

SUPPORTING INFORMATION

Planar Hexaphyrin-like Macrocycles Turning to *bis*-BODIPYs with Box-Shaped Structures Exhibiting Excitonic Coupling

Arumugam Kalaiselvan,^{a§} Shaina Dhamija,^{b§} C. Aswathi,^a Arijit K. De,^{b*} Sabapathi Gokulnath^{a*}

^aSchool of Chemistry, Indian Institute of Science Education and Research Thiruvananthapuram, Kerala-695551, India.

^bDepartment of Chemical Sciences, Indian Institute of Science Education and Research Mohali, Punjab-140306, India

S. No.	Table of Contents	Page No
S1.	General Information	2-4
S2.	Synthetic Procedures and Compound Data	5-6
S3.	High-Resolution ESI-TOF-MS and MALDI-TOF data	8-11
S4.	¹ H, ¹ H- ¹ H COSY, ¹³ C and ¹⁹ F NMR Spectra	12-16
S5.	UV/Vis Absorption and Near-IR emission Spectra	17-19
S6.	X-ray Crystallographic Data	20-22
S7.	Supramolecular Interactions through C-H...F in 2 and 2a	23
S8.	Cyclic Voltammetry	24
S9.	Photophysical Studies 9.1 Dipole-dipole interaction model: calculating the excitonic coupling strength 9.2 Steady-state measurements 9.3 Fluorescence lifetime measurements 9.4 Femtosecond transient absorption measurements	25 26 27-28 28-33
S10.	Computational Studies	34-46
S11.	Supporting References	47
S12.	Cartesian coordinates of optimized geometries and minimized energies	48-65

S1. General Information

All reagents and solvents were of commercial reagent grade and were used without further purification except where noted. Dry CH₂Cl₂ were obtained by refluxing and distillation over CaH₂. Dry THF were obtained by refluxing and distillation over Na-metal and benzophenone. Silica gel column chromatography was performed on Wakogel C-200 and C-300. Alumina column chromatography was performed on Active alumina (basic). Thin-layer chromatography (TLC) was carried out on aluminium sheets coated with silica gel 60 F254 (Merck 5554). Recrystallized samples of porphyrinoids were utilized for all the spectroscopic measurements. ¹H NMR (500 MHz) and ¹³C NMR (125 MHz) spectra were recorded on Bruker 400 (AVANCE III) and INOVA 500 (Varian) spectrometer, and chemical shifts were reported as the delta scale in ppm relative to CHCl₃ as an internal reference for ¹H (δ = 7.26 ppm) and for ¹³C (δ = 77.0 ppm). High-resolution mass spectra (HRMS) were recorded on Agilent 6520 ESI-QTOP mass spectrometer. Cyclic and differential-pulse voltammetric measurements were performed on a PC-controlled electrochemical analyzer (CH instruments model CHI620C) using a conventional three-electrode cell for samples (1 mM) dissolved in dry DMF containing 0.1 M *n*-Bu₄NPF₆ (TBAPF₆) as the supporting electrolyte. Measurements were carried out under an Argon atmosphere. A platinum working electrode, a calomel reference electrode and platinum wire counter electrode were used in all electrochemical experiments. The potentials were calibrated using the ferrocenium/ferrocene couple. The optical absorption spectra were recorded on a Shimadzu (Model UV-3600) spectrophotometer.

X-Ray Crystallography: X-Ray quality crystals were prepared by slow diffusion of *n*-hexane into a chloroform solution of **1**. Similarly, slow diffusion of *i*-PrOH into to a toluene solution of **2**. Single crystals, suitable for facile structural determination were mounted at 100 K on a three-circle Bruker SMART APEX CCD area detector system under a Mo-K α (λ = 0.71073 Å) graphite monochromatic X-ray beam; 2400 frames were recorded with an ω scan width of 0.3°, each for 10 s; crystal-detector distance 60 mm, collimator 0.5 mm. Data reduction was performed by using SAINTPLUS.^[S1] Empirical absorption corrections were performed with equivalent reflections by using the program SADABS.^[S2] The structures were solved by direct methods and least-square refinement on F² for all the compounds **2** and **2a** by using SHELXS-97.^[S2] All non-hydrogen atoms were refined anisotropically. The hydrogen atoms were included in the structure factor calculation by using a riding model. The

crystallographic parameters, data collection, and structure refinement of compounds **2** and **2a** are summarized in Fig.

Computational Methods: All calculations were carried out using the Gaussian 09 program.^[S3] Initial geometries were obtained from X-ray structures. Calculations were performed by the density functional theory (DFT) method with restricted B3LYP (Becke's three-parameter hybrid exchange functionals and the Lee-Yang-Parr correlation functional)^[S4] level, employing a basis sets 6-31G(d). Vertical electronic excitations based on B3LYP optimized geometries were computed using the time-dependent density functional theory (TDDFT) formalism.^[S5] NICS values were calculated with GIAO method at the B3LYP level employing a basis sets 6-31G(d).

Materials and sample preparation:

The samples are dissolved in chloroform (ACS spectrophotometric grade, Sigma Aldrich). The samples are stored in dark to minimize photo-bleaching.

Steady-state measurements:

Absorption spectrum is recorded on a UV-VIS spectrophotometer (Cary 60 UV VIS-NIR spectrophotometer, Agilent Technologies). Fluorescence spectra are recorded on a steady-state fluorimeter (Cary Eclipse fluorescence spectrophotometer, Agilent Technologies). Steady-state spectra are deconvoluted using Origin 2018.

Fluorescence lifetime measurements:

Time-resolved measurements are done using a time-correlated single photon counting (TCSPC) fluorimeter (Deltaflex, Horiba Scientific). Laser diode head producing pulses centered at 510 nm (N-510L, Horiba Scientific) having pulse width < 200 ps and 1MHz repetition rate is used as excitation source. The instrument response is found to be ~305 ps (by measuring the FWHM of the scatter time trace using 0.1% ludox solution, Sigma-Aldrich). The fluorescence lifetime decays are collected across the spectrum keeping the emission polarization at magic angle (54.7^0) and the peak preset at 10,000 counts. The data is fitted using DAS6 analysis software (Horiba Scientific) by maintaining the best-fitting parameters.

Transient absorption measurements:

In transient absorption studies, a pump pulse excites the sample, and a time-delayed probe pulse (broadband) tracks this initially photoexcited sample. Depending on the spectral content, the probe can interrogate various processes: it can re-excite the initially excited

molecules (known as excited-state absorption, ESA) or dump them back to the ground state (stimulated emission, SE) or recovery of ground state bleach (GSB, i.e. re-absorption). Thus, by noting the sign (positive or negative) of differential absorption ($\Delta\text{OD} > 0$ or $\Delta\text{OD} < 0$) and recording the time evolution of different spectral regions of the probe, we can map these signals. Details of customized femtosecond transient absorption spectrometer (TAS, Newport Corp.) can be found elsewhere.^[S6-S8] Ultrashort pulses centered on 500 nm or 515 nm at 1 kHz repetition rate from a commercial non-collinear optical parametric amplifier (Topas White, Light Conversion), pumped by a Ti:Sapphire regenerative amplifier centered on ~800 nm having ~54 fs pulse width (Libra, Coherent Inc.) are used to electronically excite the carbazole based expanded porphyrins and their corresponding *bis*-BODIPY complexes. A time delayed broadband (390 nm to 720 nm) white-light (generated by pumping a CaF₂ crystal) probe is used to study the excited state dynamics. The spectra for 500 nm and 515 nm pump are shown in Figures 1 and 2 having transform limited pulse widths ~ 37 fs and ~20 fs respectively but it is expected to be chirped at the sample position. Pulse width measurement using autocorrelation couldn't be done due to limited bandwidth of the second harmonic generation (SHG) crystal and the solvent scattering data is noisy to have a conclusive determination of pulse width. The fast rise component of ground state bleach (GSB) (Tables S9-2 to S9-5) is a measure of pulse width.^[S9] The optical densities for the compounds **2**, **2a**, **3** and **3a** are 0.30 (at 492 nm), 0.22 (at 516 nm), 0.28 (at 483 nm) and 0.25 (at 517 nm) respectively at pump maximum wavelengths. The pump polarization is kept at magic angle (54.7°) with respect to the vertically polarized probe to prevent polarization dependent signals. To obtain the differential absorption signal (ΔOD) at a specific time, the pump pulses are chopped at 500 Hz. At sample position, the pump and probe powers are kept <200 μW and <10 μW respectively. The measurements are done in a 1 mm pathlength cuvette. The data are collected in four different segments at different step-sizes (-1 ps to +1 ps at 0.01 ps step-size, 1.1 ps to 10 ps at 0.1 ps step-size, 11 ps to 100 ps at 1 ps step-size, 101 ps to 3000 ps at 10 ps step-size) and the entire data (averaged over 2,000 laser shots for compounds **2a** and **3a** and 3,000 laser shots for compounds **2** and **3**) are joined and fitted using MATLAB programming (MATLAB, 2018a, Mathworks). The rise parts are fitted with a sigmoidal:

$$\left(\frac{A_2 + (A_1 - A_2)}{1 + e^{\frac{t-t_0}{\tau_{rise}}}} \right)$$

(For a discussion on the equivalence of Gaussian function, see supplementary information in [S8]) and the decay with a sum of exponentials:

$$a_1 e^{-\frac{(t-t_0)}{\tau_1}} + a_2 e^{-\frac{(t-t_0)}{\tau_2}} + a_3 e^{-\frac{(t-t_0)}{\tau_3}}$$

After the experiment, the absorption spectrum is checked to rule out any degradation or photo-bleaching of samples during the experiment.

S2. Synthetic Procedures and Compound Data

1 was prepared by following our reported procedures.^[S10]

Synthesis of macrocycle 2: The solution of 1, 8-Di-(*1H*-pyrrole)-3, 6-di (*tert*-butyl)carbazole, **1** (115 mg, 0.281 mmol) and 2,3,4,5,6 pentafluorobenzaldehyde (34 μ L, 0.281 mmol) in dry DCM was degassed with a stream of Argon for 10 min. To this solution kept at dark, TFA (32 μ L, 0.422 mmol) was added and the reaction mixture was allowed to stir for 5 h. After confirming the complete consumption of the starting material, the reaction mixture was quenched using a drop of Et₃N followed by the oxidation with DDQ (96 mg, 0.422 mmol) and the resulting mixture was stirred at room temperature for 1 h. The reaction mixture was passed through a pad of alumina column which was then purified via flash column chromatography on silica gel and identified the target macrocycle as an intense purple colored fraction. The colored fraction was concentrated under vacuo and recrystallized with *n*-hexane yielded pure macrocycle **2** as shiny violet solids in 52% yield (85 mg). ¹H NMR (500 MHz, CD₂Cl₂, 213 K): δ = 10.83 (s, 2H, pyrrole NH), 8.48 (s, 2H, imino or amino pyrrole β -CH), 8.35 (s, 2H, carbazole NH), 8.28 (s, 2H, carbazole phenyl-CH), 8.20 (s, 2H, carbazole phenyl-CH), 7.96 (s, 2H, carbazole phenyl-CH), 7.43-7.36 (m, 4H, imino or amino pyrrole β -CH), 7.34 (s, 2H, carbazole phenyl-CH), 6.79 (d, *J* = 4.4, 2H, imino or amino pyrrole β -CH), 1.45 (s, 18H), 1.40 (s, 18H); HRMS (ESI): *m/z* = 1171.4485 [M+H]⁺, calcd for C₇₀H₅₇F₁₀N₆; found = 1171.4510 [M+H]⁺. UV-Vis (CH₂Cl₂): λ_{max} /nm (ϵ [mol⁻¹ dm³ cm⁻¹]): 492 (66700), 540 (49085). Fluorescence (CHCl₃, $\lambda_{\text{ex}} = 492$ nm), $\lambda_{\text{em}} = 710$ nm.

Synthesis of macrocycle 3: The solution of 1, 8-Di (-*1H*-pyrrole)-3, 6-di (*tert*-butyl)carbazole **1** (115 mg, 0.281 mmol) and mesitaldehyde (42 μ L, 0.281 mmol) in dry CH₂Cl₂ was degassed with a stream of Argon for 10 min. To this solution kept at dark, TFA (32 μ L, 0.422 mmol) was added and the reaction mixture was allowed to stir for 48 h. The reaction mixture was then quenched using a drop of Et₃N followed by the oxidation with DDQ (96 mg, 0.422

mmol) and the resulting mixture was stirred at room temperature for 1 h. Then, the reaction mixture was passed through a pad of alumina column, which was further purified via flash column chromatography on silica gel and identified the target macrocycle as an intense red colored fraction. The colored fraction was concentrated under vacuo and recrystallized with *n*-hexane to yield the pure macrocycle **3** as shiny violet solids in 46% yield (70 mg). ¹H NMR (500 MHz, CDCl₃, 298 K): δ = 11.36 (s, 2H, pyrrole NH), 8.44 (s, 2H, imino or amino pyrrole β-CH), 8.18 (s, 2H, carbazole phenyl-CH), 8.09 (s, 2H, carbazole phenyl-CH), 8.01 (s, 2H, carbazole NH), 8.00 (s, 2H, carbazole phenyl-CH), 7.51 (s, 2H, imino or amino pyrrole β-CH), 7.31 (d, *J* = 4.4 Hz, 2H, imino or amino pyrrole β-CH), 7.11 (s, 4H, mesityl CH), 7.03 (s, 2H, carbazole phenyl-CH), 6.86 (d, *J* = 4.4 Hz, 2H, imino or amino pyrrole β-CH), 2.44 (s, 6H, *p*-CH₃), 2.26 (s, 12H, *o*-CH₃), 1.52 (s, 18H, Bu^t), 1.41 (s, 18H, Bu^t); HRMS (ESI): *m/z* = 1075.6366 [M+H]⁺, calcd for C₇₆H₇₉N₆; found = 1075.6367 [M+H]⁺. UV-Vis (CH₂Cl₂): λ_{max}/nm (ε [mol⁻¹ dm³ cm⁻¹]): 482 (76493), 525 (64928). Fluorescence (CHCl₃, λ_{ex} = 483 nm), λ_{max} = 653 nm.

Synthesis of 2a: To a dry toluene solution of **2** (10 mg, 0.0085 mmol) was added N, N'-DIPEA (0.297 mL, 1.71 mmol, 200 equiv) and the mixture was stirred at room temperature for 5 min under Argon. Then, BF₃.OEt₂ (0.211 mL, 1.71 mmol, 200 equiv) was added to the solution and was stirred at 70 °C for 48 h. Reaction was quenched by the addition of water and the resulting mixture was extracted with CH₂Cl₂. It was then purified via flash column chromatography on silica gel and identified the target macrocycle as an intense pink fraction. This colored fraction was collected and recrystallized with *n*-hexane yielded pure *bis*-BODIPY complex **2a** as purple solids in 47% yield. ¹H NMR (500 MHz, CDCl₃, 298 K): δ = 8.51 (brs, 2H, carbazole NH), 8.04 (s, 4H, carbazole phenyl-CH), 7.29 (s, 4H, carbazole phenyl-CH), 6.83 (d, *J* = 5.0 Hz, 4H, pyrrole β-CH), 6.41 (d, *J* = 5.0 Hz, 4H, pyrrole β-CH), 1.38 (s, 36H, Bu^t); HRMS (ESI): *m/z* = 1399.3427 [M•Cs]⁺, calcd for C₇₀H₅₄B₂CsF₁₄N₆; found = 1399.3286 [M•Cs]⁺. UV-Vis (CH₂Cl₂): λ_{max}/nm (ε [mol⁻¹ dm³ cm⁻¹]) 523 (71058). Fluorescence (CHCl₃, λ_{ex} = 516 nm), λ_{max} = 742 nm.

Similar procedure was adapted using **3** to obtain the corresponding *bis*-BODIPY, **3a**: Yield: 43%. ¹H NMR (500 MHz, CDCl₃): δ = 8.60 (s, 2H, carbazole NH), 8.02 (s, 4H, carbazole phenyl-CH), 7.32 (d, *J* = 1.3 Hz, 4H, carbazole phenyl-CH), 7.02 (s, 2H, mesityl CH), 6.69 (d, *J* = 3.9 Hz, 4H, pyrrole β-CH), 6.28 (d, *J* = 3.9 Hz, 4H, pyrrole β-CH), 2.41 (s, 6H, *p*-

CH_3), 2.26 (d, 12H, $J = 5.0$ Hz, *o*- CH_3), 1.38 (s, 36H, Bu^t); HRMS (ESI): $m/z = 1303.5308$ [$\text{M}\bullet\text{Cs}$]⁺, calcd for $\text{C}_{76}\text{H}_{76}\text{B}_2\text{CsF}_4\text{N}_6$; found = 1303.5242 [$\text{M}\bullet\text{Cs}$]⁺. UV-Vis (CH_2Cl_2): $\lambda_{\text{max}}/\text{nm}$ (ϵ [mol⁻¹ dm³ cm⁻¹]) = 515 (77712). Fluorescence (CHCl_3 , $\lambda_{\text{ex}} = 517$ nm), $\lambda_{\text{em}} = 664$ nm.

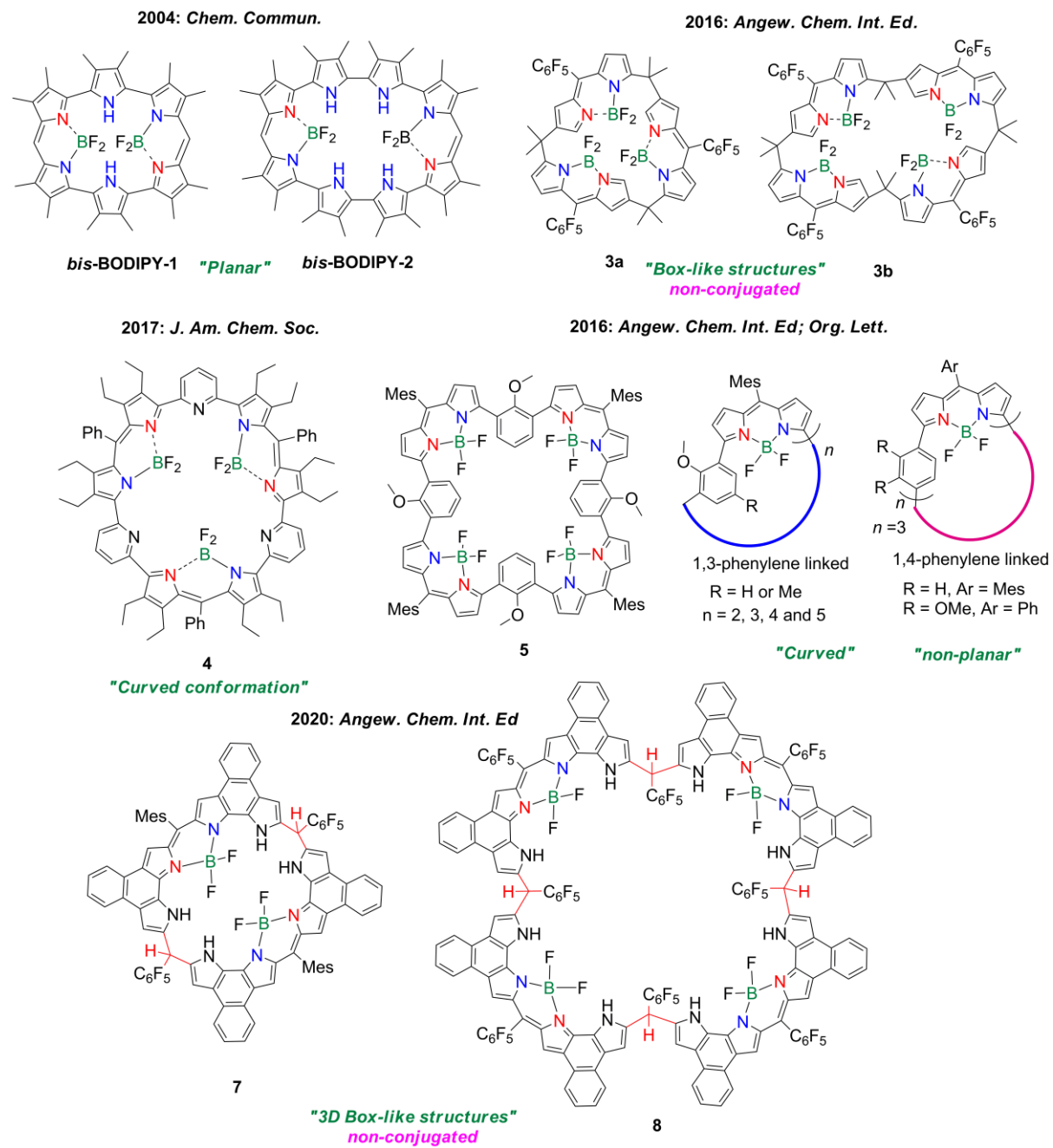


Figure S2-1. Representative examples of cyclic BODIPYs known in the literature.

S3. High-Resolution ESI-TOF-MS

Z:\Data\...\VAUG2017\AKT-253_170830105148

30-08-2017 10:51:48

AKT-253_170830105148 #36-42 RT: 0.53-0.62 AV: 7 NL: 2.33E6
T: FTMS {1,1} + p ESI Full lock ms [100.00-2000.00]

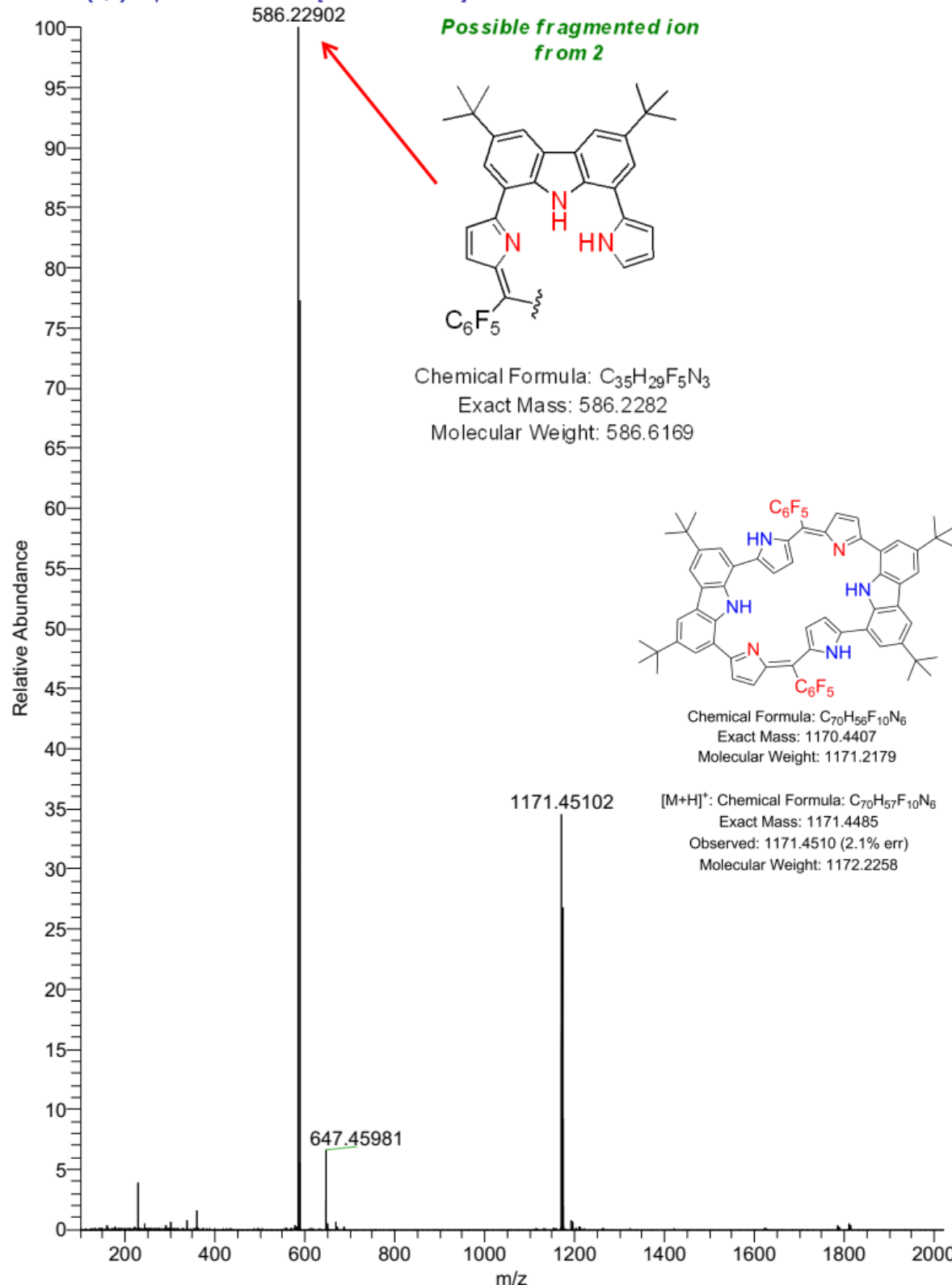


Figure S3-1. HR-mass spectrum (ESI) of macrocycle 2.

JR-546-A #310 RT: 4.67 AV: 1 NL: 1.10E5
T: FTMS {1,1} + p ESI Full lock ms [100.00-1500.00]

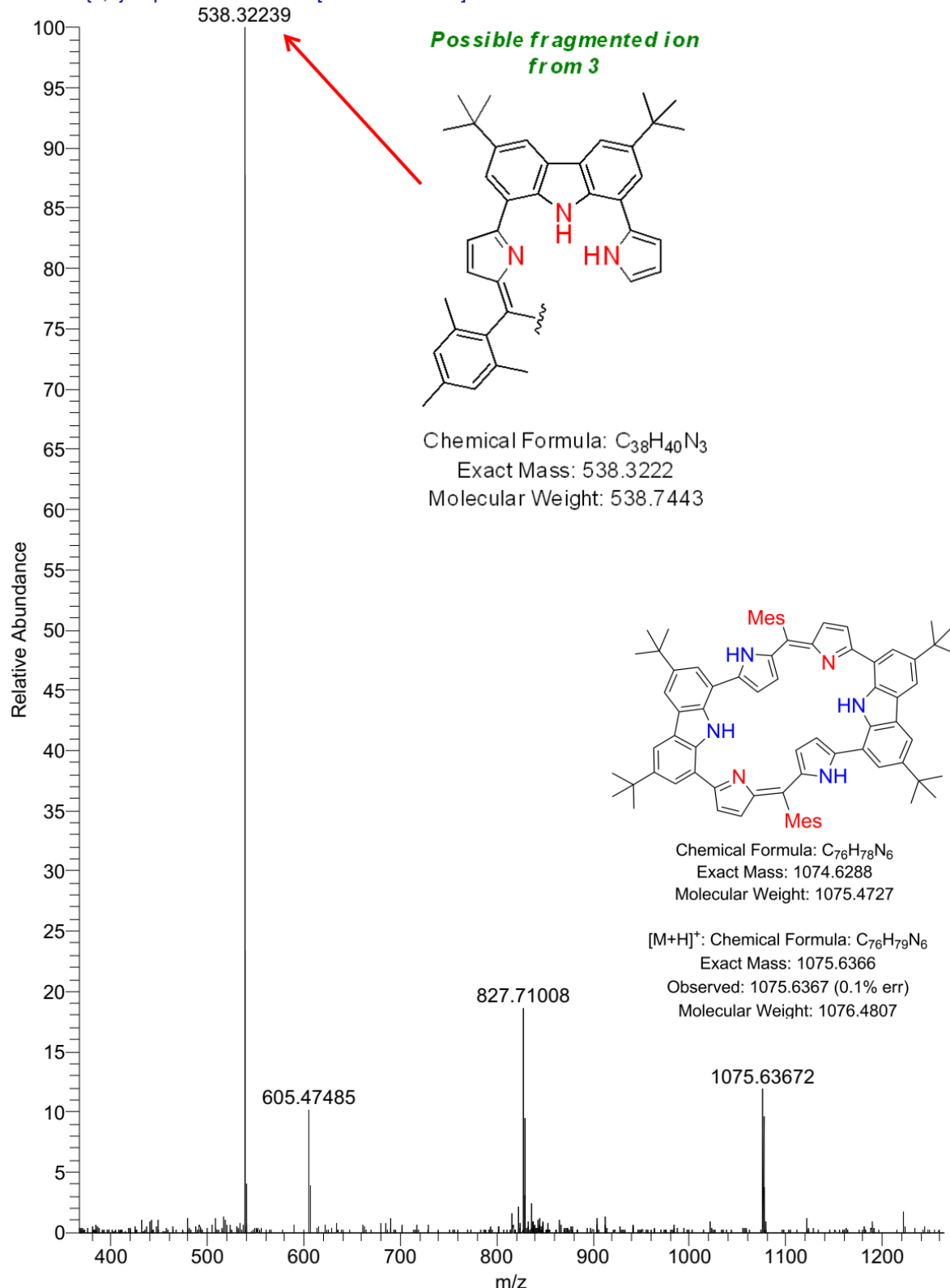


Figure S3-2. HR-mass spectrum (ESI) of macrocycle 3.

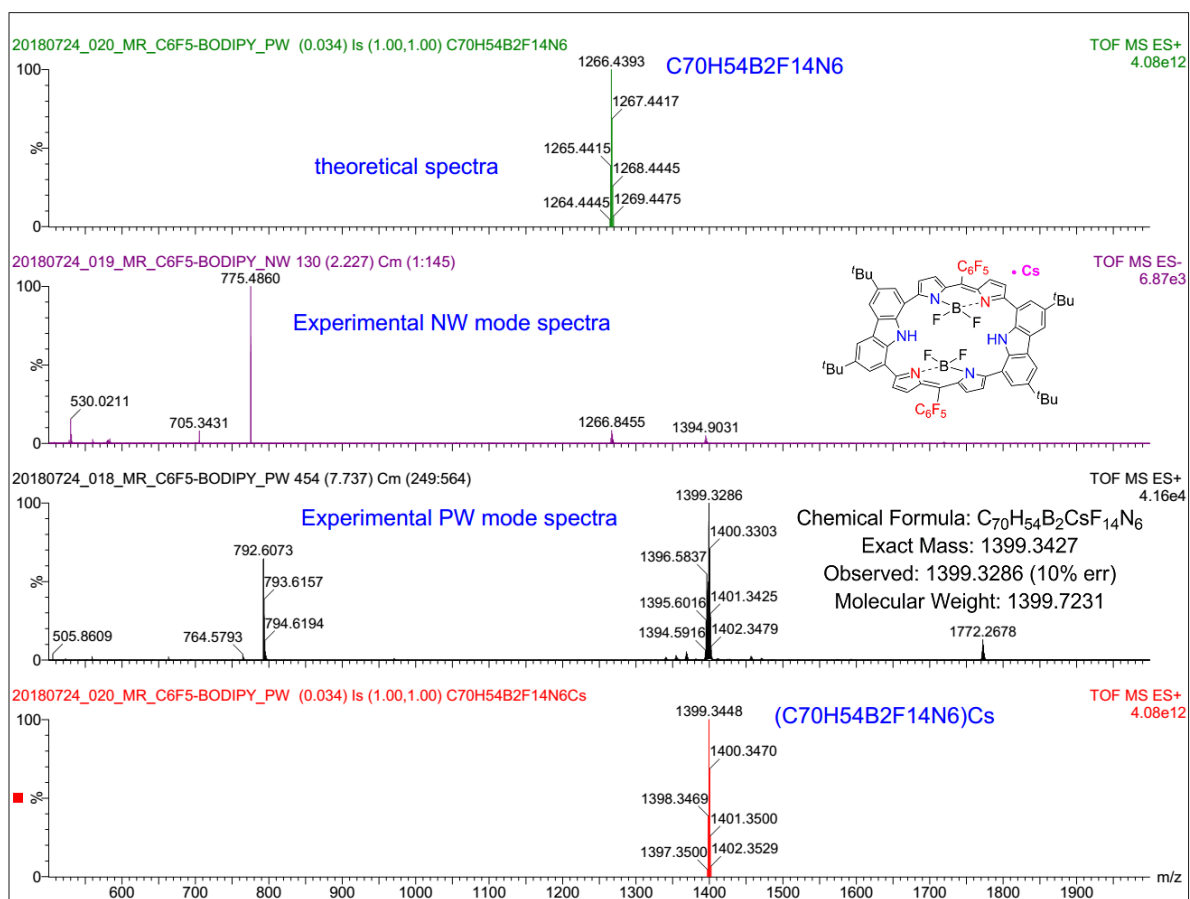


Figure S3-3. ESI-TOF of **2a**.

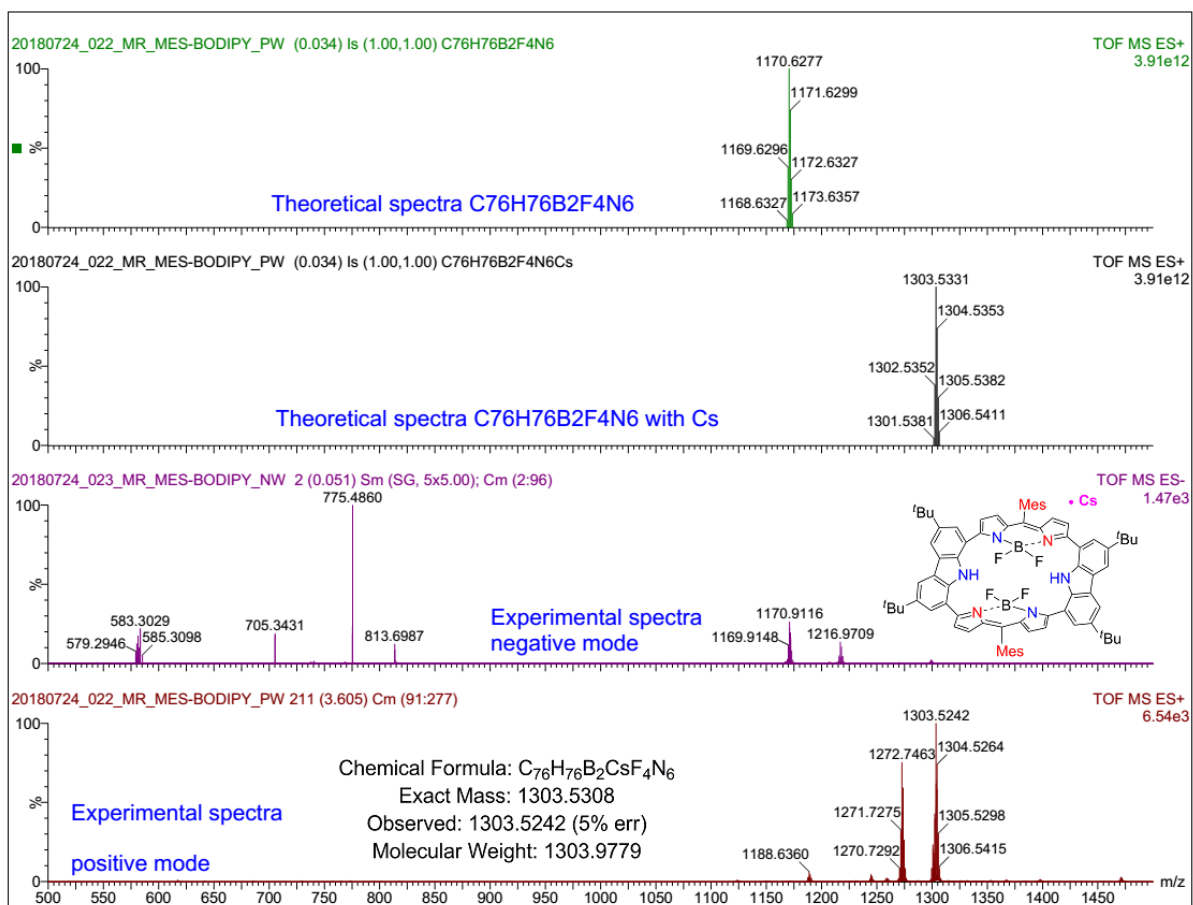


Figure S3-4. ESI-TOF of 3a.

S4. ^1H and ^1H - ^1H COSY NMR characterization

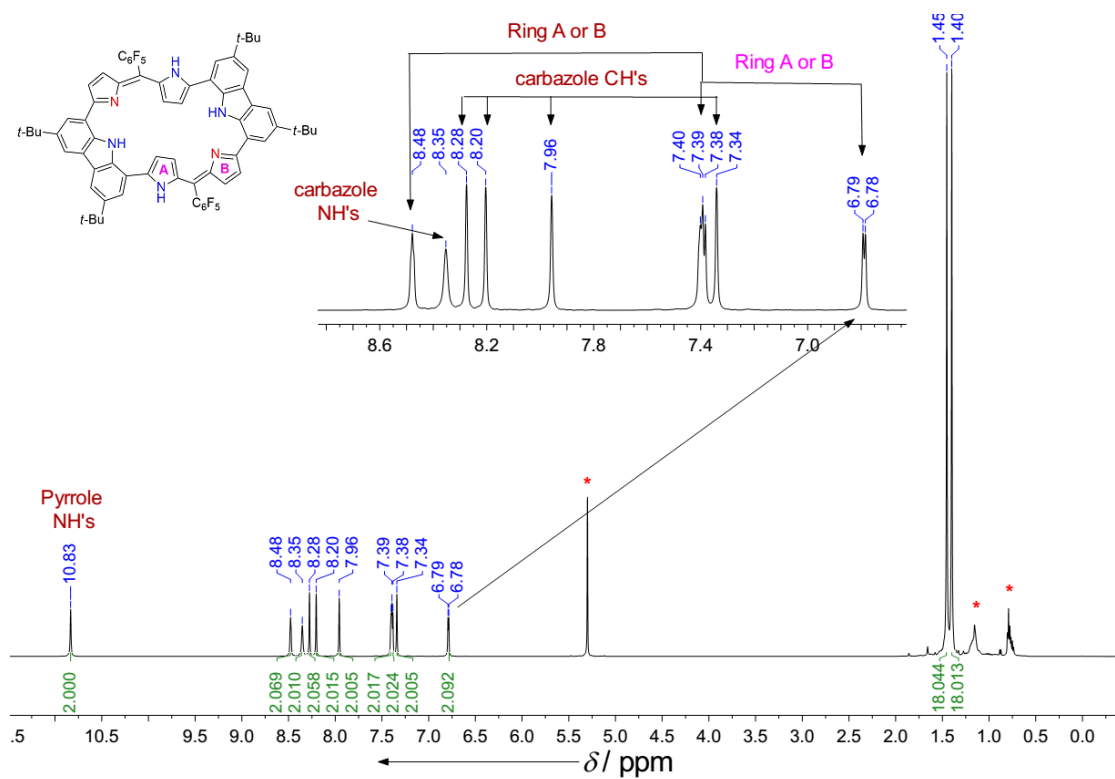


Figure S4-1. ^1H NMR spectrum of **2** in CDCl_3 at 213 K. Signals marked with (*) denotes residual solvents or impurities.

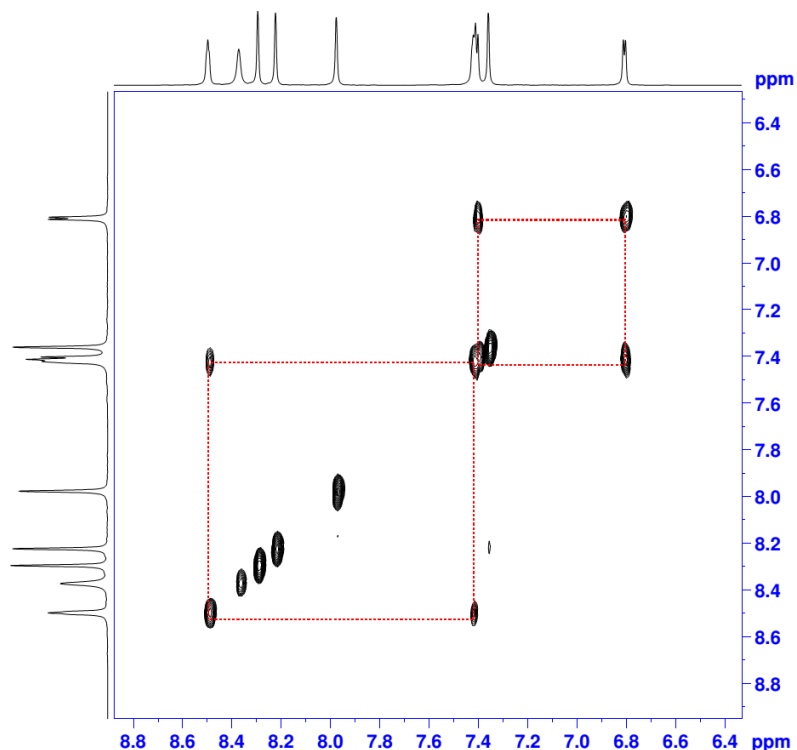


Figure S4-2. ^1H - ^1H COSY spectrum of **2** in CDCl_3 at 213 K. Signals marked with (*) denotes residual solvents or impurities.

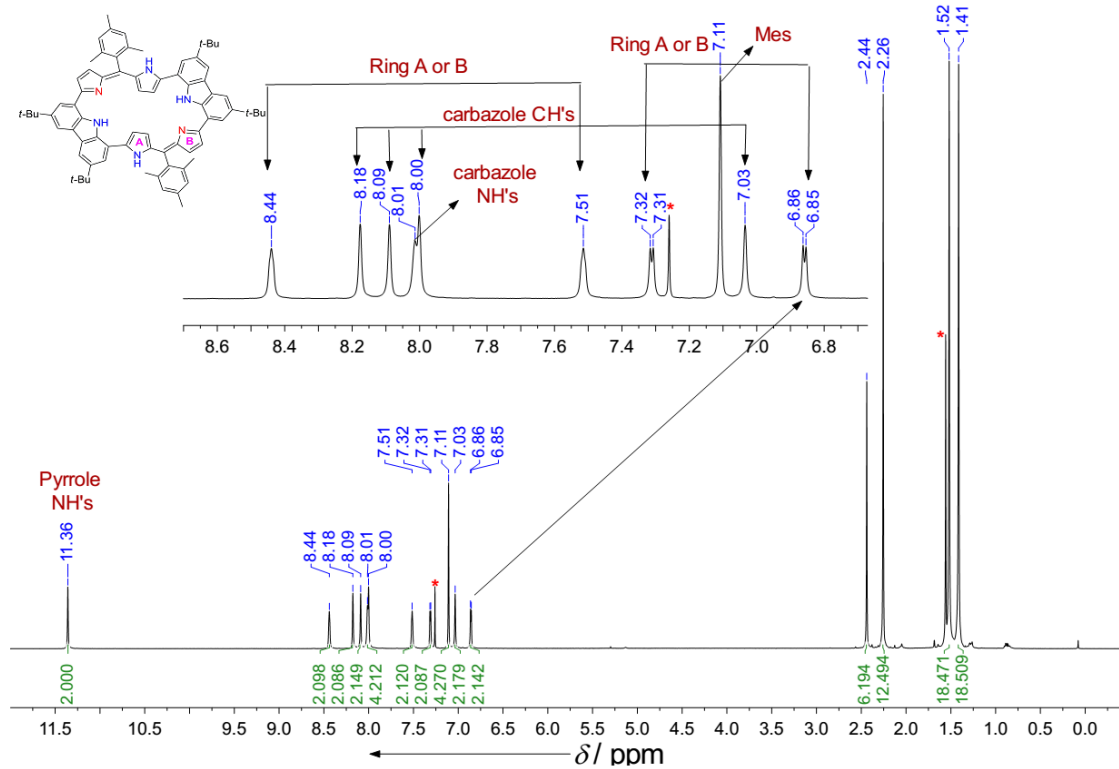


Figure S4-3. ^1H NMR spectrum of **3** in CD_2Cl_2 at 298 K. Signals marked with (*) denotes residual solvents or impurities.

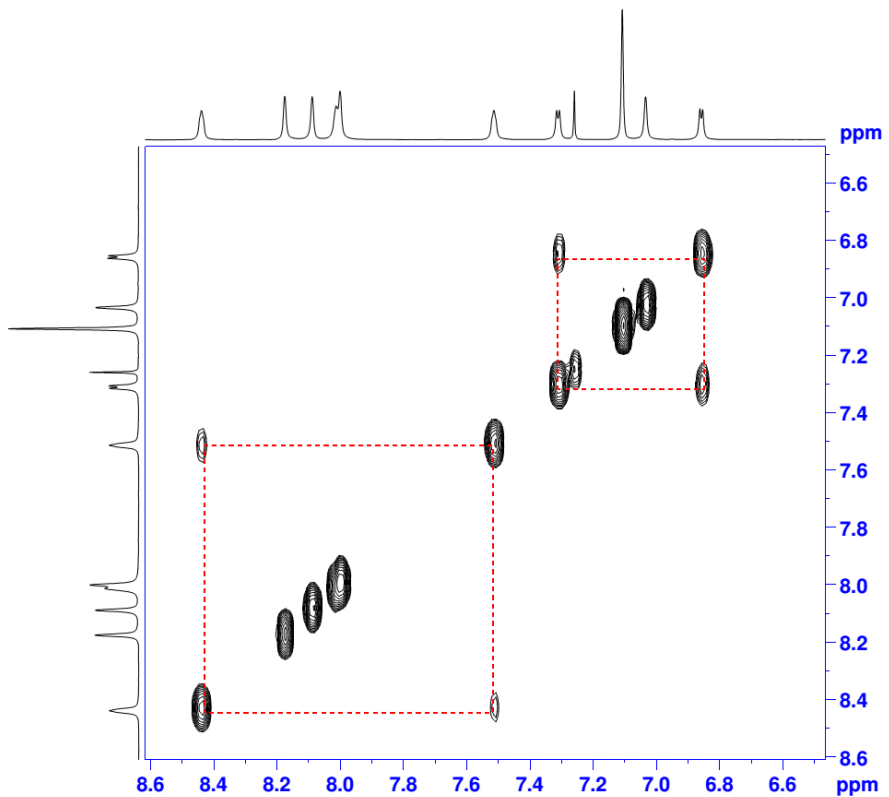


Figure S4-4. ^1H - ^1H COSY spectrum of **3** in CDCl_3 at 298 K. Signals marked with (*) denotes residual solvents or impurities.

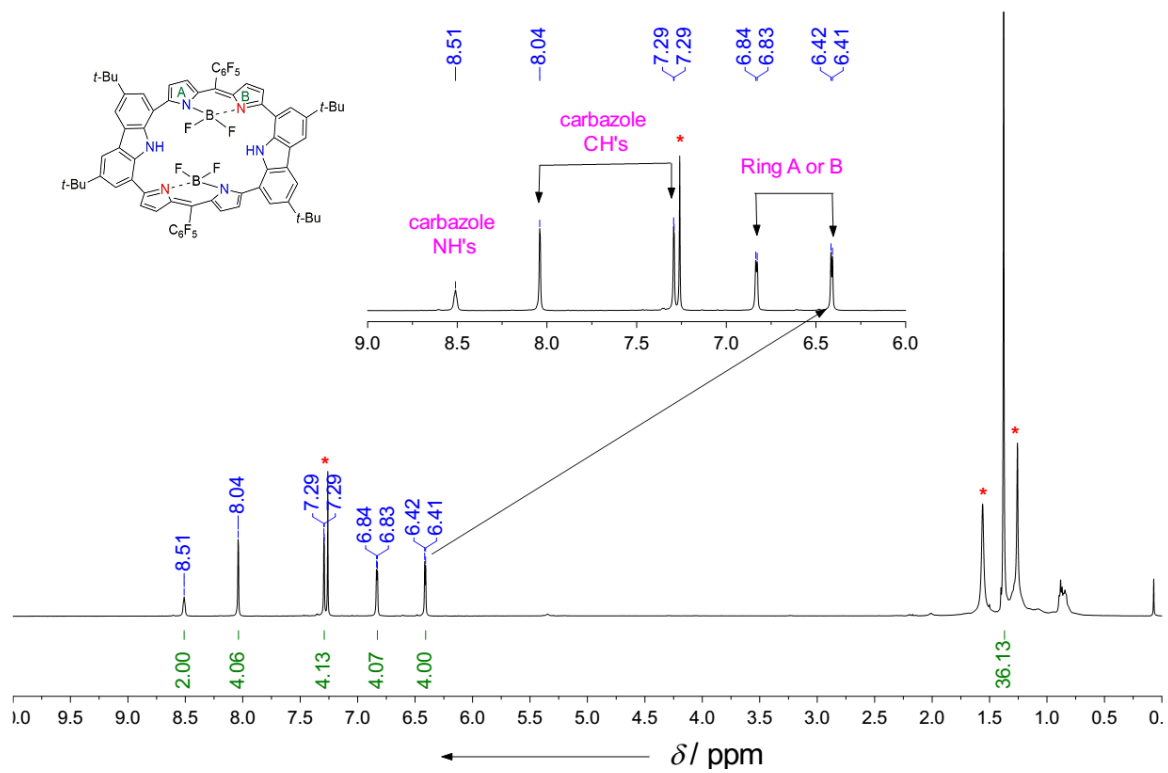


Figure S4-5. ^1H NMR spectrum of **2a** in CDCl_3 at 298 K. Signals marked with (*) denotes residual solvents or impurities.

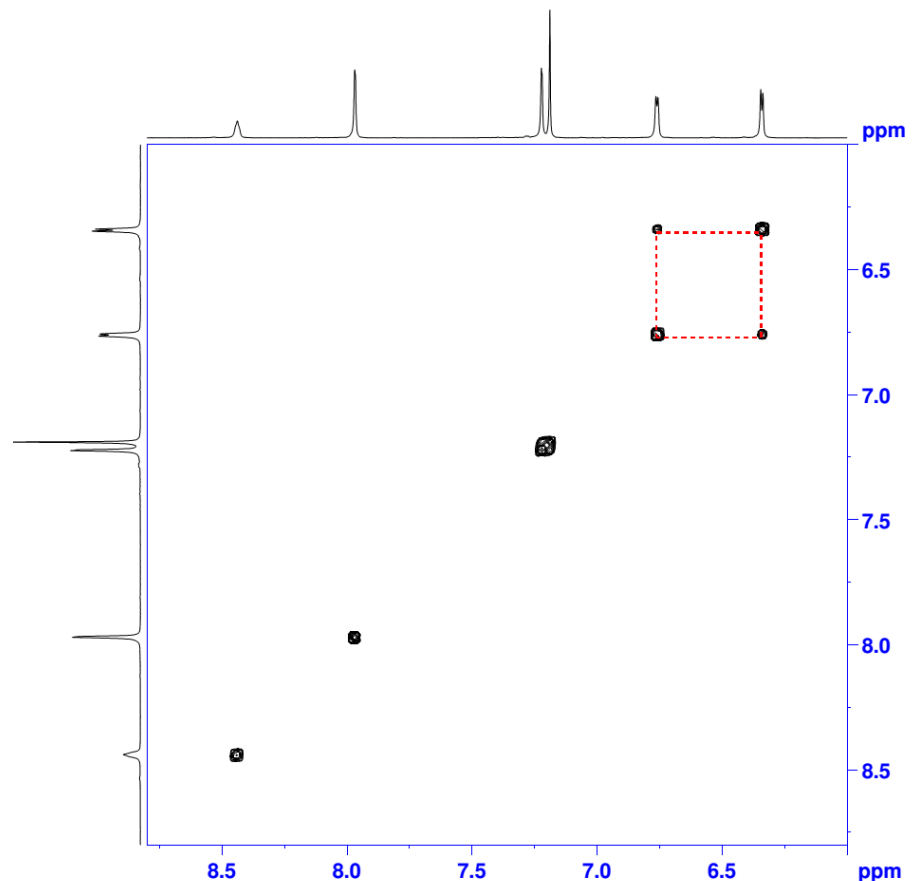


Figure S4-6. ^1H - ^1H COSY spectrum of **2a** in CDCl_3 at 298 K.

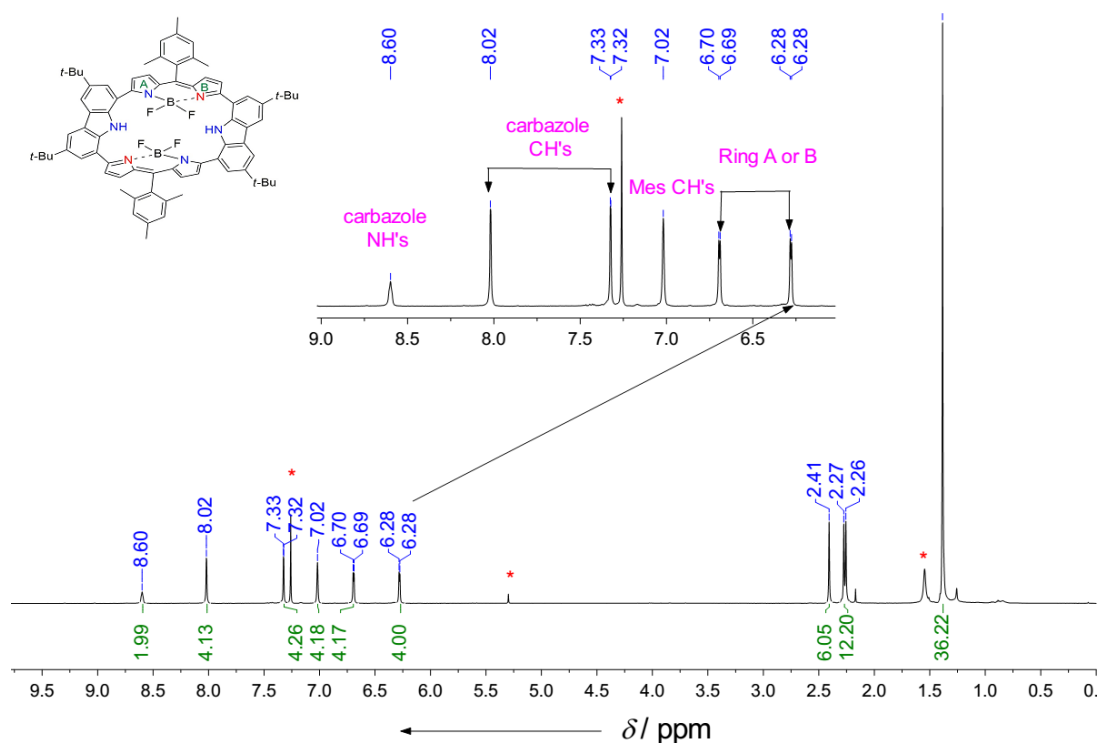


Figure S4-7. ^1H NMR spectrum of **3a** in CDCl_3 at 298 K. Signals marked with (*) denotes residual solvents or impurities.

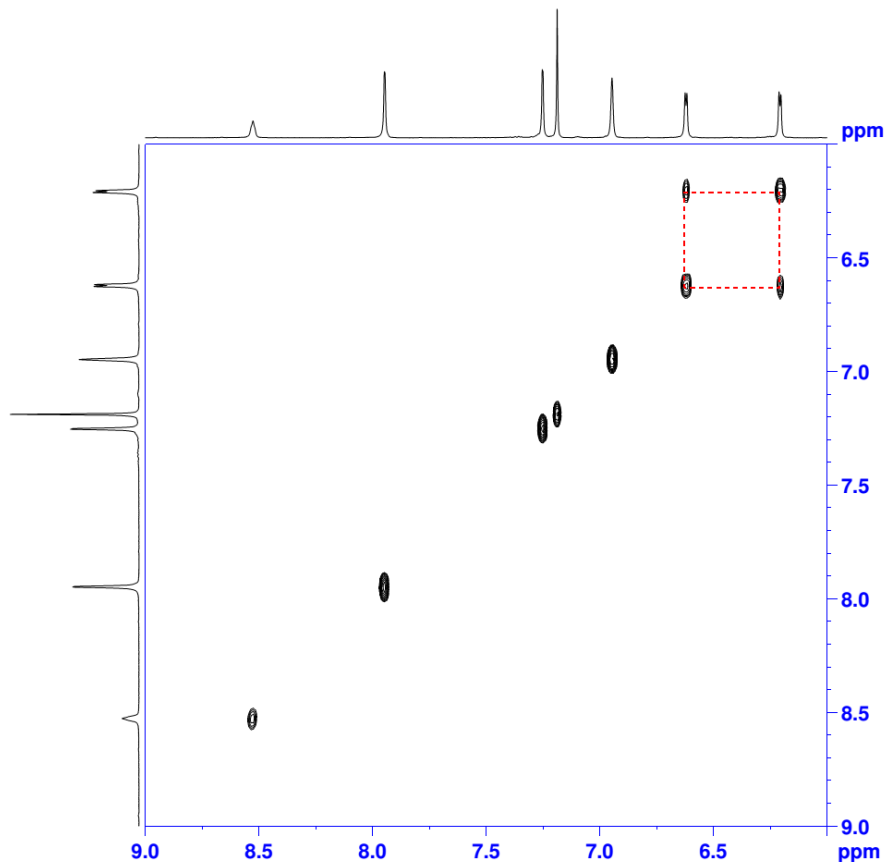


Figure S4-8. ^1H - ^1H COSY spectrum of **3a** in CDCl_3 at 298 K.

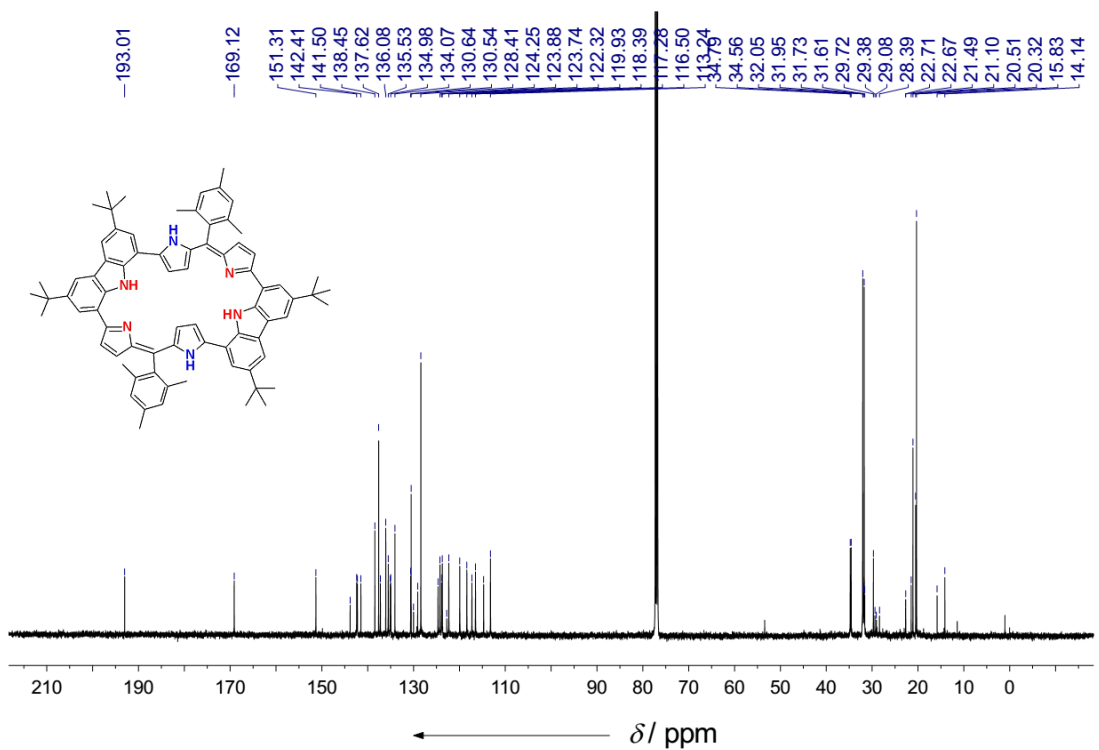


Figure S4-9. ^{13}C NMR spectrum of **3** in CDCl_3 at 298 K.

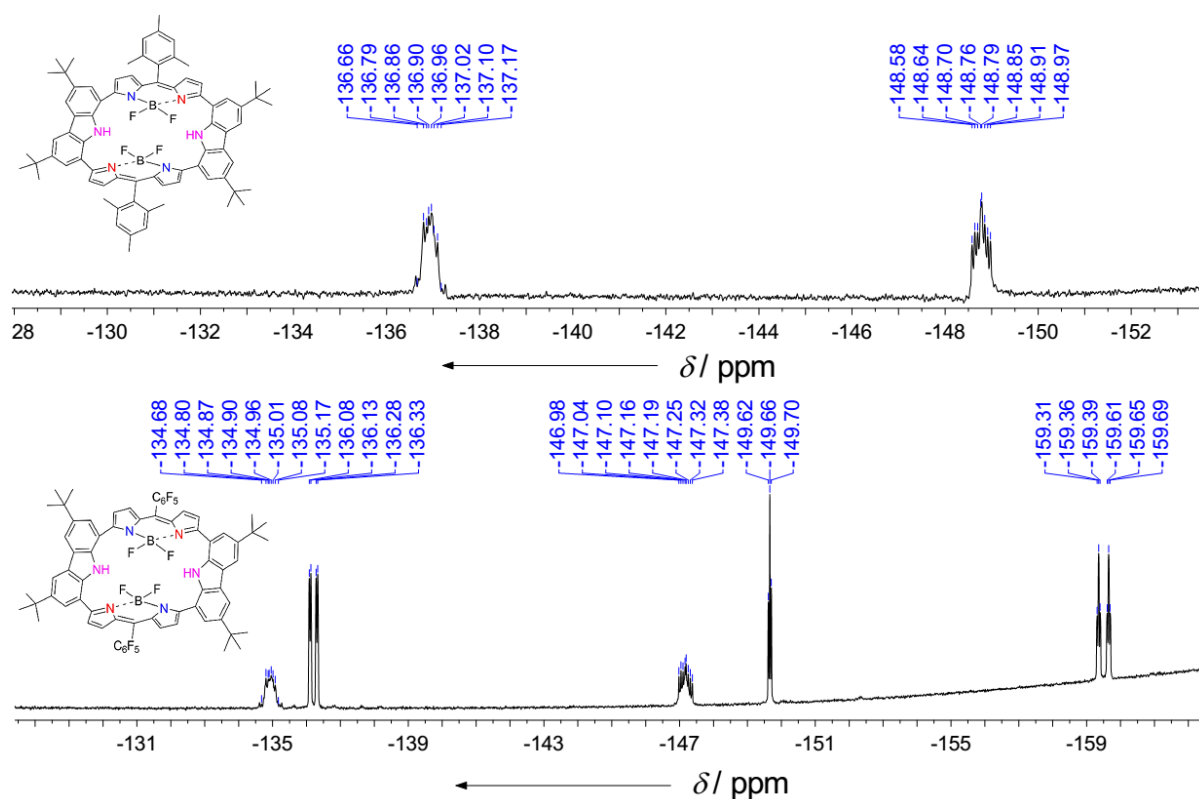


Figure S4-10. ^{19}F NMR spectrum of **2a** (bottom) and **3a** (top) in CDCl_3 at 298 K.

S5. UV/Vis Absorption and Near-IR emission Spectra

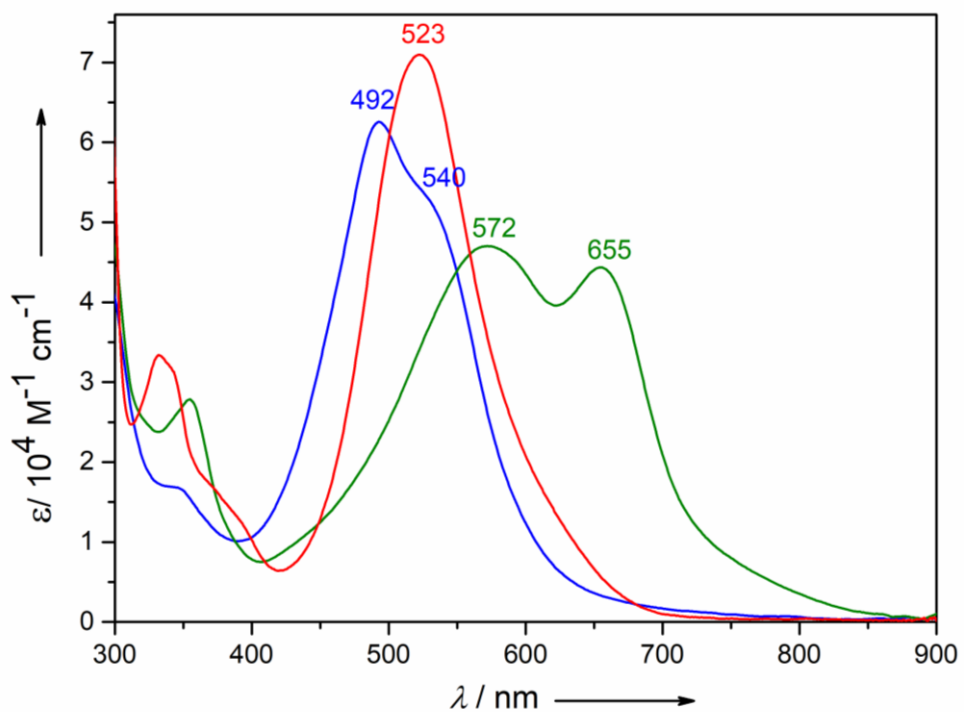


Figure S5-1. UV-Vis absorption spectra of **2** (blue), **2a** (red) and **2•2H⁺** (green) recorded in CH₂Cl₂.

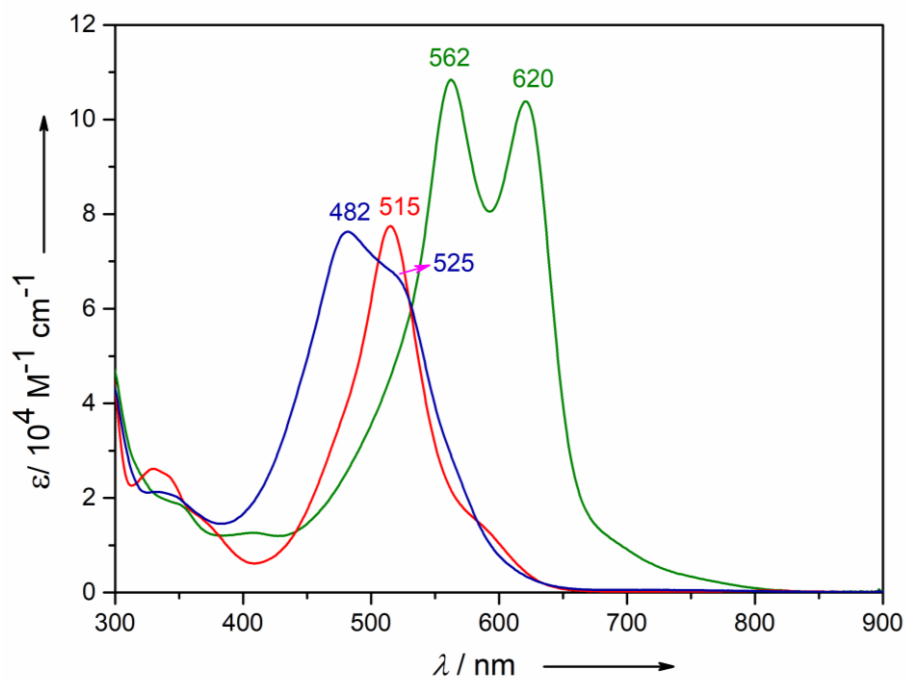


Figure S5-2. UV-Vis absorption spectra of **3** (blue), **3a** (red) and **3•2H⁺** (green) recorded in CH₂Cl₂.

S5.1 Solvent Dependent Absorption Spectra

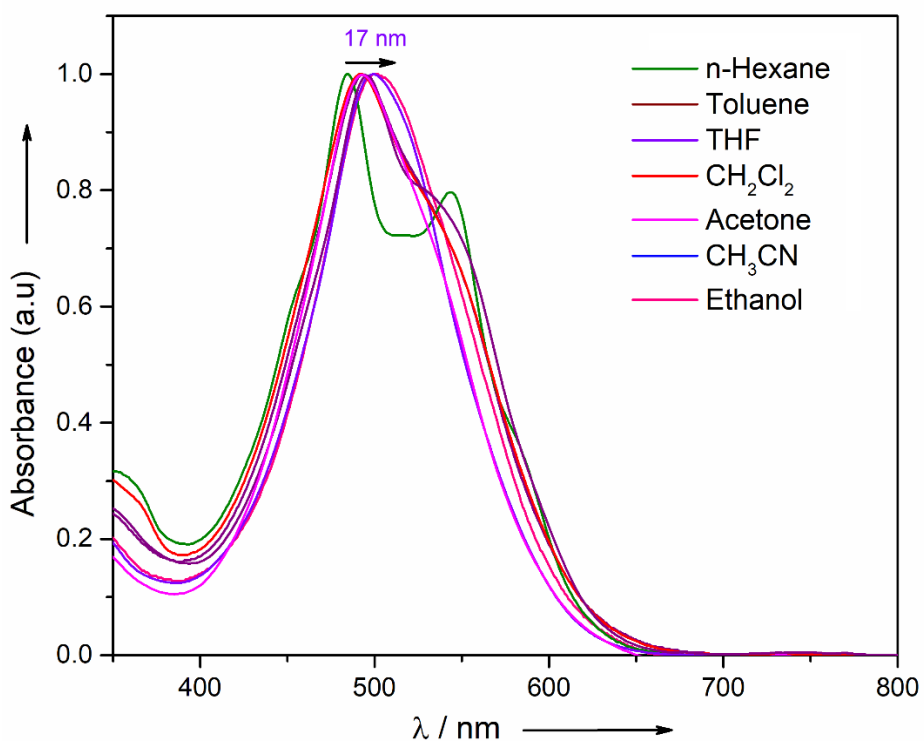


Figure S5-3. UV-Vis absorption spectra of **2** recorded in different solvents.

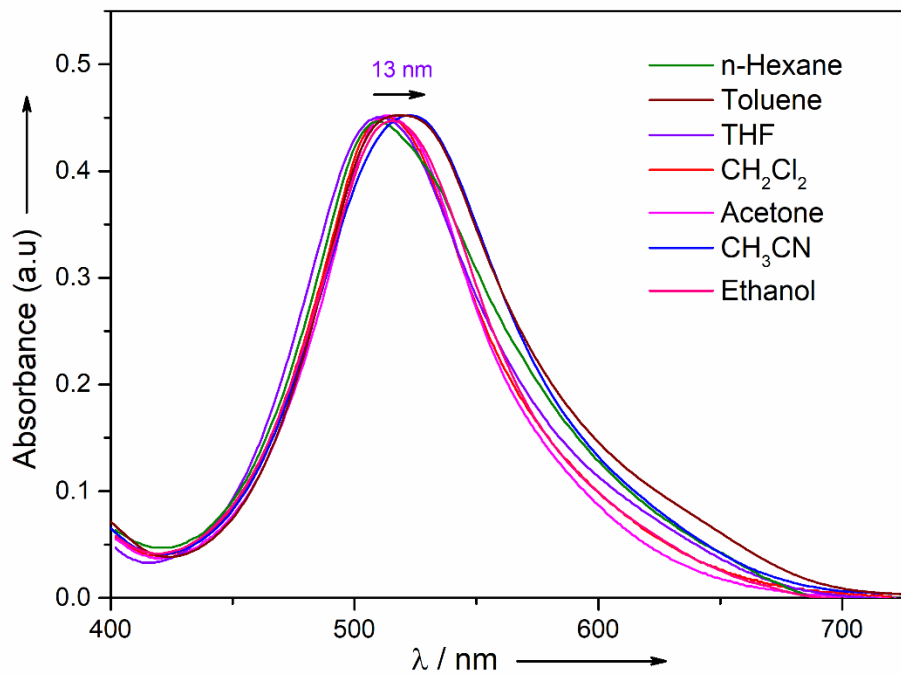


Figure S5-4. UV-Vis absorption spectra of **2a** recorded in different solvents.

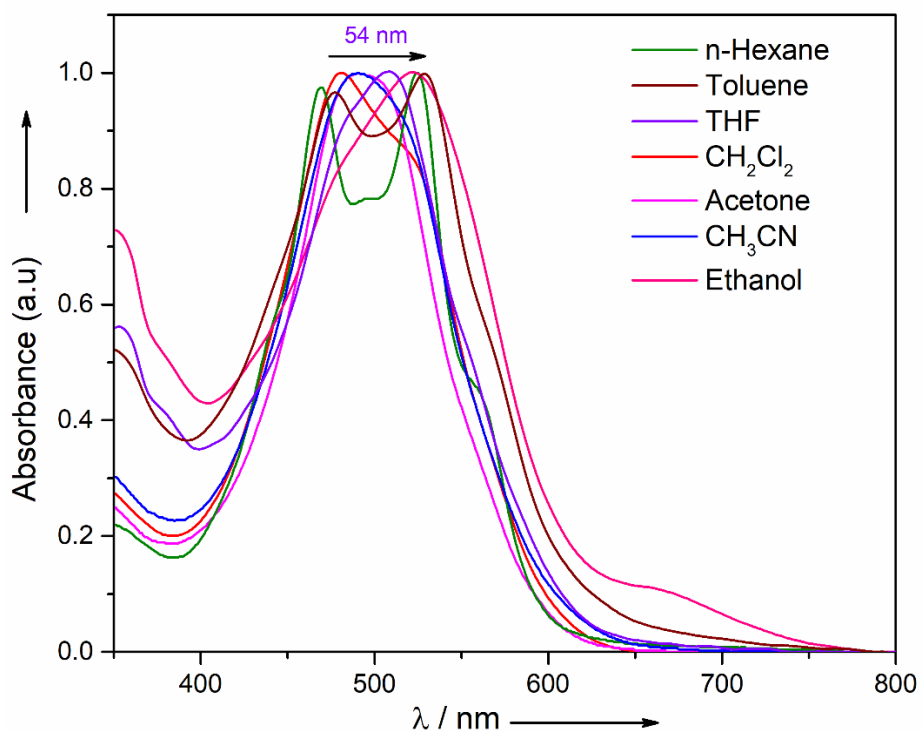


Figure S5-5. UV-Vis absorption spectra of **3** recorded in different solvents.

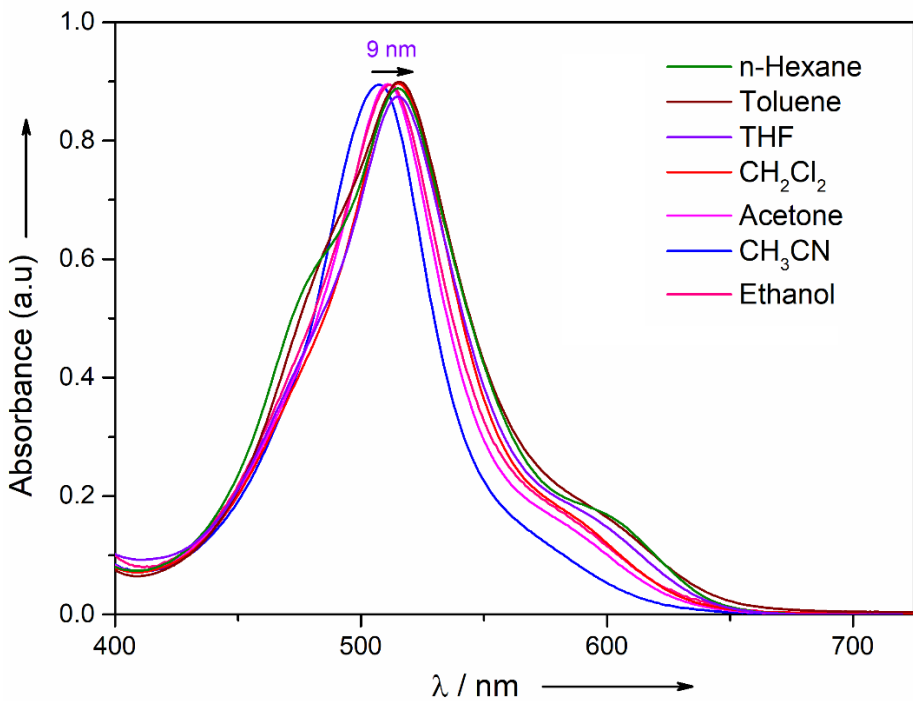


Figure S5-6. UV-Vis absorption spectra of **3a** recorded in different solvents.

S6. Crystallographic Data

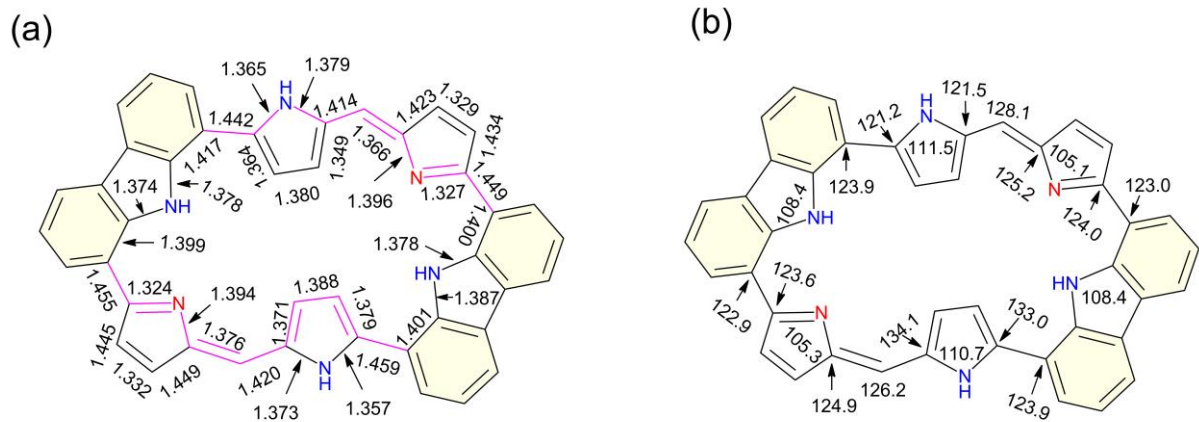


Figure S6-1: (a) Bond lengths (\AA) and (b) bond angles ($^\circ$) of **2**.

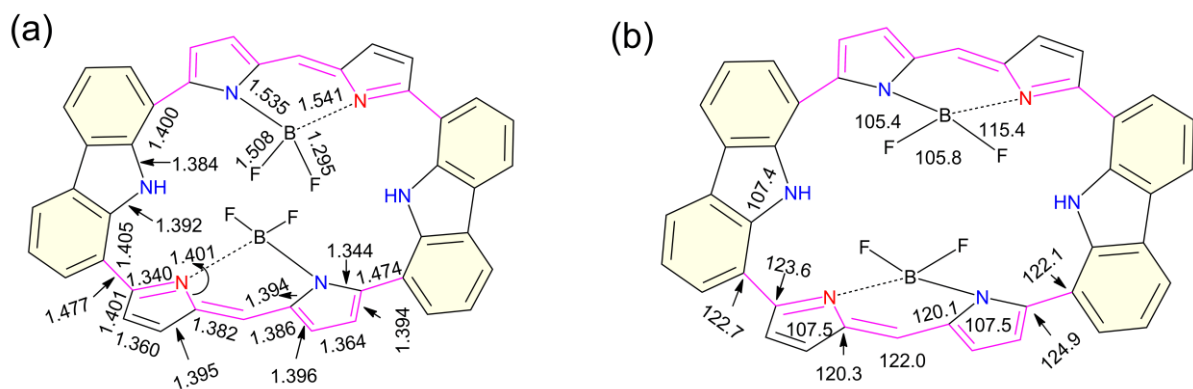


Figure S6-2: (a) Bond lengths (\AA) and (b) bond angles ($^\circ$) of **2a**.

Table S6-1. Crystal data and structure refinement for **2**

Empirical formula	C ₇₀ H ₅₆ N ₆ F ₁₀
Formula weight	1171.20
Temperature/K	293.15
Crystal system	triclinic
Space group	P-1
a/Å	12.713(7)
b/Å	16.637(8)
c/Å	17.026(13)
α/°	94.06(4)
β/°	105.49(5)
γ/°	104.83(3)
Volume/Å ³	3317(4)
Z	2
ρ _{calc} g/cm ³	1.173
μ/mm ⁻¹	0.089
F(000)	1216.0
Crystal size/mm ³	0.2 × 0.15 × 0.02
Radiation	MoKα ($\lambda = 0.71073$)
2Θ range for data collection/°	3.846 to 49.992
Index ranges	-15 ≤ h ≤ 15, -19 ≤ k ≤ 19, -20 ≤ l ≤ 20
Reflections collected	94101
Independent reflections	9677 [$R_{\text{int}} = 0.1481$, $R_{\text{sigma}} = 0.1103$]
Data/restraints/parameters	9677/0/803
Goodness-of-fit on F ²	1.013
Final R indexes [I>=2σ (I)]	$R_1 = 0.0735$, $wR_2 = 0.1934$
Final R indexes [all data]	$R_1 = 0.2048$, $wR_2 = 0.2767$
Largest diff. peak/hole / eÅ ⁻³	0.39/-0.27
CCDC Number	2064001

Table S6-2. Crystal data and structure refinement for **2a**

Empirical formula	C ₇₀ H ₅₄ B ₂ F ₁₄ N ₆
Formula weight	1266.81
Temperature/K	296(2)
Crystal system	monoclinic
Space group	I2/a
a/Å	17.626(3)
b/Å	16.380(3)
c/Å	24.678(6)
α/°	90
β/°	95.021(5)
γ/°	90
Volume/Å ³	7098(3)
Z	4
ρ _{calcg} /cm ³	1.186
μ/mm ⁻¹	0.095
F(000)	2608.0
Crystal size/mm ³	0.240 × 0.200 × 0.200
Radiation	MoKα ($\lambda = 0.71073$)
2Θ range for data collection/°	4.604 to 49.994
Index ranges	-20 ≤ h ≤ 20, -19 ≤ k ≤ 19, -29 ≤ l ≤ 29
Reflections collected	37794
Independent reflections	6243 [R _{int} = 0.0576, R _{sigma} = 0.0460]
Data/restraints/parameters	6243/0/451
Goodness-of-fit on F ²	1.035
Final R indexes [I>=2σ (I)]	R ₁ = 0.0630, wR ₂ = 0.1631
Final R indexes [all data]	R ₁ = 0.1175, wR ₂ = 0.2088
Largest diff. peak/hole / e Å ⁻³	0.27/-0.23
CCDC Number	2059517

S7. Supramolecular Interactions

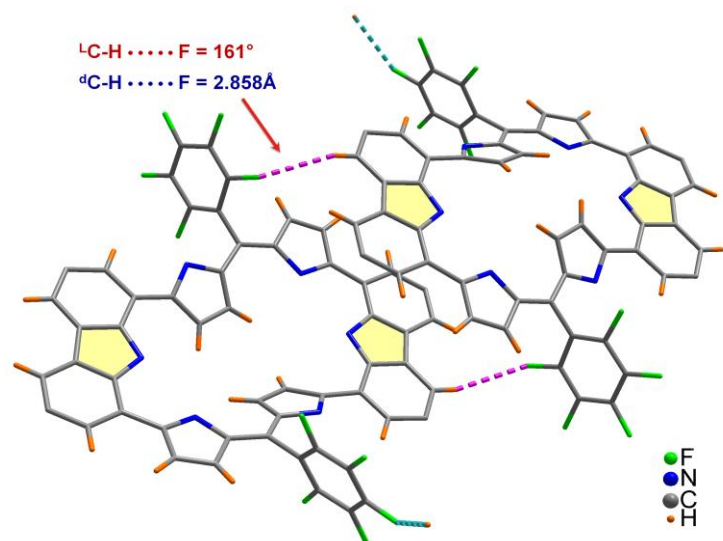


Figure S7-1: Secondary interactions in **2**.

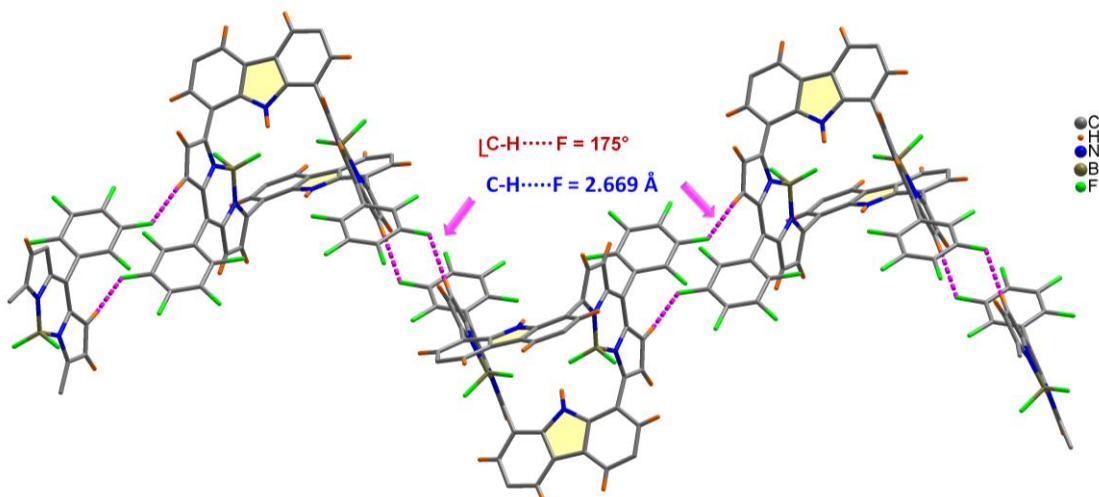


Figure S7-2: Secondary interactions in **2a**. View along X-axis

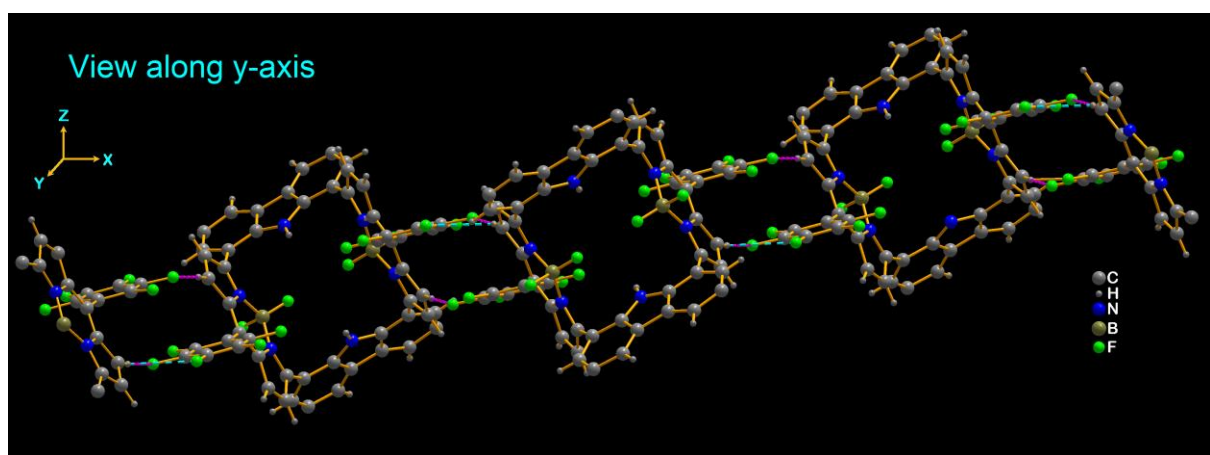


Figure S7-3: Secondary interactions in **2a**. View along Y-axis

S8. Cyclic Voltammetry

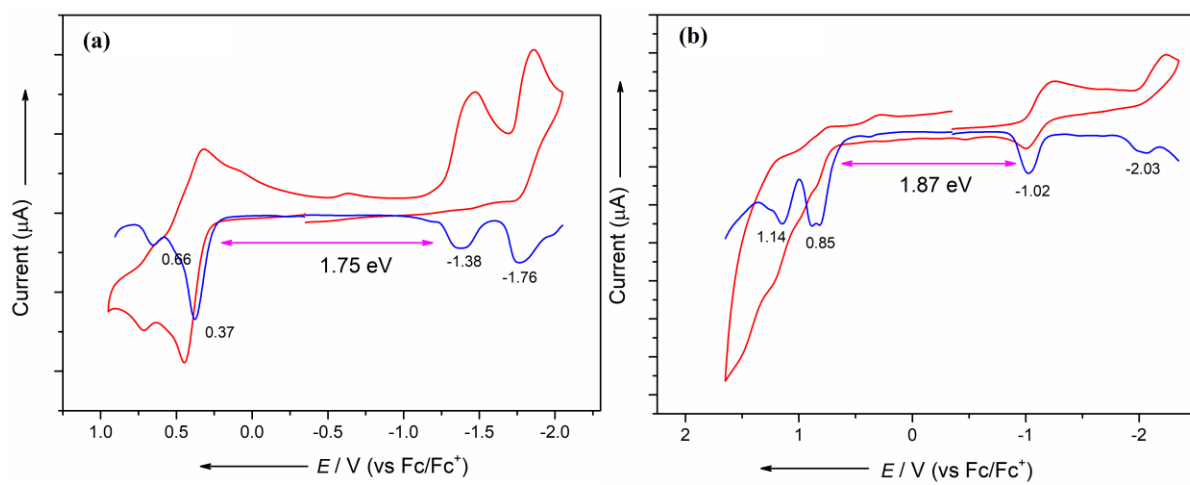


Figure S8-1. Cyclic Voltammetry and DPV for (a) **2** (b) **2a** recorded in CH_3CN .

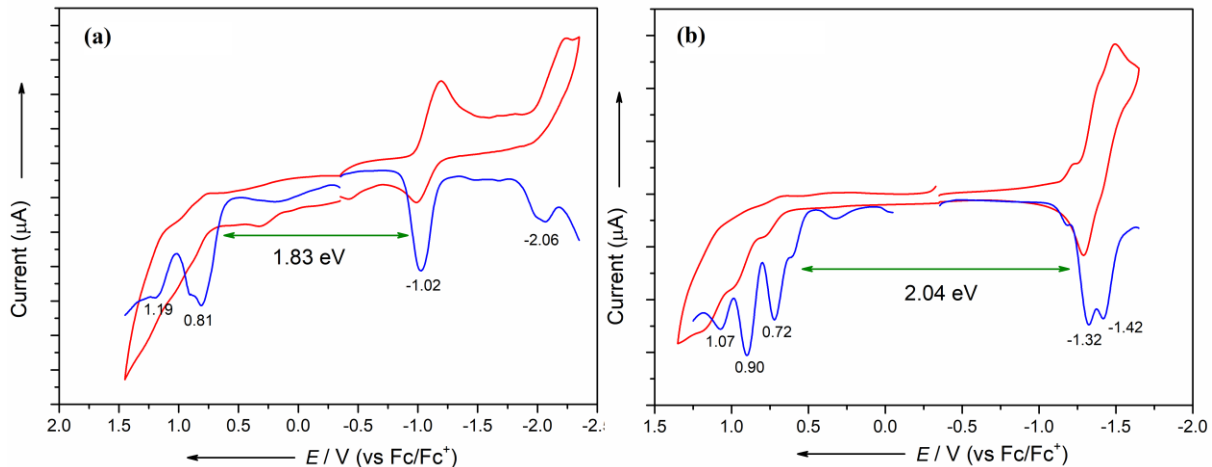


Figure S8-2. Cyclic Voltammetry and DPV for (a) **3** (b) **3a** recorded in CH_3CN .

S9. Photophysical Studies

S9.1 Dipole-dipole interaction model: calculating the excitonic coupling strength

The absorption spectra for free bases show Q-like bands in the visible region which are similar to those reported for Zn complexes of carbazole containing porphyrin oligomers.^[S11] Further, for the *bis*-BODIPY derivatives, similar bands are retained which show sub-bands due to excitonic coupling between the BODIPY units^[S12]. A large Stokes ($\Delta\nu_{\max}$) shift of 6029 cm⁻¹ for **2a** was calculated, which is two-fold higher than previously reported multiply N-confused calix-BODIPYs, whereas for **3a** it was estimated to be 4282 cm⁻¹.

The experimental absorption spectrum is fitted as a sum of Gaussians. The difference between the two peaks, centered on 14,880 cm⁻¹ (690 nm) and 19,663 cm⁻¹ (508 nm) is 4,782 cm⁻¹ for **2a** and this difference is 3,270 cm⁻¹, for bands centered on 17,938 cm⁻¹ (557 nm) and 21,208 cm⁻¹ (471 nm), for **3a**. Therefore, these two bands are assigned as pure electronic transition ($0 \leftarrow 0$) from ground state (S_0) to the Q-like bands, denoted as Q_1 (forbidden/weakly allowed for **2a/3a**) and Q_2 (allowed for both **2a/3a**) whereas the other bands, centered on 18,167 cm⁻¹ (550 nm) and 19,379 cm⁻¹ (516 nm) for **2a** and **3a**, respectively, are assigned as vibrational features (allowed for both **2a** and **3a**) of Q_1 , denoted as Q_1^* . The amplitude of transition is less and the splitting of bands is more in **2a** as compared to **3a**, suggesting stronger coupling in **2a** due to separation between the transition dipoles.

The strength of excitonic coupling, defined as coupling energies (cm⁻¹) due to interaction between the transition dipoles 1 and 2, can be calculated (in SI units) using^[S12]

$$\nu_{12} = \frac{5.04 f_L^2 \overrightarrow{|\mu_1|} \overrightarrow{|\mu_2|} \kappa_{12}}{(4\pi\epsilon_0) \epsilon_r R_{TS}^3}$$

where f_L is the Lorentz field correction factor given by $f_L^2 = \frac{(\epsilon_r + 2)}{3}$, $\overrightarrow{\mu_1}$ and $\overrightarrow{\mu_2}$ are the transition dipoles for the BODIPY monomer, ϵ_r is the relative permittivity or the dielectric constant, ϵ_0 is the vacuum permittivity, R_{TS} is the center-to-center distance (taken to be the C_{meso}-C_{meso} distance), κ_{12} is the orientation factor. Using the value of R_{TS} from DFT optimized geometry as 0.77 nm for **2a** (0.7081 nm from crystal structure) and 0.76 nm for **3a**, $\overrightarrow{\mu_1} = \overrightarrow{\mu_2} = 5.35$ Debye, $\epsilon_r = 4.81$ (in chloroform), $\kappa_{12} = 1$. By considering the parallel orientation between the dipoles^[S13] (ignoring the small angle between the dipole and the molecular axis),^[S14] a 2 x 2 square matrix was obtained by diagonalization to give the

coupling energies as $\pm 1697\text{ cm}^{-1}$ and $\pm 1765\text{ cm}^{-1}$ (or, equivalently, energy gaps between split energy levels as 3394 cm^{-1} and 3530 cm^{-1}) for **2a** and **3a**, respectively.

This calculation estimates the order of magnitude of the coupling strength ($3,394\text{ cm}^{-1}$ and $3,530\text{ cm}^{-1}$, compared with $4,782\text{ cm}^{-1}$ and $3,270\text{ cm}^{-1}$ from spectra). However, the experimentally observed trend is reversed which may be ascribed to the explicit electronic effect due to presence of electron withdrawing/donating substituents in **2a/3a** as well as fluxional behaviour (leading to a modification in the orientation factor, κ_{12}), which is not accounted in the simplified model.

S9.2. Steady-state measurements:

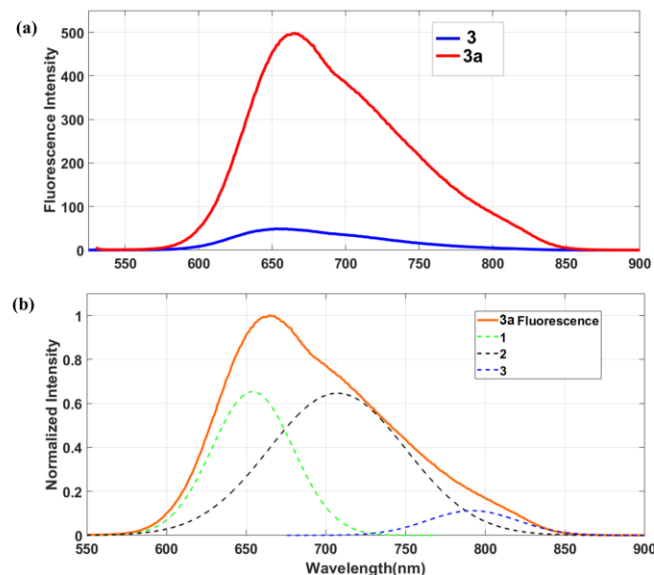


Figure S9-1: (a) Fluorescence (at excitation maxima) for **3** and **3a** showing an increase in fluorescence upon forming *bis*-BODIPY complex and (b) Fluorescence spectrum for **3a** deconvoluted as a sum of three Gaussians.

S9.3. Fluorescence lifetime measurements:

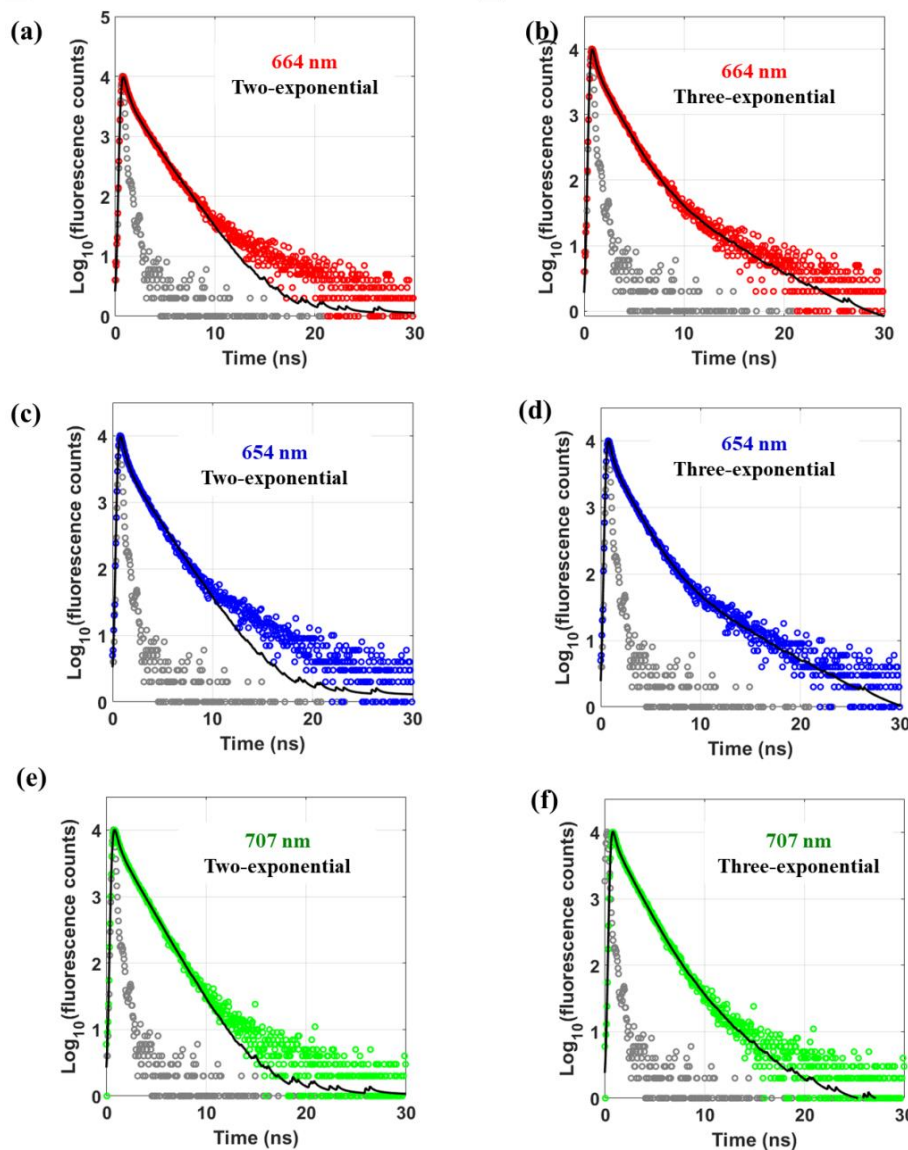


Figure S9-2: Fluorescence lifetime decay for compound **3a** at 510 nm excitation recorded at 664 nm (a-b); 654 nm (c-d) and 707 nm (e-f), respectively.

Fluorescence lifetime data for **3a** is recorded (510 nm excitation) at 664 nm (fluorescence maximum) and the maxima for Gaussians obtained after deconvolution (654 nm and 707 nm as shown in Figure S9-1). Lifetime data couldn't be recorded at 792 nm (third peak after Gaussian deconvolution) because the fluorescence counts were too low. Fluorescence lifetime data shows a sharp decay component of ~300 ps. Although the tail doesn't fit properly upon fitting the data as two exponentials, but three exponential fitting gives two similar lifetime components.

To account for the existence of multiple bands (centered on 654 nm, 707 nm and 792 nm) and their relative intensities in the steady-state fluorescence spectrum for **3a** (Figure S9-1b), we note that both GSB1*/ESA1* and ESA2b showed longer radiative decay components of 1.7 ns/2.4 ns (from $S_0 \leftarrow Q_1^*$) and 3.8 ns (from $S_0 \leftarrow Q_2$), respectively, compared with a shorter component of 465 ps for GSB1 (from $S_0 \leftarrow Q_1$). This is consistent with the fluorescence lifetime measurements which show radiative components apart from dominant non-radiative components (accounting for moderate fluorescence from these compounds). Thus, these bands are ascribed to fluorescence from Q_2 , Q_1^* and Q_1 , respectively (fluorescence lifetime measurements could not be performed for Q_1). Notably, the TA data do not show any SE band due to spectral overlap with ESA and higher probe intensities beyond 700 nm.

Similar multiple fluorescence might also be present in the free base **3** (Figure 3 in the main text) for which the spectral kinetics of the SE band is governed by non-radiative relaxation (see section S9.4), accounting for its feeble fluorescence (fluorescence lifetime measurements could not be performed for **3**).

S9.4. Femtosecond transient absorption measurements:

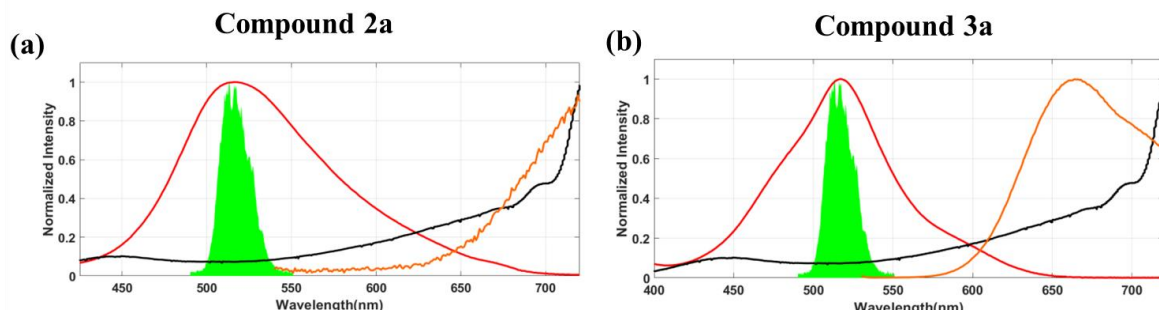


Figure S9-3: Absorption spectrum (red), fluorescence (orange), pump spectrum (green) and white light (black) for (a) **2a** and (b) **3a**.

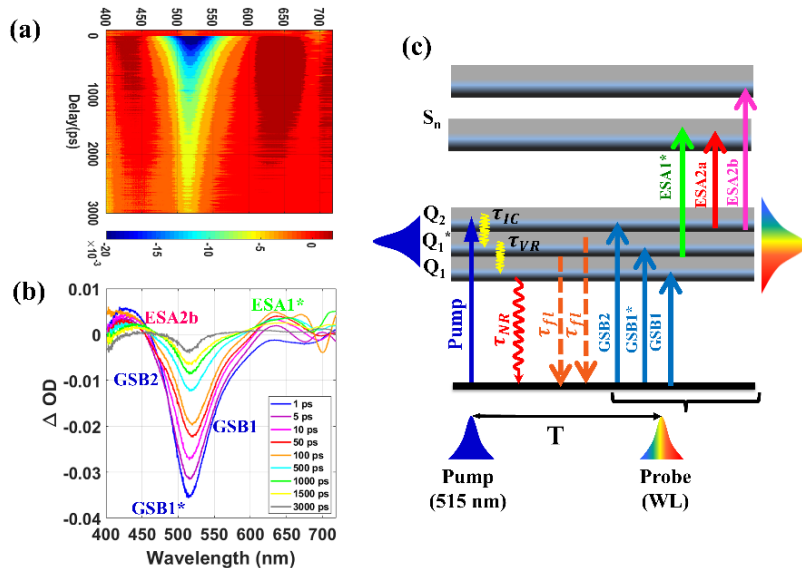
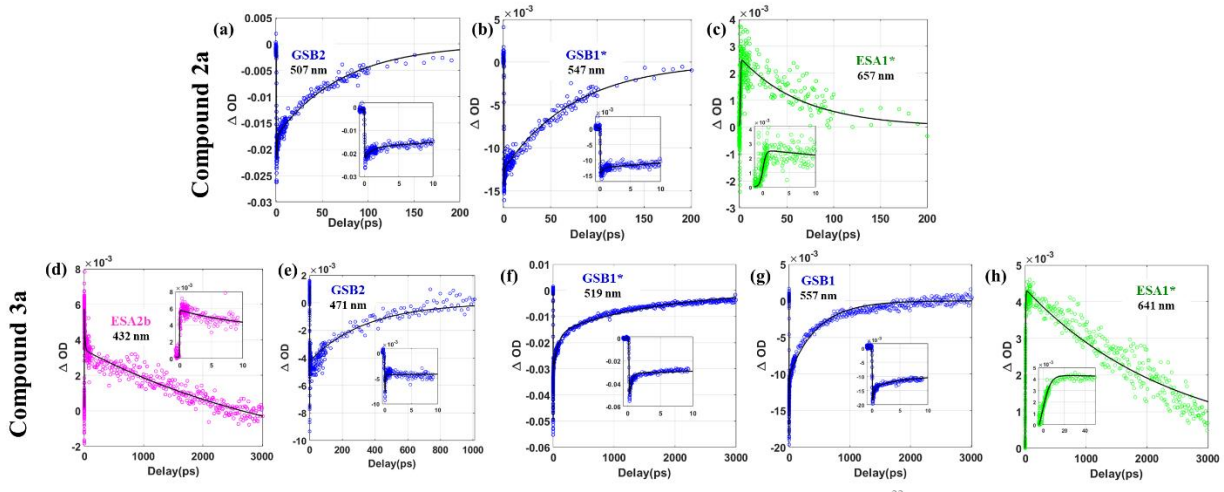


Figure S9-4: (a) Transient absorption contour (b) Spectral traces at various probe delays and (c) kinetic model depicting various states and photophysical processes for compound **3a**

Since all the bands are red-shifted in **3a** (compared with **2a**), ESA from Q₂ (ESA2a) most likely falls out of the spectral range probed and is quite weak due to strong probe intensity at this wavelength. However, another ESA band (ESA2b) at 432 nm was observed which was assigned to a transition from Q₂ to a higher lying state (since ESA2b rises with the pump pulse). ESA2b also shows a long decay component of 3.8 ns which is due to radiative relaxation. The 10 ps component of ESA2b and two decay components (60 fs and 341 ps) of GSB2 are difficult to assign due to their spectral overlap. GSB1* exhibits 330 fs and 79 ps decay components which account for intra-band VR within Q₁^{*} manifold (as well as inter-band IC from Q₁^{*} to Q₁) and non-radiative relaxation from Q₁^{*}/Q₁ to S₀. In addition, GSB1* shows a radiative decay component of 1.7 ns. In contrast, apart from a similar 230 fs component, GSB1 exhibits very different time constants of 4 ps and 465 ps which is most likely due to spectral overlap with a broad ESA band. Similarly, the ESA band (ESA1*) at 641 nm exhibits a 4 ps component and a radiative component of 2.4 ns time constant like GSB1*.



33

Figure S9-5: Kinetic traces for **2a** (a-c) and for **3a** (d-h).

The transient absorption measurements for compound **2** show two GSB and two ESA bands. GSB2 band corresponds to Q₂ and a weak GSB1 to Q₁. GSB1 and ESA1 are spectrally overlapping. The kinetic traces for GSB2, ESA1 and ESA2 are shown in Figure S9-6. The kinetic trace for GSB1 is not shown since it is dominated by ESA1 at later times and the timescales thus extracted won't be very accurate. GSB2 decay timescales of 70 fs, 5 ps and 75 ps are assigned to vibrational relaxation, internal conversion and non-radiative decay to S₀, respectively. ESA1 band broadens at longer probe delays as ground state bleach is recovered and the spectral overlap is reduced (i.e. the complete spectrum of ESA1 is not observed at early times since it is masked by GSB signal). ESA1 also shifts to bluer wavelengths at a later time (as evident from the spectral traces in Figure S9-6). A timescale of 470 fs for ESA1 corresponds to very fast vibrational relaxation and hence blue shift. Decay timescales of 100 ps for both ESA1 and ESA2 are due to non-radiative relaxation to ground state.

In case of compound **3**, GSB and SE (as evident from the steady-state fluorescence spectrum) and a weak ESA1 are observed. In addition to these, a blue shifted ESA band denoted as ESA1b (which corresponds to the population getting excited to a higher excited state) is also observed showing a rise time of 200 fs. ESAs showing rise time are assigned to Q₁ band involving relaxation from Q₂ to Q₁. 100 ps decay components are due to non-radiative relaxation to ground state. The kinetic traces are shown in Figure S9-7. ESA2 band in this case is quite shifted and is weak due to high probe intensity.

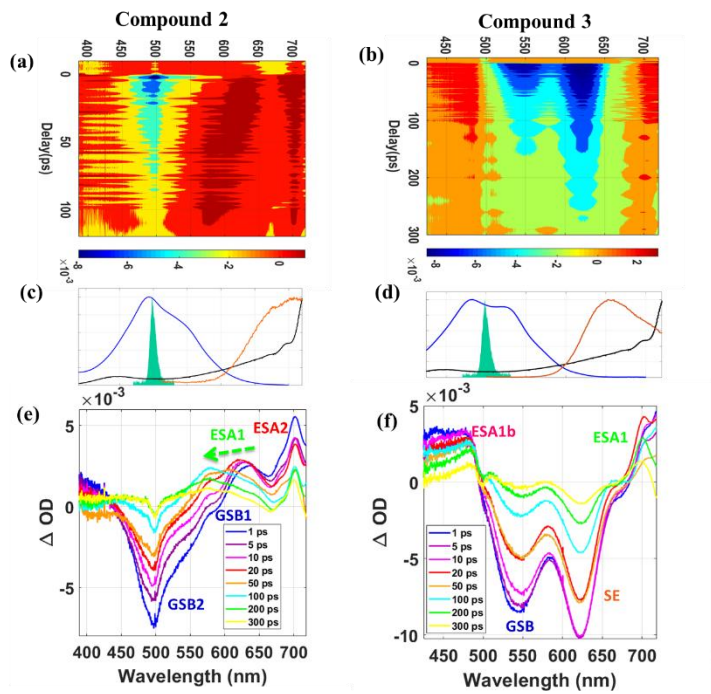


Figure S9-6: Top panel: Transient absorption contours for compounds (a) 2 and (b) 3. Middle panel: Plots for spectra in which blue corresponds to absorption spectrum, green to pump spectrum, orange to fluorescence and black to white light probe for (c) 2 and (d) 3. Bottom panel: Spectral traces at various probe delays for (e) 2 and (f) 3.

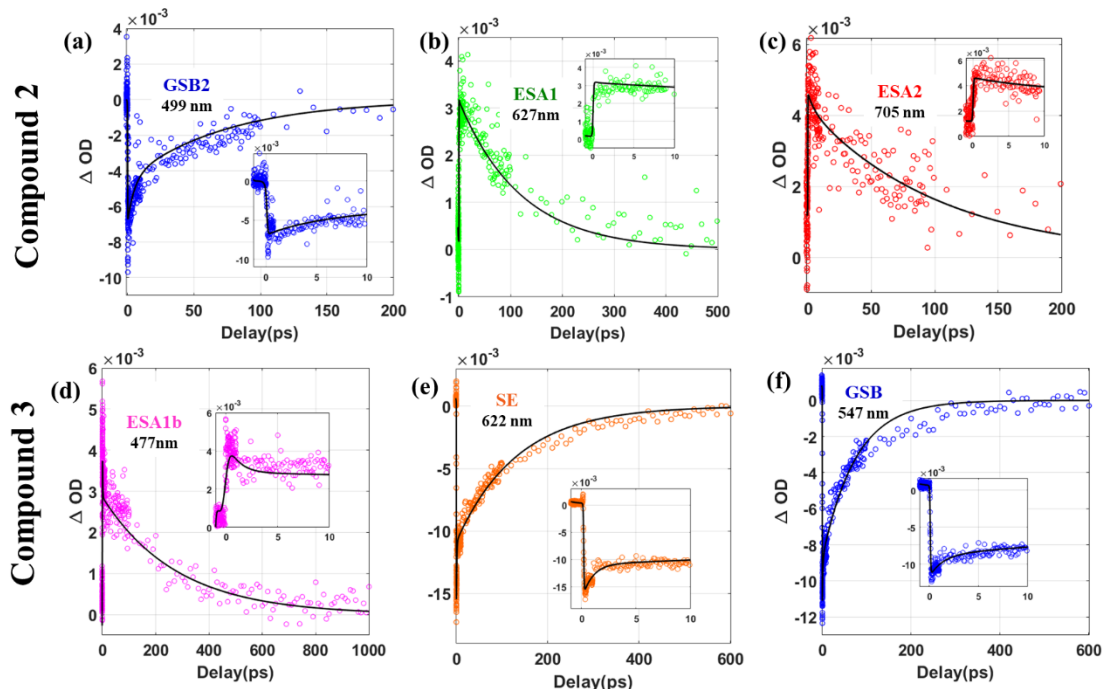


Figure S9-7: Kinetic traces for 2 (a-c) and for 3 (d-f).

Table S9-1: Table for photophysical properties of compounds in CHCl₃

Compound	λ_{abs} (nm)	λ_{em} (nm)
2	492	708
2a	516	749
3	483	653
3a	517	664

Table S9-2: Fitting data for kinetic traces for **2a**.

λ (nm)	A_1	A_2	τ_{rise} (ps)	a_1	τ_1 (ps)	a_2	τ_2 (ps)	a_3	τ_3 (ps)	R^2
507 (GSB2)	3.07×10^{-3}	0.075	0.02	0.06	0.94	0.23	72.18	---	---	0.97
547 (GSB1*)	3.44×10^{-4}	0.013	0.02	0.18	0.40	0.89	76.56	---	---	0.98
657 (ESA1*)	3.25×10^{-5}	0.004	0.31	0.56	67.25	---	---	---	---	0.62

Table S9-3: Fitting data for kinetic traces for **3a**.

λ (nm)	A_1	A_2	τ_{rise} (ps)	a_1	τ_1 (ps)	a_2	τ_2 (ps)	a_3	τ_3 (ps)	R^2
432 (ESA2b)	1.12×10^{-4}	0.004	0.02	0.61	10.73	1.79	3863	---	---	0.93
471 (GSB2)	-3.17×10^{-10}	0.011	0.02	0.87	0.06	0.37	341.70	---	---	0.90
519 (GSB1*)	9.55×10^{-6}	0.015	0.02	1.60	0.33	0.90	79.03	1.05	1689	0.99
557 (GSB1)	-3.97×10^{-5}	0.022	0.02	0.31	0.23	0.17	4.43	0.46	465.40	0.99
641 (ESA1*)	-2.1×10^{-3}	0.005	3.83	0.78	2441	---	---	---	---	0.95

Table S9-4: Fitting data for kinetic traces for **2**.

λ (nm)	A_1	A_2	τ_{rise} (ps)	a_1	τ_1 (ps)	a_2	τ_2 (ps)	a_3	τ_3 (ps)	R^2
499 (GSB2)	-5.34×10^{-12}	0.003	0.05	0.54	0.07	0.77	5.31	1.44	74.86	0.85
627 (ESA1)	1.66×10^{-5}	3.3×10^{-4}	0.04	0.24	0.47	9.55	119.4	---	---	0.84
705 (ESA2)	1.24×10^{-4}	4.8×10^{-4}	0.05	0.84	5.74	8.64	105.8	---	---	0.74

Table S9-5: Fitting data for kinetic traces for **3**.

λ (nm)	A_1	A_2	τ_{rise} (ps)	a_1	τ_1 (ps)	a_2	τ_2 (ps)	a_3	τ_3 (ps)	R^2
477 (ESA1b)	3.86×10^{-6}	4.6×10^{-4}	0.20	0.26	0.12	3.96	1.12	6.15	279	0.79
547 (GSB)	1.0×10^{-3}	0.018	0.03	0.15	1.37	0.48	74.93	---	---	0.98
622 (SE)	3.6×10^{-4}	0.016	0.02	0.32	0.95	0.64	132.30	---	---	0.98

Table S9-6: Fitting data for fluorescence lifetimes for **3a** at 510 nm excitation.

Wavelength (nm)	Two-exponential						Three-exponential					
	a_1	τ_1 (ps)	a_2	τ_2 (ns)	χ^2	a_1	τ_1 (ps)	a_2	τ_2 (ns)	a_3	τ_3 (ns)	χ^2
	0.74	332	0.26	1.78	2.09	0.70	246	0.29	1.47	0.01	4.74	0.85
664	0.76	366	0.24	1.89	2.69	0.71	252	0.28	1.48	0.01	4.99	0.96
707	0.65	292	0.35	1.64	1.33	0.63	220	0.35	1.43	0.02	3.17	0.92

S10. Computational Studies

Position	NICS (ppm)	Position	NICS (ppm)
1	+0.33	10	-10.05
2	+2.24	11	-1.02
3	-1.02	12	-10.21
4	-10.20	13	+1.05
5	+1.07	14	-1.81
6	-1.83	15	+1.26
7	+1.29	16	-9.30
8	-9.34	17	-9.39
9	-9.71	18	-10.23

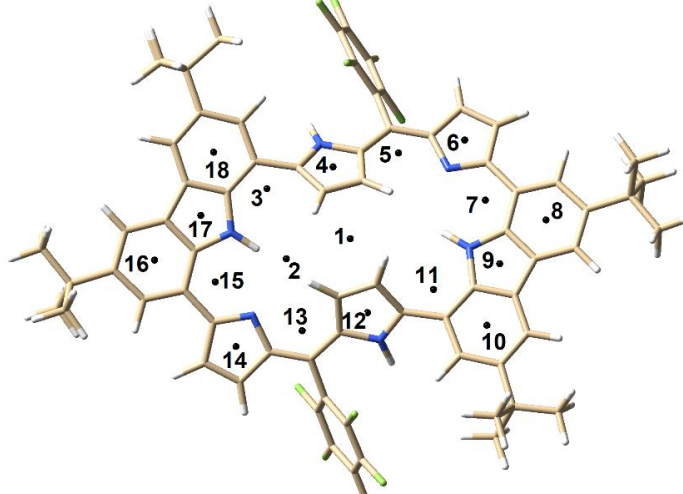


Figure S10-1. NICS(0) values at various positions of **2**.

Position	NICS (ppm)	Position	NICS (ppm)
1	+0.38	10	-1.61
2	-0.14	11	-9.10
3	-8.73	12	-0.26
4	-0.39	13	-6.08
5	-5.62	14	-0.27
6	-0.89	15	-7.68
7	-7.70	16	-6.91
8	-7.59	17	-8.81
9	-9.18		

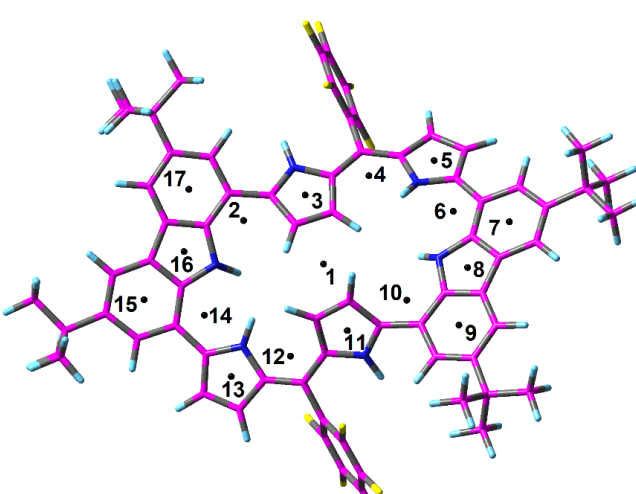
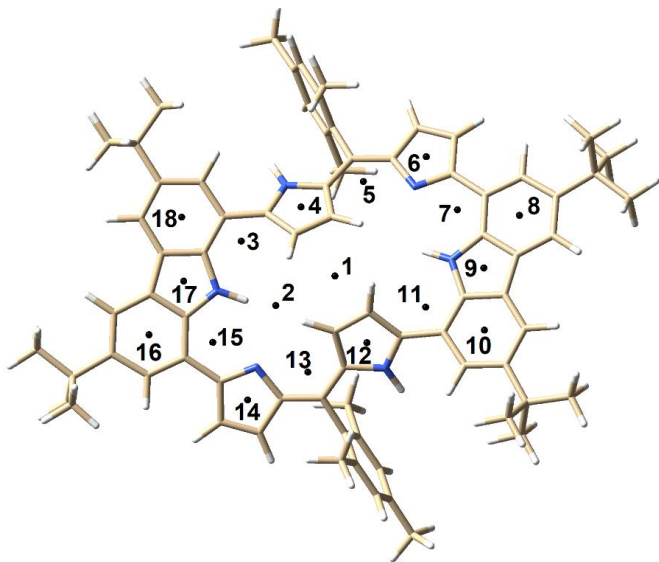
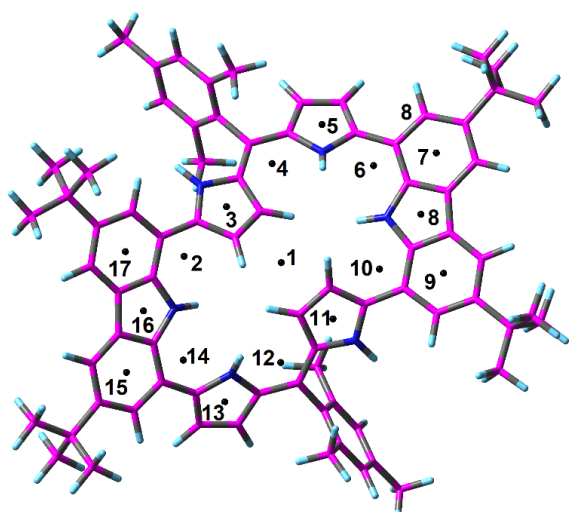


Figure S10-2. NICS(0) values at various positions of **2.2H+**.



Position	NICS (ppm)	Position	NICS (ppm)
1	-0.02	10	-10.13
2	+2.26	11	-0.76
3	-0.79	12	-10.14
4	-10.13	13	+1.35
5	+1.36	14	-2.31
6	-2.34	15	+1.11
7	+1.14	16	-9.54
8	-9.59	17	-9.46
9	-9.80	18	-10.31

Figure S10-3. NICS(0) values at various positions of **3**.



Position	NICS (ppm)	Position	NICS (ppm)
1	-0.90	10	-3.63
2	-3.55	11	-9.50
3	-9.53	12	-3.93
4	-3.97	13	-10.11
5	-10.05	14	-3.58
6	-3.64	15	-11.03
7	-10.95	16	-6.13
8	-5.86	17	-12.05
9	-11.89		

Figure S10-4. NICS(0) values at various positions of **3.2H⁺**

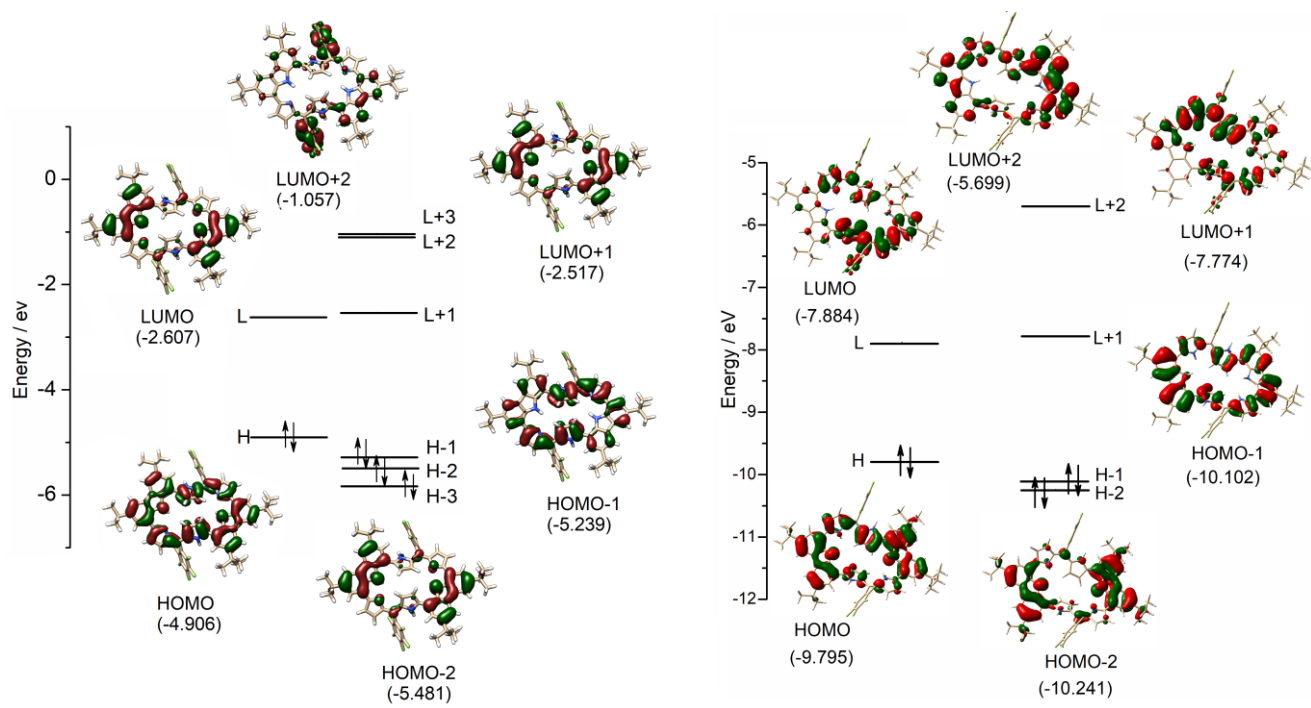


Figure S10-5. Selected frontier MOs of **2** (left) and **2•2H⁺** (right) at the B3LYP/6-31G(d,p) level.

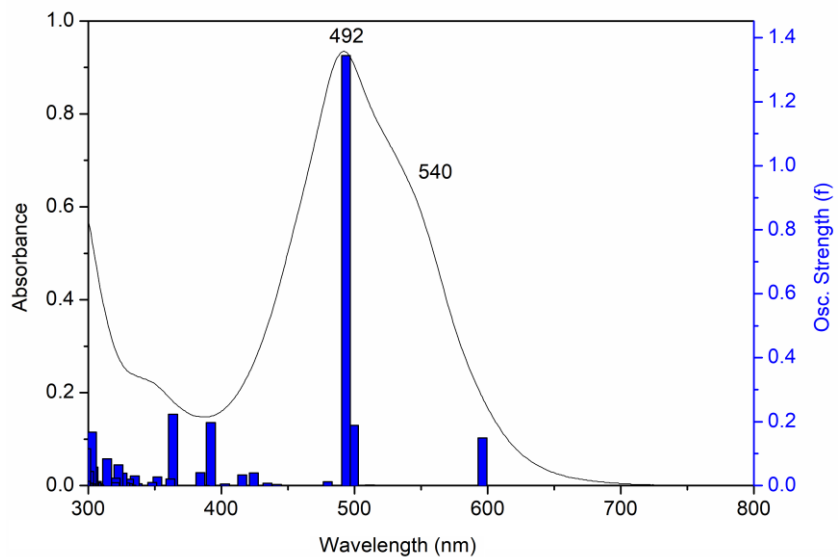


Figure S10-6. Steady-state absorption spectra (black lines) of **2** recorded in CH₂Cl₂ along with the theoretical vertical excitation energies (blue bar) obtained from TD-DFT calculations carried out at the B3LYP/6-31G(d,p) level.

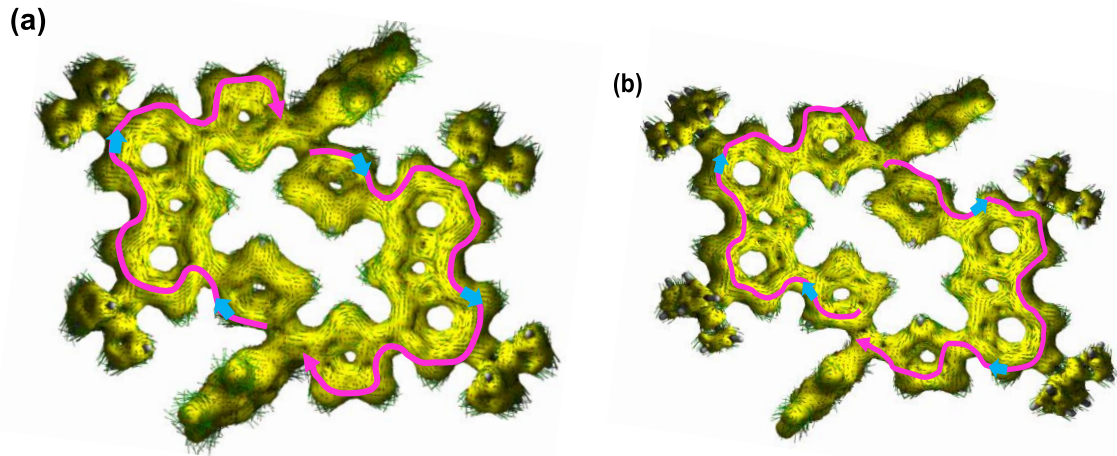


Figure S10-7. ACID plots for (a) **2** and (b) **2•2H⁺**. Vectors moving clock-wise direction is indicated by the appropriate arrows.

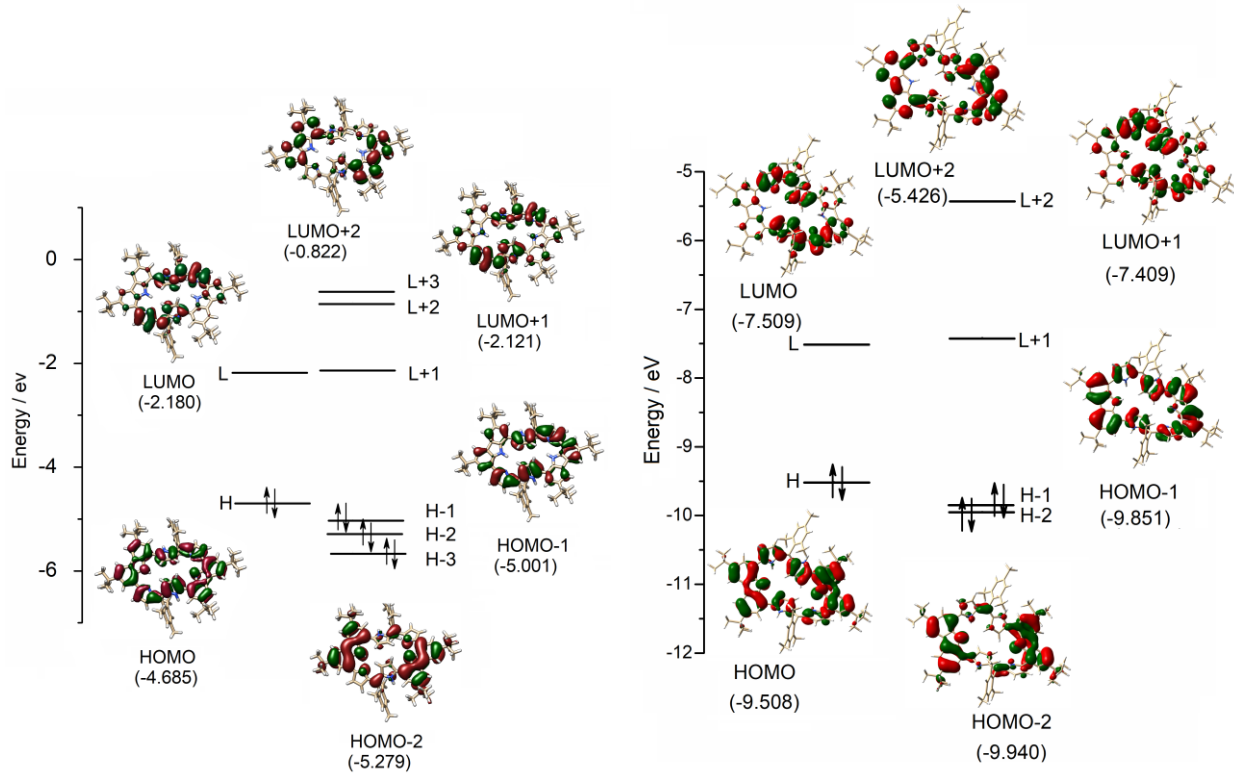


Figure S10-8. Selected frontier MOs of **3** (left) and **3•2H⁺** (right) at the B3LYP/6-31G(d,p) level.

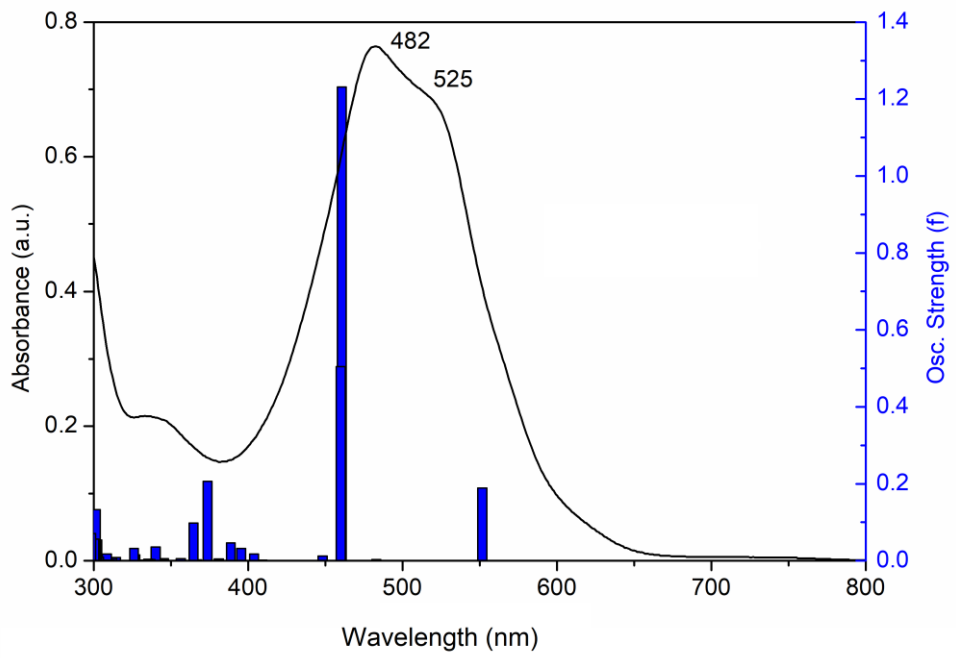


Figure S10-9. Steady-state absorption spectra (black lines) of **3** recorded in CH_2Cl_2 along with the theoretical vertical excitation energies (blue bar) obtained from TD-DFT calculations carried out at the B3LYP/6-31G(d,p) level

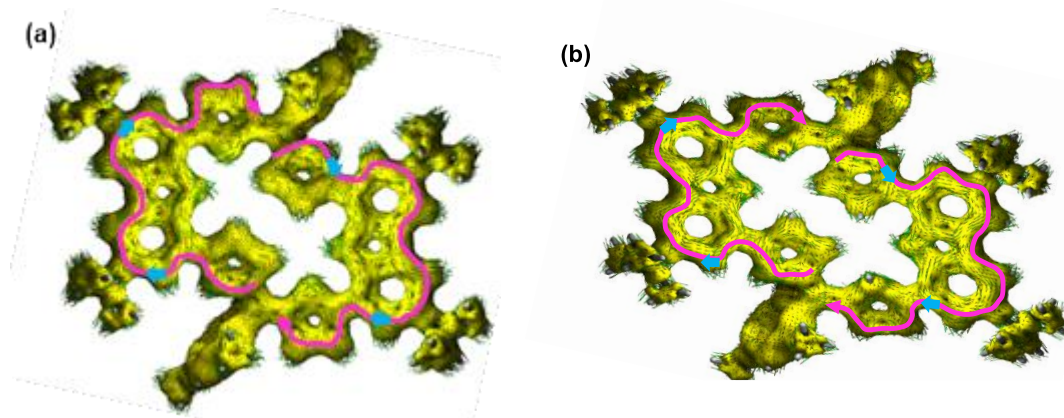


Figure S10-10. ACID plots for (a) **3** and (b) **3•2H⁺**. Vectors moving clock-wise direction is indicated by the appropriate arrows.

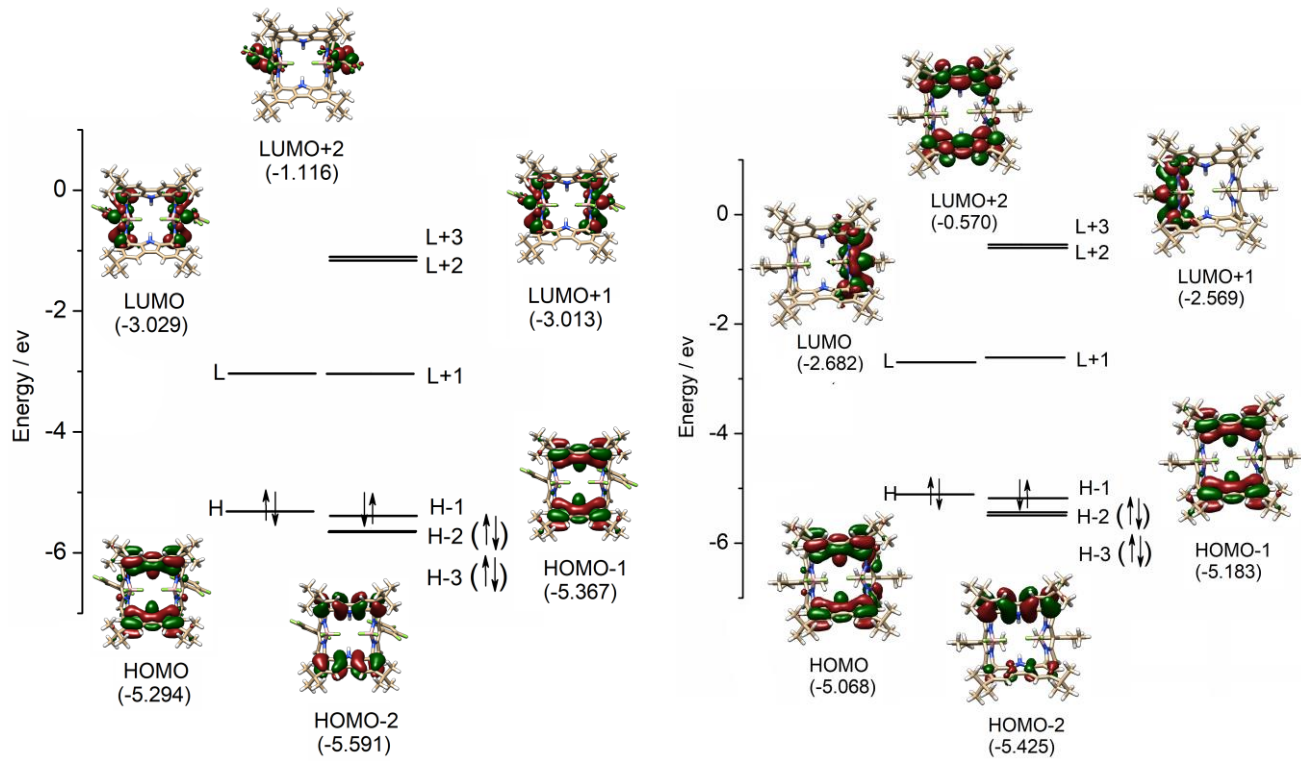


Figure S10-11. Selected frontier MOs of **2a** at the B3LYP/6-31G(d,p) level.

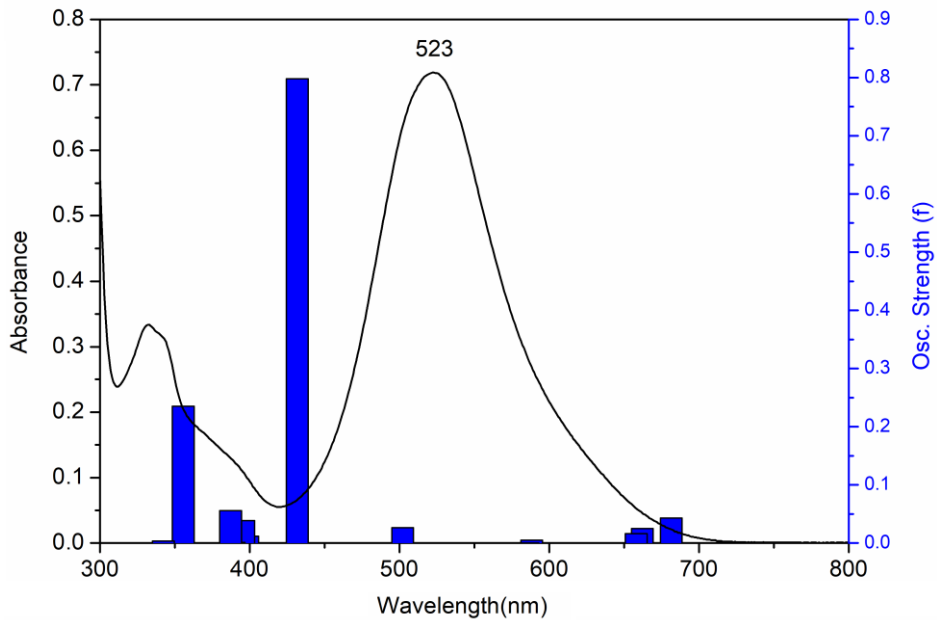


Figure S10-12. Steady-state absorption spectra (black lines) of **2a** recorded in CH_2Cl_2 along with the theoretical vertical excitation energies (blue bar) obtained from TD-DFT calculations carried out at the B3LYP/6-31G(d,p) level.

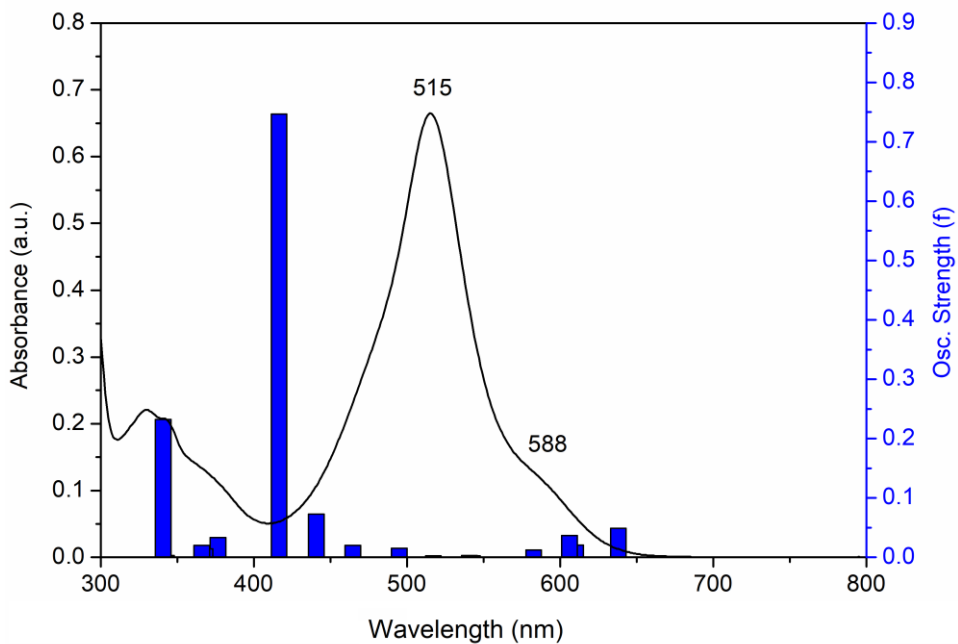


Figure S10-13. Steady-state absorption spectra (black lines) of **3a** recorded in CH_2Cl_2 along with the theoretical vertical excitation energies (blue bar) obtained from TD-DFT calculations carried out at the B3LYP/6-31G(d,p) level.

Table S10-1. Open-shell diradical character calculations were carried out at **DFT UCAM-B3LYP/6-31G (d, p)** basis set and the Closed-shell calculations were carried out at **DFT RB3LYP/6-31G (d, p)**.

Molecule	γ_0	$E_{\text{HOMO}} - E_{\text{LUMO}}$ (eV)	E_{HOMO} (eV)	E_{LUMO} (eV)
2	0	-2.2983	-4.9057	-2.6074
3	0	-2.5048	-4.6852	-2.1804
2a	0	-2.2645	-5.2939	-3.0294
3a	0	-2.3867	-5.0683	-2.6816

Table S10-2. Calculated singlet excited energies and states of **2** by the time-dependent DFT calculation at B3LYP/6-31g(d,p)

Energy (cm^{-1})	Wavelength (nm)	Osc. Strength	Major contribs
15150.42304	660.04758	4E-4	HOMO->LUMO (98%)
16777.25456	596.04508	0.1492	H-1->LUMO (20%), HOMO->L+1 (79%)
19547.78816	511.56683	0.0015	H-1->L+1 (95%)
20016.39952	499.59035	0.1886	H-2->LUMO (94%)
20261.59376	493.54459	1.3451	H-1->LUMO (73%), HOMO->L+1 (19%)
20839.09072	479.86739	0.0123	H-2->L+1 (95%)
22636.91296	441.75635	0.0038	H-3->LUMO (83%)
23011.96336	434.55658	0.0075	H-4->LUMO (61%), H-3->L+1 (31%)
23567.6832	424.30984	0.0393	H-4->LUMO (25%), H-4->L+1 (15%), H-3->L+1 (51%)

24058.07168	415.66091	0.0331	H-4->LUMO (10%), H-4->L+1 (74%)
24836.40208	402.63481	0.0054	H-5->LUMO (84%)
25511.4928	391.9802	0.1977	H-7->LUMO (10%), H-5->L+1 (72%)
25819.59872	387.30269	3E-4	H-7->L+1 (23%), H-6->LUMO (60%)
26027.6912	384.20619	0.0403	H-7->LUMO (40%), H-6->L+1 (33%), H-5->L+1 (19%)
27494.82384	363.70482	0.223	HOMO->L+2 (84%)
27652.10304	361.63615	0.0205	HOMO->L+3 (65%), HOMO->L+4 (14%)
28216.69504	354.40012	6E-4	H-7->L+1 (12%), HOMO->L+3 (12%), HOMO->L+4 (59%)
28418.33504	351.8855	0.0273	H-7->LUMO (38%), H-6->L+1 (51%)
28728.05408	348.0918	0.0098	H-7->L+1 (46%), H-6->LUMO (25%)
29660.43744	337.14944	0.0031	H-16->LUMO (10%), H-16->L+1 (11%), H-15->LUMO (22%), H-9->LUMO (18%), HOMO->L+5 (10%)
29674.95552	336.9845	0.0062	H-15->LUMO (12%), H-15->L+1 (14%), HOMO->L+5 (28%)
29859.65776	334.90002	0.0305	H-16->LUMO (13%), H-15->L+1 (16%), H-12->LUMO (10%), HOMO->L+5 (39%)
30096.7864	332.26139	1E-3	HOMO->L+6 (84%)
30262.93776	330.43719	0.0195	HOMO->L+7 (65%)
30323.42976	329.778	0.0063	H-8->LUMO (47%), H-1->L+2 (18%)
30506.51888	327.79879	0.0083	H-8->LUMO (17%), H-1->L+2 (61%)
30697.6736	325.75758	0.0389	H-8->L+1 (49%), H-1->L+3 (22%)
30990.45488	322.68	0.0643	H-8->L+1 (12%), H-1->L+3 (46%), H-1->L+4 (17%)
31190.48176	320.61063	0.0226	H-8->L+1 (15%), H-1->L+3 (12%), H-1->L+4 (59%)
31267.10496	319.82494	0.009	H-15->LUMO (11%), H-9->LUMO (62%), H-8->LUMO (10%)
31836.53632	314.10452	0.0837	H-9->L+1 (67%)
32450.32848	308.16329	0.0015	H-2->L+2 (78%)
32560.02064	307.12511	0.0061	H-2->L+3 (60%), H-2->L+4 (18%)
32643.90288	306.33592	0.0128	H-14->LUMO (37%), H-14->L+1 (14%)
32668.90624	306.10146	0.0094	H-13->LUMO (31%), H-13->L+1 (21%), H-1->L+5 (14%)
32819.73296	304.69474	0.0128	H-13->LUMO (16%), H-1->L+5 (51%)
32918.93984	303.77649	0.0579	H-14->LUMO (18%), H-11->LUMO (11%), H-10->LUMO (31%), HOMO->L+8 (13%)
33035.08448	302.70847	0.1669	H-10->LUMO (21%), H-2->L+3 (13%), H-2->L+4 (18%), HOMO->L+8 (30%)
33087.51088	302.22884	0.0051	H-1->L+6 (67%), H-1->L+7 (12%)
33258.5016	300.675	0.0447	H-2->L+3 (12%), H-2->L+4 (52%), HOMO->L+8 (22%)
33331.092	300.02017	0.0076	H-1->L+6 (13%), H-1->L+7 (57%)
33513.37456	298.38833	0.1154	H-16->LUMO (13%), H-12->LUMO (41%), H-11->LUMO (23%)
33572.25344	297.86502	0.014	H-11->L+1 (17%), H-10->L+1 (45%)
33718.2408	296.57538	0.0935	H-11->LUMO (35%), H-10->LUMO (18%), HOMO->L+8 (14%)
33988.4384	294.21769	0.0036	H-11->L+1 (46%), HOMO->L+9 (11%)

Table S10-3. Calculated singlet excited energies and states of **2a** by the time-dependent DFT calculation at B3LYP/6-31g(d,p)

Energy (cm ⁻¹)	Wavelength (nm)	Osc. Strength	Major contribs
14569.69984	686.35594	4E-4	HOMO->L+1 (99%)
14672.93952	681.5267	0.0432	HOMO->LUMO (96%)
15102.02944	662.16266	0.0248	H-1->LUMO (99%)
15198.01008	657.98088	0.0163	H-1->L+1 (98%)
16949.05184	590.00351	3E-4	H-2->LUMO (99%)
16999.86512	588.23996	0.0054	H-3->LUMO (100%)
17071.64896	585.7665	1E-4	H-2->L+1 (100%)
17112.78352	584.35847	0	H-3->L+1 (100%)
19736.5232	506.67485	0	H-5->L+1 (19%), H-4->LUMO (80%)
19920.41888	501.99748	0.0263	H-5->LUMO (36%), H-4->L+1 (63%)
21926.3336	456.0726	7E-4	H-5->L+1 (78%), H-4->LUMO (17%)
23160.3704	431.77202	0.7977	H-5->LUMO (58%), H-4->L+1 (32%)
25089.66192	398.57054	0.0119	H-6->LUMO (98%)
25246.13456	396.10024	0.0386	H-6->L+1 (98%)
25665.54576	389.62741	0.0012	H-7->LUMO (92%)
25829.27744	387.15756	0.0559	H-7->L+1 (86%)
27929.55968	358.0436	0	H-9->LUMO (44%), H-8->L+1 (46%)
28123.13408	355.57915	0.2352	H-9->L+1 (36%), H-8->LUMO (48%)
29207.15072	342.38191	0.0014	H-11->LUMO (45%), H-10->L+1 (42%)
29216.02288	342.27794	0.0036	H-11->L+1 (39%), H-10->LUMO (48%)

Table S10-4. Calculated singlet excited energies and states of **3** by the time-dependent DFT calculation at B3LYP/6-31g(d,p)

Energy (cm ⁻¹)	Wavelength (nm)	Osc. Strength	Major contribs
16701.43792	598.75084	9E-4	HOMO->LUMO (98%)
18128.24256	551.62545	0.1889	H-1->LUMO (19%), HOMO->L+1 (80%)
20705.20176	482.97042	0.0039	H-1->L+1 (96%)
21710.98208	460.59639	1.2318	H-2->LUMO (22%), H-1->LUMO (61%), HOMO->L+1 (13%)
21742.43792	459.93002	0.505	H-2->LUMO (76%), H-1->LUMO (17%)
22309.4496	448.24055	0.0126	H-2->L+1 (96%)

24436.34832	409.22645	0.0013	H-3->LUMO (76%), H-3->L+1 (13%)
24772.68384	403.67043	0.0176	H-4->LUMO (47%), H-3->L+1 (38%)
25288.07568	395.4433	0.032	H-4->LUMO (31%), H-4->L+1 (23%), H-3->L+1 (36%)
25722.00496	388.77218	0.047	H-4->LUMO (15%), H-4->L+1 (67%), H-3->L+1 (10%)
26251.91488	380.92459	0.0052	H-5->LUMO (77%)
26758.43456	373.71394	0.2062	H-7->LUMO (15%), H-6->L+1 (12%), H-5->L+1 (63%)
27266.56736	366.7495	0.0032	H-7->L+1 (22%), H-6->LUMO (51%), H-5->LUMO (16%)
27428.68592	364.58181	0.0983	H-7->LUMO (36%), H-6->L+1 (32%), H-5->L+1 (26%)
28068.288	356.27396	0.0059	HOMO->L+2 (83%)
28955.504	345.35748	0.0059	H-9->LUMO (61%), H-9->L+1 (28%)
28984.54016	345.01151	0.0048	H-8->LUMO (46%), H-8->L+1 (43%)
29407.98416	340.04371	0.0359	H-7->LUMO (11%), H-6->L+1 (16%), HOMO->L+3 (62%)
29690.28016	336.81056	0.0037	H-7->LUMO (24%), H-7->L+1 (10%), H-6->LUMO (12%), H-6->L+1 (24%), HOMO->L+3 (22%)
29833.04128	335.19881	0.0043	H-7->L+1 (49%), H-6->LUMO (22%), H-6->L+1 (11%)
30260.51808	330.46361	7E-4	H-12->LUMO (60%), H-12->L+1 (30%)
30275.84272	330.29634	0.0014	H-10->LUMO (42%), H-10->L+1 (45%)
30584.7552	326.96028	0.0151	H-16->LUMO (10%), H-1->L+2 (70%)
30618.63072	326.59854	7E-4	H-18->L+1 (10%), H-17->LUMO (45%), H-16->L+1 (31%)
30667.83088	326.07458	0.0322	H-18->LUMO (11%), H-17->L+1 (27%), H-16->LUMO (28%), H-1->L+2 (23%)
31815.56576	314.31156	0.0091	H-11->LUMO (53%), H-1->L+3 (11%)
32058.34032	311.93131	0.0068	H-11->L+1 (51%)
32209.16704	310.47062	0.0011	H-1->L+3 (32%), HOMO->L+5 (41%)
32281.75744	309.77248	0.0023	H-1->L+3 (26%), HOMO->L+5 (44%)
32328.53792	309.32423	3E-4	H-1->L+4 (12%), HOMO->L+4 (68%)
32426.13168	308.39325	0.0172	H-8->L+1 (11%), H-2->L+2 (64%)
32497.91552	307.71204	0.0021	H-8->LUMO (31%), H-8->L+1 (28%), H-2->L+2 (12%)
32618.89952	306.57073	3E-4	H-9->LUMO (28%), H-9->L+1 (53%)
32960.0744	303.39737	0.0098	H-13->LUMO (32%), H-11->LUMO (11%), H-10->LUMO (16%), H-10->L+1 (20%)
33077.83216	302.31727	0.0544	H-13->LUMO (12%), H-13->L+1 (12%), H-12->LUMO (12%), H-12->L+1 (16%), H-10->L+1 (15%), HOMO->L+6 (15%)

33191.55712	301.28144	0.133	H-13->LUMO (10%), H-11->L+1 (12%), H-10->LUMO (16%), HOMO->L+6 (36%)
33281.08528	300.47097	0.0562	H-13->LUMO (12%), H-12->LUMO (16%), H-12->L+1 (46%), HOMO->L+6 (15%)
33530.31232	298.2376	0.0713	H-13->L+1 (56%)
33780.34592	296.03012	5E-4	H-2->L+3 (75%)
34098.93712	293.26427	0.0019	HOMO->L+7 (66%), HOMO->L+8 (16%)
34221.53424	292.21367	0.0067	H-1->L+7 (10%), HOMO->L+7 (15%), HOMO->L+8 (71%)
34586.90592	289.12676	0.0014	H-14->L+1 (10%), H-3->L+2 (17%), HOMO->L+9 (42%)
34809.51648	287.27776	0.0443	H-18->LUMO (16%), H-16->LUMO (28%), H-15->LUMO (25%), H-14->LUMO (13%), H-13->L+1 (11%)
35120.04208	284.7377	0.0011	H-18->L+1 (11%), H-16->L+1 (22%), H-15->L+1 (44%)
35300.71152	283.28041	0.0071	H-1->L+4 (71%), HOMO->L+4 (13%)

Table S10-5. Calculated singlet excited energies and states of **3a** by the time-dependent DFT calculation at B3LYP/6-31g(d,p)

Energy (cm ⁻¹)	Wavelength (nm)	Osc. Strength	Major contribs
15673.88048	638.0041	0.0487	HOMO->LUMO (95%)
16392.52544	610.03413	0.0207	HOMO->L+1 (96%)
16498.99136	606.09766	0.0366	H-1->LUMO (99%)
17163.5968	582.62846	0.0123	H-1->L+1 (99%)
18423.44352	542.78669	0.0028	H-2->LUMO (98%)
18494.4208	540.70361	0.0031	H-3->LUMO (99%)
19266.29872	519.04105	7E-4	H-2->L+1 (99%)
19334.85632	517.20064	0.0026	H-3->L+1 (99%)
20212.3936	494.74596	0.0153	H-4->LUMO (91%)
21523.0536	464.61809	0.0204	H-5->LUMO (10%), H-5->L+1 (31%), H-4->L+1 (57%)
22690.95248	440.70429	0.0728	H-5->LUMO (58%), H-5->L+1 (33%)
24020.96992	416.30292	0.7464	H-5->LUMO (20%), H-5->L+1 (33%), H-4->L+1 (38%)
25471.1648	392.60081	7E-4	H-10->LUMO (96%)
25741.3624	388.47983	0	H-8->L+1 (91%)
26560.0208	376.50573	0.0333	H-6->LUMO (98%)

26681.0048	374.79848	0	H-11->LUMO (98%)
27002.01568	370.34272	3E-4	H-9->L+1 (95%)
27179.45888	367.92491	0.0145	H-13->LUMO (10%), H-7->LUMO (84%)
27325.44624	365.95926	0.0204	H-6->L+1 (98%)
27787.60512	359.87268	2E-4	H-12->L+1 (12%), H-7->L+1 (80%)
28626.42752	349.32756	3E-4	H-8->LUMO (94%)
29074.06832	343.94911	0	H-9->LUMO (95%)
29168.43584	342.83635	0.0033	H-13->LUMO (50%), H-12->L+1 (36%)

S11. Supporting References

[S1] SADABS, SMART, SAINT, and SHELXTL, Bruker AXS Inc., Madison, Wisconsin, USA, **2000**.

[S2] G. M. Sheldrick, *Acta Crystallogr. C* 2015, **71**, 3.

[S3] Gaussian 09, Revision A.02, M. J. Frisch, G. W. Trucks, H. B. Schlegel, G. E. Scuseria, M. A. Robb, J. R. Cheeseman, G. Scalmani, V. Barone, G. A. Petersson, H. Nakatsuji, X. Li, M. Caricato, A. V. Marenich, J. Bloino, B. G. Janesko, R. Gomperts, B. Mennucci, H. P. Hratchian, J. V. Ortiz, A. F. Izmaylov, J. L. Sonnenberg, D. Williams-Young, F. Ding, F. Lipparini, F. Egidi, J. Goings, B. Peng, A. Petrone, T. Henderson, D. Ranasinghe, V. G. Zakrzewski, J. Gao, N. Rega, G. Zheng, W. Liang, M. Hada, M. Ehara, K. Toyota, R. Fukuda, J. Hasegawa, M. Ishida, T. Nakajima, Y. Honda, O. Kitao, H. Nakai, T. Vreven, K. Throssell, J. A. Montgomery, J. E. Peralta, F. Ogliaro, M. J. Bearpark, J. J. Heyd, E. N. Brothers, K. N. Kudin, V. N. Staroverov, T. A. Keith, R. Kobayashi, J. Normand, K. Raghavachari, A. P. Rendell, J. C. Burant, S. S. Iyengar, J. Tomasi, M. Cossi, J. M. Millam, M. Klene, C. Adamo, R. Cammi, J. W. Ochterski, R. L. Martin, K. Morokuma, O. Farkas, J. B. Foresman, D. J. Fox, Gaussian, Inc., Wallingford CT, 2010.

[S4] a) A. D. Becke, *J. Chem. Phys.*, 1993, **98**, 1372; b) Lee, C.; Yang, W.; Parr, R. G. *Phys. Rev. B*, 1988, **37**, 785.

[S5] a) R. Bauernschmitt, R. Ahlrichs, *Chem. Phys. Lett.* 1996, **256**, 454-464; b) R. E. Stratmann, G. E. Scuseria, M. J. Frisch, *J. Chem. Phys.* 1998, **109**, 8218-8224; c) M. E. Casida, C. Jamorski, K. C. Casida, D. R. Salahub, *J. Chem. Phys.* 1998, **108**, 4439-4449.

[S6] S. Dhamija, B. Thakur, P. Guptasarma, P, A. K. De, *Faraday Discuss.* 2018, **207**, 39–54.

[S7] Y. Silori, P. Seliya, A. K. De, *Chem. Phys. Chem.* 2019, **20**, 1488–1496.

[S8] Y. Silori, S. Chawla, A. K. De, *Chem. Phys. Chem.* 2020, **21**, 1908-1917.

[S9] Ultrafast optics, Weiner, A. M. John Wiley and Sons, 2009, 441-442.

[S10] A. Kalaiselvan, I. S. V. Krishna, A. P. Nambiar, A. Edwin, V. S. Reddy, S. Gokulnath, *Org. Lett.* 2020, **22**, 4494-4499.

[S11] T. Wu, T. Kim, B. Yin, K. Wang, L. Xu, M. Zhou, D. Kim, J. Song, *Chem. Commun.* 2019, **55**, 11454-11457.

[S12] X.-S. Ke, T. Kim, V. M. Lynch, D. Kim, J. L. Sessler, *J. Am. Chem. Soc.* 2017, **139**, 13950-13956.

[S13] B. Valeur, M. N. Barberan-Santos, Molecular Fluorescence: Principles and Applications, Second Edition, Wiley-VCH, 2013, 228-229.

[S14] A. Toffoletti, Z. Wang, J. Zhao, M. Tommasini, A. Barbon, *Phys. Chem. Chem. Phys.* 2018, **20**, 20497-20503.

S12. Cartesian coordinates of optimized geometries and minimized energies

Table S12-1: Fractional Atomic Coordinates ($\times 10^4$) and Equivalent Isotropic Displacement Parameters ($\text{\AA}^2 \times 10^3$) for 2. Ueq is defined as 1/3 of the trace of the orthogonalised \mathbf{U}_{IJ} tensor

	x	y	z	U(eq)
C1	1789 (4)	-443 (3)	992 (3)	65.5 (14)
C2	519 (5)	-797 (4)	896 (4)	104 (2)
C3	2257 (5)	-1173 (3)	837 (3)	95 (2)
C4	1920 (6)	128 (3)	340 (3)	105 (2)
C5	2401 (4)	25 (3)	1871 (3)	54.1 (12)
C6	2353 (4)	-394 (3)	2531 (3)	59.3 (13)
C7	2887 (4)	26 (3)	3328 (3)	52.8 (12)
C8	3468 (4)	892 (3)	3472 (3)	53.3 (12)
C9	3529 (4)	1339 (3)	2810 (3)	53.2 (12)
C10	2990 (4)	879 (3)	2024 (3)	59.1 (13)
C11	3001 (4)	-242 (3)	4129 (3)	53.5 (12)
C12	3661 (4)	463 (3)	4709 (3)	53.2 (12)
C13	3982 (4)	399 (3)	5550 (3)	55.3 (13)
C14	3548 (4)	-395 (3)	5754 (3)	61.6 (13)
C15	2855 (4)	-1094 (3)	5192 (3)	56.0 (13)
C16	2604 (4)	-1015 (3)	4372 (3)	60.7 (14)
C17	2384 (5)	-1931 (3)	5474 (3)	63.7 (14)
C18	4713 (4)	1099 (3)	6178 (3)	53.1 (12)
C19	5135 (4)	1031 (3)	7033 (3)	61.5 (14)
C20	5812 (4)	1790 (3)	7398 (3)	65.1 (14)
C21	5823 (4)	2326 (3)	6783 (3)	58.3 (13)
C22	6438 (4)	3153 (3)	6910 (3)	60.7 (13)
C23	7235 (6)	3487 (3)	7759 (3)	72.6 (16)
C24	8215 (7)	3266 (4)	8043 (5)	100 (2)
C25	8924 (8)	3519 (6)	8811 (7)	148 (4)
C26	8678 (12)	4030 (7)	9346 (6)	160 (6)
C27	7711 (11)	4268 (5)	9103 (5)	137 (4)
C28	7007 (8)	3997 (4)	8310 (4)	106 (2)
C29	6406 (4)	3733 (3)	6343 (3)	57.3 (13)
C30	5691 (5)	3712 (3)	5591 (3)	77.2 (17)
C31	6033 (5)	4471 (3)	5320 (3)	79.6 (17)

C32	6966 (4)	4986 (3)	5905 (3)	54.0 (13)
C33	7597 (4)	5858 (3)	5995 (3)	52.0 (12)
C34	8200 (4)	6321 (3)	6762 (3)	58.0 (13)
C35	8783 (4)	7173 (3)	6912 (3)	56.0 (13)
C36	9458 (5)	7604 (3)	7795 (3)	64.3 (14)
C38	8726 (6)	7415 (4)	8368 (4)	113 (2)
C39	10479 (6)	7293 (5)	8095 (4)	139 (3)
C40	9832 (6)	8560 (3)	7851 (4)	123 (3)
C41	8732 (4)	7602 (3)	6242 (3)	56.6 (13)
C42	8154 (4)	7178 (3)	5459 (3)	51.9 (12)
C43	7607 (4)	6321 (3)	5328 (3)	55.4 (13)
C44	7417 (4)	6724 (3)	4087 (3)	56.2 (13)
C45	8025 (4)	7447 (3)	4663 (3)	53.8 (12)
C46	8425 (4)	8204 (3)	4409 (3)	57.2 (13)
C47	8239 (4)	8259 (3)	3575 (3)	58.0 (13)
C48	7636 (4)	7537 (3)	3018 (3)	65.4 (14)
C49	7212 (4)	6759 (3)	3242 (3)	60.2 (13)
C50	8725 (4)	9072 (3)	3256 (3)	60.3 (14)
C54	6700 (4)	6014 (3)	2618 (3)	64.3 (14)
C55	6687 (5)	5998 (3)	1766 (3)	86.8 (19)
C56	6212 (5)	5201 (3)	1406 (3)	83.4 (18)
C57	5908 (5)	4723 (3)	2033 (3)	65.1 (15)
C58	5358 (4)	3876 (3)	1911 (3)	58.0 (13)
C59	4918 (4)	3421 (3)	2484 (3)	57.3 (13)
C60	4673 (4)	3647 (3)	3190 (3)	62.7 (14)
C61	4164 (4)	2917 (3)	3455 (3)	62.2 (14)
C62	4086 (4)	2239 (3)	2906 (3)	54.2 (13)
C63	5179 (5)	3402 (3)	1096 (3)	58.9 (13)
C64	6029 (6)	3250 (3)	833 (4)	79.5 (17)
C65	5860 (8)	2787 (4)	70 (4)	92 (2)
C66	4777 (9)	2477 (4)	-435 (4)	103 (3)
C67	3909 (7)	2606 (4)	-190 (4)	93 (2)
C68	4115 (6)	3072 (3)	549 (3)	71.8 (16)
C51	9354 (9)	9792 (4)	3923 (4)	196 (5)
C52	7803 (6)	9315 (4)	2670 (5)	147 (3)
C53	9513 (7)	8914 (5)	2787 (6)	169 (4)
C69	1605 (16)	-2630 (7)	4745 (8)	93 (7)
C70	3293 (12)	-2212 (9)	5984 (11)	91 (7)
C71	1589 (14)	-1818 (8)	5991 (12)	88 (6)
C69'	2840 (15)	-1892 (9)	6467 (9)	105 (6)
C70'	1147 (10)	-2132 (8)	5266 (11)	87 (5)
C71'	2743 (15)	-2630 (6)	5066 (10)	103 (7)
N1	3931 (3)	1149 (2)	4315 (2)	53.4 (10)
N2	5110 (3)	1871 (2)	6024 (2)	58.9 (11)
N3	7180 (3)	4521 (2)	6526 (2)	64.1 (12)

N4	7148 (3)	6051 (2)	4492 (2)	57.4 (11)
N6	6222 (3)	5261 (2)	2774 (2)	62.3 (11)
N5	4543 (3)	2559 (2)	2320 (2)	56.0 (11)
F1	6086 (5)	4249 (3)	8084 (3)	161 (2)
F2	7461 (6)	4760 (4)	9637 (3)	236 (3)
F3	9342 (5)	4255 (3)	10126 (3)	239 (4)
F4	9868 (5)	3276 (3)	9059 (4)	226 (3)
F5	8505 (3)	2756 (3)	7547 (3)	138.7 (16)
F6	7113 (3)	3522 (2)	1331 (2)	112.1 (12)
F7	6741 (4)	2649 (2)	-141 (3)	145.5 (17)
F8	4620 (4)	2036 (2)	-1161 (2)	159.4 (19)
F9	2845 (4)	2291 (2)	-698 (2)	135.6 (15)
F10	3218 (3)	3200 (2)	747 (2)	104.2 (11)

Table S12-2 Anisotropic Displacement Parameters ($\text{\AA}^2 \times 10^3$) for 2. The Anisotropic displacement factor exponent takes the form: $-2\pi^2[h^2a^*{}^2U_{11}+2hka^*b^*U_{12}+\dots]$.

Atom	U₁₁	U₂₂	U₃₃	U₂₃	U₁₃	U₁₂
C1	69 (4)		63 (3)	51 (3)	-2 (3)	4 (3)
C2	77 (5)		121 (5)	80 (5)	-23 (4)	-3 (3)
C3	134 (6)		92 (4)	56 (4)	-13 (3)	6 (4)
C4	169 (7)		78 (4)	43 (4)	4 (3)	2 (4)
C5	58 (3)		54 (3)	42 (3)	0 (2)	3 (2)
C6	63 (3)		50 (3)	52 (3)	-2 (3)	6 (3)
C7	55 (3)		52 (3)	44 (3)	4 (2)	12 (2)
C8	53 (3)		54 (3)	45 (3)	-2 (2)	12 (2)
C9	58 (3)		54 (3)	43 (3)	10 (2)	11 (2)
C10	68 (3)		56 (3)	44 (3)	6 (2)	9 (3)
C11	55 (3)		52 (3)	49 (3)	7 (2)	16 (2)
C12	56 (3)		48 (3)	50 (3)	4 (3)	18 (3)
C13	61 (3)		54 (3)	49 (3)	13 (2)	18 (3)
C14	70 (4)		62 (3)	51 (3)	12 (3)	23 (3)
C15	66 (3)		49 (3)	51 (3)	12 (2)	16 (3)
C16	66 (3)		47 (3)	63 (4)	4 (3)	22 (3)
C17	70 (4)		54 (3)	65 (4)	17 (3)	25 (3)
C18	57 (3)		50 (3)	50 (3)	10 (2)	18 (3)
C19	67 (3)		59 (3)	48 (3)	18 (3)	8 (3)
C20	77 (4)		65 (3)	44 (3)	16 (3)	10 (3)
C21	66 (3)		53 (3)	44 (3)	6 (3)	8 (3)
C22	76 (4)		55 (3)	41 (3)	10 (2)	5 (3)
C23	95 (5)		54 (3)	50 (4)	13 (3)	5 (3)
C24	104 (6)		72 (4)	93 (6)	9 (4)	-1 (5)
C25	123 (7)		97 (6)	130 (8)	25 (6)	-69 (7)
C26	192 (12)		114 (8)	60 (6)	15 (5)	-43 (7)
						-66 (8)

C27	194 (10)	112 (7)	59 (6)	-9 (5)	21 (7)	-12 (7)
C28	148 (7)	90 (5)	59 (5)	-1 (4)	20 (5)	12 (5)
C29	74 (4)	47 (3)	43 (3)	6 (2)	13 (3)	8 (3)
C30	102 (5)	55 (3)	52 (4)	8 (3)	2 (3)	6 (3)
C31	104 (5)	62 (3)	50 (3)	11 (3)	2 (3)	5 (3)
C32	79 (4)	47 (3)	36 (3)	5 (2)	14 (3)	20 (3)
C33	63 (3)	45 (3)	44 (3)	0 (2)	14 (2)	13 (2)
C34	75 (4)	51 (3)	44 (3)	4 (2)	14 (3)	17 (3)
C35	64 (3)	55 (3)	45 (3)	3 (2)	13 (3)	14 (3)
C36	75 (4)	62 (3)	44 (3)	-2 (2)	10 (3)	9 (3)
C38	137 (6)	123 (5)	57 (4)	-10 (4)	33 (4)	-2 (4)
C39	129 (6)	172 (7)	91 (5)	-35 (5)	-30 (5)	78 (6)
C40	186 (7)	70 (4)	63 (4)	-6 (3)	5 (4)	-8 (4)
C41	64 (3)	50 (3)	50 (3)	0 (3)	16 (3)	6 (2)
C42	64 (3)	47 (3)	43 (3)	2 (2)	18 (2)	12 (2)
C43	69 (3)	52 (3)	42 (3)	5 (2)	14 (3)	16 (3)
C44	66 (3)	48 (3)	50 (3)	8 (3)	16 (3)	9 (2)
C45	66 (3)	46 (3)	45 (3)	1 (2)	19 (3)	7 (2)
C46	69 (3)	44 (3)	53 (3)	2 (2)	16 (3)	11 (2)
C47	70 (4)	50 (3)	49 (3)	8 (2)	17 (3)	12 (3)
C48	88 (4)	54 (3)	41 (3)	4 (2)	15 (3)	2 (3)
C49	75 (4)	47 (3)	50 (3)	5 (2)	16 (3)	5 (3)
C50	73 (4)	47 (3)	52 (3)	12 (2)	15 (3)	7 (3)
C54	87 (4)	49 (3)	48 (3)	7 (3)	16 (3)	8 (3)
C55	145 (6)	54 (3)	51 (4)	12 (3)	33 (4)	6 (3)
C56	132 (5)	56 (3)	50 (3)	5 (3)	30 (3)	4 (3)
C57	99 (4)	48 (3)	41 (3)	4 (2)	22 (3)	9 (3)
C58	80 (4)	49 (3)	41 (3)	1 (2)	19 (3)	12 (3)
C59	74 (4)	45 (3)	44 (3)	1 (2)	16 (3)	5 (2)
C60	86 (4)	51 (3)	43 (3)	-3 (2)	19 (3)	8 (3)
C61	73 (4)	66 (3)	40 (3)	5 (3)	16 (3)	8 (3)
C62	61 (3)	52 (3)	41 (3)	4 (2)	8 (2)	10 (2)
C63	77 (4)	49 (3)	46 (3)	3 (2)	21 (3)	7 (3)
C64	93 (5)	63 (4)	73 (4)	2 (3)	29 (4)	5 (3)
C65	137 (7)	66 (4)	86 (5)	-4 (4)	70 (5)	17 (4)
C66	158 (8)	74 (4)	60 (5)	-7 (3)	46 (5)	-6 (5)
C67	123 (6)	78 (4)	47 (4)	0 (3)	15 (4)	-15 (4)
C68	93 (5)	67 (3)	50 (4)	7 (3)	26 (4)	7 (3)
C51	341 (13)	75 (5)	75 (5)	9 (4)	26 (6)	-72 (6)
C52	123 (6)	101 (5)	172 (8)	74 (5)	-14 (6)	3 (5)
C53	191 (9)	124 (6)	270 (11)	85 (7)	180 (9)	48 (6)
C69	121 (16)	58 (8)	103 (11)	29 (8)	46 (10)	11 (9)
C70	86 (11)	76 (10)	99 (16)	49 (11)	5 (9)	12 (8)
C71	87 (12)	77 (9)	105 (15)	32 (9)	50 (11)	5 (8)
C69'	128 (15)	102 (10)	78 (10)	39 (8)	32 (9)	10 (9)

C70'	72 (9)	70 (8)	122 (15)	29 (10)	41 (9)	9 (7)
C71'	128 (16)	46 (6)	165 (17)	29 (8)	79 (14)	37 (8)
N1	64 (3)	46 (2)	41 (2)	6.2 (19)	13 (2)	0.9 (19)
N2	71 (3)	49 (2)	47 (3)	10 (2)	13 (2)	4 (2)
N3	77 (3)	52 (2)	46 (3)	8 (2)	4 (2)	4 (2)
N4	77 (3)	43 (2)	45 (3)	4.4 (19)	15 (2)	7 (2)
N6	88 (3)	48 (2)	43 (3)	4 (2)	19 (2)	7 (2)
N5	79 (3)	47 (2)	36 (2)	2.2 (18)	18 (2)	8 (2)
F1	187 (5)	171 (4)	124 (4)	-34 (3)	40 (4)	71 (4)
F2	329 (8)	218 (6)	105 (4)	-71 (4)	76 (5)	-7 (5)
F3	284 (7)	183 (5)	84 (3)	27 (3)	-74 (4)	-85 (5)
F4	153 (5)	183 (5)	228 (6)	61 (5)	-96 (5)	3 (4)
F5	107 (3)	123 (3)	164 (4)	8 (3)	-2 (3)	43 (3)
F6	95 (3)	115 (3)	118 (3)	-12 (2)	34 (2)	23 (2)
F7	197 (5)	124 (3)	149 (4)	-5 (3)	113 (4)	47 (3)
F8	256 (5)	125 (3)	73 (3)	-35 (2)	68 (3)	7 (3)
F9	161 (4)	127 (3)	61 (2)	-7 (2)	-6 (2)	-12 (3)
F10	103 (3)	120 (3)	74 (2)	7 (2)	15 (2)	20 (2)

Table S12-3 Bond Lengths for 2.

Atom	Atom	Length/Å	Atom	Atom	Length/Å
C1	C2	1.530 (7)	C32	C33	1.442 (6)
C1	C3	1.517 (7)	C32	N3	1.364 (5)
C1	C4	1.527 (7)	C33	C34	1.382 (6)
C1	C5	1.535 (6)	C33	C43	1.417 (6)
C5	C6	1.369 (6)	C34	C35	1.391 (6)
C5	C10	1.395 (6)	C35	C36	1.534 (6)
C6	C7	1.386 (6)	C35	C41	1.383 (6)
C7	C8	1.412 (6)	C36	C38	1.515 (7)
C7	C11	1.446 (6)	C36	C39	1.497 (8)
C8	C9	1.401 (6)	C36	C40	1.528 (7)
C8	N1	1.387 (5)	C41	C42	1.376 (6)
C9	C10	1.395 (6)	C42	C43	1.390 (6)
C9	C62	1.459 (6)	C42	C45	1.437 (6)
C11	C12	1.394 (6)	C43	N4	1.378 (5)
C11	C16	1.391 (6)	C44	C45	1.399 (6)
C12	C13	1.401 (6)	C44	C49	1.399 (6)
C12	N1	1.378 (5)	C44	N4	1.374 (5)
C13	C14	1.402 (6)	C45	C46	1.378 (6)
C13	C18	1.450 (6)	C46	C47	1.390 (6)
C14	C15	1.383 (6)	C47	C48	1.381 (6)
C15	C16	1.371 (6)	C47	C50	1.537 (6)
C15	C17	1.533 (6)	C48	C49	1.392 (6)
C17	C69	1.556 (14)	C49	C54	1.455 (6)

C17	C70	1.451(13)	C50	C51	1.481(7)
C17	C71	1.544(14)	C50	C52	1.486(8)
C17	C69'	1.625(14)	C50	C53	1.498(8)
C17	C70'	1.459(12)	C54	C55	1.445(6)
C17	C71'	1.539(12)	C54	N6	1.324(5)
C18	C19	1.435(6)	C55	C56	1.332(6)
C18	N2	1.327(5)	C56	C57	1.450(6)
C19	C20	1.330(6)	C57	C58	1.376(6)
C20	C21	1.424(6)	C57	N6	1.393(5)
C21	C22	1.366(6)	C58	C59	1.420(6)
C21	N2	1.396(5)	C58	C63	1.478(6)
C22	C23	1.497(7)	C59	C60	1.371(6)
C22	C29	1.414(6)	C59	N5	1.373(5)
C23	C24	1.363(8)	C60	C61	1.388(6)
C23	C28	1.358(9)	C61	C62	1.380(6)
C24	C25	1.341(10)	C62	N5	1.357(5)
C24	F5	1.339(8)	C63	C64	1.348(7)
C25	C26	1.352(15)	C63	C68	1.368(7)
C25	F4	1.336(11)	C64	C65	1.397(8)
C26	C27	1.357(14)	C64	F6	1.351(7)
C26	F3	1.336(9)	C65	C66	1.357(9)
C27	C28	1.374(11)	C65	F7	1.331(7)
C27	F2	1.335(10)	C66	C67	1.339(9)
C28	F1	1.315(9)	C66	F8	1.330(7)
C29	C30	1.350(6)	C67	C68	1.354(8)
C29	N3	1.379(5)	C67	F9	1.341(7)
C30	C31	1.381(6)	C68	F10	1.333(6)
C31	C32	1.364(6)			

Table S12-4 Bond Angles for 2.

Atom	Atom	Atom	Angle/ [°]	Atom	Atom	Atom	Angle/ [°]
C2	C1	C5	109.1(4)	C34	C33	C32	121.3(4)
C3	C1	C2	108.3(5)	C34	C33	C43	114.6(4)
C3	C1	C4	108.7(5)	C43	C33	C32	124.0(4)
C3	C1	C5	109.9(4)	C33	C34	C35	125.4(4)
C4	C1	C2	108.3(5)	C34	C35	C36	120.0(4)
C4	C1	C5	112.4(4)	C41	C35	C34	117.6(4)
C6	C5	C1	119.9(4)	C41	C35	C36	122.4(4)
C6	C5	C10	118.4(4)	C38	C36	C35	110.6(4)
C10	C5	C1	121.7(4)	C38	C36	C40	106.1(5)
C5	C6	C7	120.4(4)	C39	C36	C35	109.8(4)
C6	C7	C8	120.6(4)	C39	C36	C38	108.8(5)
C6	C7	C11	132.9(4)	C39	C36	C40	109.8(5)
C8	C7	C11	106.5(4)	C40	C36	C35	111.7(4)

C9	C8	C7	120.5 (4)	C42	C41	C35	120.0 (4)
N1	C8	C7	108.7 (4)	C41	C42	C43	120.9 (4)
N1	C8	C9	130.8 (4)	C41	C42	C45	131.7 (4)
C8	C9	C62	123.9 (4)	C43	C42	C45	107.3 (4)
C10	C9	C8	116.2 (4)	C42	C43	C33	121.3 (4)
C10	C9	C62	119.9 (4)	N4	C43	C33	129.8 (4)
C9	C10	C5	124.0 (4)	N4	C43	C42	108.9 (4)
C12	C11	C7	106.5 (4)	C49	C44	C45	120.4 (4)
C16	C11	C7	132.4 (4)	N4	C44	C45	109.5 (4)
C16	C11	C12	121.1 (4)	N4	C44	C49	130.0 (4)
C11	C12	C13	120.5 (4)	C44	C45	C42	105.8 (4)
N1	C12	C11	109.9 (4)	C46	C45	C42	133.4 (4)
N1	C12	C13	129.6 (4)	C46	C45	C44	120.6 (4)
C12	C13	C14	115.6 (4)	C45	C46	C47	120.4 (4)
C12	C13	C18	123.1 (4)	C46	C47	C50	122.7 (4)
C14	C13	C18	121.4 (4)	C48	C47	C46	117.9 (4)
C15	C14	C13	124.8 (5)	C48	C47	C50	119.3 (4)
C14	C15	C17	121.3 (4)	C47	C48	C49	123.9 (5)
C16	C15	C14	117.8 (4)	C44	C49	C54	122.9 (4)
C16	C15	C17	120.9 (4)	C48	C49	C44	116.7 (4)
C15	C16	C11	120.1 (4)	C48	C49	C54	120.0 (4)
C15	C17	C69	113.0 (6)	C51	C50	C47	113.2 (4)
C15	C17	C71	109.4 (6)	C51	C50	C52	108.2 (6)
C15	C17	C69'	112.4 (6)	C51	C50	C53	108.9 (6)
C15	C17	C71'	109.8 (6)	C52	C50	C47	110.8 (4)
C70	C17	C15	111.3 (6)	C52	C50	C53	106.9 (6)
C70	C17	C69	111.1 (9)	C53	C50	C47	108.6 (4)
C70	C17	C71	107.8 (10)	C55	C54	C49	124.4 (4)
C71	C17	C69	103.9 (9)	N6	C54	C49	123.6 (4)
C70'	C17	C15	109.5 (6)	N6	C54	C55	111.9 (4)
C70'	C17	C69'	105.8 (9)	C56	C55	C54	106.6 (5)
C70'	C17	C71'	111.1 (9)	C55	C56	C57	106.7 (5)
C71'	C17	C69'	108.1 (9)	C58	C57	C56	125.6 (4)
C19	C18	C13	124.1 (4)	C58	C57	N6	125.0 (4)
N2	C18	C13	124.0 (4)	N6	C57	C56	109.4 (4)
N2	C18	C19	111.9 (4)	C57	C58	C59	126.3 (4)
C20	C19	C18	106.1 (4)	C57	C58	C63	116.7 (4)
C19	C20	C21	107.8 (4)	C59	C58	C63	117.0 (4)
C22	C21	C20	125.7 (4)	C60	C59	C58	134.1 (4)
C22	C21	N2	125.2 (4)	C60	C59	N5	106.5 (4)
N2	C21	C20	109.1 (4)	N5	C59	C58	119.2 (4)
C21	C22	C23	115.9 (4)	C59	C60	C61	108.1 (4)
C21	C22	C29	128.1 (4)	C62	C61	C60	108.2 (4)
C29	C22	C23	116.0 (4)	C61	C62	C9	133.1 (5)
C24	C23	C22	122.0 (6)	N5	C62	C9	120.0 (4)

C28	C23	C22		122.4 (7)	N5	C62	C61	106.5 (4)
C28	C23	C24		115.5 (7)	C64	C63	C58	123.6 (5)
C25	C24	C23		123.8 (9)	C64	C63	C68	114.6 (5)
F5	C24	C23		119.9 (7)	C68	C63	C58	121.8 (5)
F5	C24	C25		116.3 (9)	C63	C64	C65	123.7 (7)
C24	C25	C26		119.4 (10)	C63	C64	F6	119.9 (5)
F4	C25	C24		121.3 (12)	F6	C64	C65	116.3 (7)
F4	C25	C26		119.3 (10)	C66	C65	C64	118.0 (7)
C25	C26	C27		119.6 (9)	F7	C65	C64	120.3 (8)
F3	C26	C25		120.3 (14)	F7	C65	C66	121.7 (7)
F3	C26	C27		119.9 (14)	C67	C66	C65	120.0 (7)
C26	C27	C28		119.3 (10)	F8	C66	C65	117.7 (8)
F2	C27	C26		119.4 (11)	F8	C66	C67	122.3 (8)
F2	C27	C28		121.3 (12)	C66	C67	C68	120.0 (7)
C23	C28	C27		122.3 (9)	C66	C67	F9	119.0 (7)
F1	C28	C23		119.5 (7)	F9	C67	C68	121.0 (8)
F1	C28	C27		118.2 (9)	C67	C68	C63	123.7 (7)
C30	C29	C22		132.9 (5)	F10	C68	C63	119.2 (5)
C30	C29	N3		105.5 (4)	F10	C68	C67	117.1 (6)
N3	C29	C22		121.6 (4)	C12	N1	C8	108.4 (4)
C29	C30	C31		108.7 (5)	C18	N2	C21	105.1 (4)
C32	C31	C30		109.5 (5)	C32	N3	C29	111.6 (4)
C31	C32	C33		133.6 (5)	C44	N4	C43	108.5 (4)
C31	C32	N3		104.7 (4)	C54	N6	C57	105.4 (4)
N3	C32	C33		121.3 (4)	C62	N5	C59	110.7 (4)

Table S12-5 Hydrogen Bonds for 2.

D	H	A	d(D-H)/Å	d(H-A)/Å	d(D-A)/Å	D-H-A/°
C30	H30	N2	0.93		2.70	3.149 (6) 110.7
C30	H30	N2	0.93		2.70	3.149 (6) 110.7
C55	H55	F9 ₁	0.93		2.59	3.494 (7) 165.0
C55	H55	F9 ₁	0.93		2.59	3.494 (7) 165.0
N1	H1	N2	0.86		2.40	2.900 (6) 117.6
N1	H1	N2	0.86		2.40	2.900 (6) 117.6
N4	H4	N6	0.86		2.42	2.913 (6) 117.1
N4	H4	N6	0.86		2.42	2.913 (6) 117.1

¹1-X,1-Y,-Z

Table S12-6 Torsion Angles for 2.

A	B	C	D	Angle/°	A	B	C	D	Angle/°
---	---	---	---	---------	---	---	---	---	---------

C1 C5 C6 C7	-179.0 (4)	C34C35C41C42	-2.3 (7)
C1 C5 C10C9	177.9 (5)	C35C41C42C43	0.6 (7)
C2 C1 C5 C6	58.8 (6)	C35C41C42C45	-175.7 (5)
C2 C1 C5 C10	-119.6 (5)	C36C35C41C42	177.2 (4)
C3 C1 C5 C6	-59.8 (6)	C41C35C36C38	129.8 (5)
C3 C1 C5 C10	121.8 (5)	C41C35C36C39	-110.2 (6)
C4 C1 C5 C6	179.0 (5)	C41C35C36C40	11.9 (7)
C4 C1 C5 C10	0.5 (7)	C41C42C43C33	1.8 (7)
C5 C6 C7 C8	1.2 (7)	C41C42C43N4	-177.1 (4)
C5 C6 C7 C11	-178.8 (5)	C41C42C45C44	175.5 (5)
C6 C5 C10C9	-0.6 (7)	C41C42C45C46	0.1 (9)
C6 C7 C8 C9	-1.0 (7)	C42C43N4 C44	1.3 (5)
C6 C7 C8 N1	-179.3 (4)	C42C45C46C47	174.2 (5)
C6 C7 C11C12	178.6 (5)	C43C33C34C35	0.4 (7)
C6 C7 C11C16	-0.4 (9)	C43C42C45C44	-1.1 (5)
C7 C8 C9 C10	0.0 (7)	C43C42C45C46	-176.5 (5)
C7 C8 C9 C62	178.3 (4)	C44C45C46C47	-0.6 (7)
C7 C8 N1 C12	0.3 (5)	C44C49C54C55	-166.7 (5)
C7 C11C12C13	-176.3 (4)	C44C49C54N6	11.0 (8)
C7 C11C12N1	1.7 (5)	C45C42C43C33	178.8 (4)
C7 C11C16C15	179.2 (5)	C45C42C43N4	-0.1 (5)
C8 C7 C11C12	-1.5 (5)	C45C44C49C48	-0.3 (7)
C8 C7 C11C16	179.5 (5)	C45C44C49C54	172.9 (5)
C8 C9 C10C5	0.8 (7)	C45C44N4 C43	-2.0 (5)
C8 C9 C62C61	-37.1 (8)	C45C46C47C48	0.6 (7)
C8 C9 C62N5	151.7 (5)	C45C46C47C50	-176.2 (4)
C9 C8 N1 C12	-177.8 (5)	C46C47C48C49	-0.5 (8)
C9 C62N5 C59	173.8 (4)	C46C47C50C51	-3.0 (8)
C10C5 C6 C7	-0.4 (7)	C46C47C50C52	-124.7 (6)
C10C9 C62C61	141.2 (6)	C46C47C50C53	118.1 (6)
C10C9 C62N5	-30.0 (7)	C47C48C49C44	0.3 (8)
C11C7 C8 C9	179.1 (4)	C47C48C49C54	-173.0 (5)
C11C7 C8 N1	0.7 (5)	C48C47C50C51	-179.8 (6)
C11C12C13C14	-3.2 (7)	C48C47C50C52	58.5 (7)
C11C12C13C18	176.9 (4)	C48C47C50C53	-58.6 (7)
C11C12N1 C8	-1.2 (5)	C48C49C54C55	6.2 (8)
C12C11C16C15	0.3 (7)	C48C49C54N6	-176.1 (5)
C12C13C14C15	0.6 (7)	C49C44C45C42	-175.6 (4)
C12C13C18C19	-174.2 (5)	C49C44C45C46	0.4 (7)
C12C13C18N2	2.8 (7)	C49C44N4 C43	175.3 (5)
C13C12N1 C8	176.5 (5)	C49C54C55C56	176.2 (5)
C13C14C15C16	2.3 (8)	C49C54N6 C57	-176.4 (5)
C13C14C15C17	-177.8 (5)	C50C47C48C49	176.5 (5)
C13C18C19C20	177.0 (4)	C54C55C56C57	1.1 (7)
C13C18N2 C21	-176.4 (4)	C55C54N6 C57	1.6 (6)

C14C13C18C19	5.8 (7)	C55C56C57C58	177.6 (6)
C14C13C18N2	-177.2 (5)	C55C56C57N6	-0.2 (7)
C14C15C16C11	-2.7 (7)	C56C57C58C59	-170.9 (5)
C14C15C17C69	178.8 (9)	C56C57C58C63	7.1 (8)
C14C15C17C70	-55.4 (11)	C56C57N6 C54	-0.9 (6)
C14C15C17C71	63.6 (10)	C57C58C59C60	16.0 (10)
C14C15C17C69'	-2.6 (11)	C57C58C59N5	-170.5 (5)
C14C15C17C70'	114.8 (9)	C57C58C63C64	69.0 (7)
C14C15C17C71'	-123.0 (9)	C57C58C63C68	-111.8 (6)
C16C11C12C13	2.8 (7)	C58C57N6 C54	-178.7 (5)
C16C11C12N1	-179.2 (4)	C58C59C60C61	174.9 (5)
C16C15C17C69	-1.3 (10)	C58C59N5 C62	-176.0 (4)
C16C15C17C70	124.5 (10)	C58C63C64C65	178.5 (5)
C16C15C17C71	-116.5 (9)	C58C63C64F6	1.4 (8)
C16C15C17C69'	177.3 (9)	C58C63C68C67	-177.3 (5)
C16C15C17C70'	-65.4 (9)	C58C63C68F10	1.9 (7)
C16C15C17C71'	56.9 (10)	C59C58C63C64	-112.8 (6)
C17C15C16C11	177.4 (4)	C59C58C63C68	66.3 (6)
C18C13C14C15	-179.4 (4)	C59C60C61C62	-0.5 (6)
C18C19C20C21	-0.3 (6)	C60C59N5 C62	-0.9 (5)
C19C18N2 C21	0.9 (5)	C60C61C62C9	-172.0 (5)
C19C20C21C22	-178.6 (5)	C60C61C62N5	0.0 (6)
C19C20C21N2	0.9 (6)	C61C62N5 C59	0.5 (5)
C20C21C22C23	5.4 (8)	C62C9 C10C5	-177.6 (4)
C20C21C22C29	-173.9 (5)	C63C58C59C60	-161.9 (6)
C20C21N2 C18	-1.1 (5)	C63C58C59N5	11.6 (7)
C21C22C23C24	72.1 (7)	C63C64C65C66	0.4 (9)
C21C22C23C28	-104.8 (6)	C63C64C65F7	-178.7 (5)
C21C22C29C30	11.7 (10)	C64C63C68C67	1.9 (8)
C21C22C29N3	-171.7 (5)	C64C63C68F10	-178.9 (5)
C22C21N2 C18	178.4 (5)	C64C65C66C67	-1.3 (10)
C22C23C24C25	-176.8 (6)	C64C65C66F8	-179.9 (5)
C22C23C24F5	2.2 (9)	C65C66C67C68	2.5 (10)
C22C23C28C27	176.5 (6)	C65C66C67F9	-179.7 (6)
C22C23C28F1	-3.8 (10)	C66C67C68C63	-2.9 (9)
C22C29C30C31	177.5 (5)	C66C67C68F10	177.9 (6)
C22C29N3 C32	-177.7 (4)	C68C63C64C65	-0.7 (8)
C23C22C29C30	-167.5 (6)	C68C63C64F6	-177.9 (5)
C23C22C29N3	9.1 (7)	N1 C8 C9 C10	177.9 (5)
C23C24C25C26	-0.6 (12)	N1 C8 C9 C62	-3.8 (8)
C23C24C25F4	179.2 (7)	N1 C12C13C14	179.3 (4)
C24C23C28C27	-0.6 (10)	N1 C12C13C18	-0.7 (8)
C24C23C28F1	179.1 (6)	N2 C18C19C20	-0.4 (6)
C24C25C26C27	1.0 (15)	N2 C21C22C23	-174.0 (5)
C24C25C26F3	176.5 (6)	N2 C21C22C29	6.7 (9)

C25C26C27C28	-1.2(15)	N3 C29C30C31	0.6(6)
C25C26C27F2	178.9(8)	N3 C32C33C34	-18.4(7)
C26C27C28C23	1.0(13)	N3 C32C33C43	165.1(4)
C26C27C28F1	-178.7(8)	N4 C44C45C42	1.9(5)
C28C23C24C25	0.3(10)	N4 C44C45C46	178.0(4)
C28C23C24F5	179.3(6)	N4 C44C49C48	-177.2(5)
C29C22C23C24	-108.5(6)	N4 C44C49C54	-4.1(9)
C29C22C23C28	74.6(7)	N6 C54C55C56	-1.8(7)
C29C30C31C32	-0.6(7)	N6 C57C58C59	6.6(9)
C30C29N3 C32	-0.3(6)	N6 C57C58C63	-175.4(5)
C30C31C32C33	-172.3(5)	N5 C59C60C61	0.8(6)
C30C31C32N3	0.4(6)	F2 C27C28C23	-179.1(7)
C31C32C33C34	153.3(6)	F2 C27C28F1	1.2(12)
C31C32C33C43	-23.2(9)	F3 C26C27C28	-176.8(6)
C31C32N3 C29	0.0(6)	F3 C26C27F2	3.3(14)
C32C33C34C35	-176.5(5)	F4 C25C26C27	-178.8(8)
C32C33C43C42	174.6(4)	F4 C25C26F3	-3.3(14)
C32C33C43N4	-6.8(8)	F5 C24C25C26	-179.5(8)
C33C32N3 C29	173.8(4)	F5 C24C25F4	0.3(11)
C33C34C35C36	-177.7(5)	F6 C64C65C66	177.7(5)
C33C34C35C41	1.8(7)	F6 C64C65F7	-1.4(8)
C33C43N4 C44	-177.5(5)	F7 C65C66C67	177.8(6)
C34C33C43C42	-2.2(7)	F7 C65C66F8	-0.8(9)
C34C33C43N4	176.5(5)	F8 C66C67C68	-179.0(5)
C34C35C36C38	-50.7(7)	F8 C66C67F9	-1.1(10)
C34C35C36C39	69.3(7)	F9 C67C68C63	179.3(5)
C34C35C36C40	-168.6(5)	F9 C67C68F10	0.1(8)

Table S12-7 Hydrogen Atom Coordinates ($\text{\AA} \times 10^4$) and Isotropic Displacement Parameters ($\text{\AA}^2 \times 10^3$) for 2

Atom	x	y	z	U(eq)
H2A	207	-344	991	157
H2B	132	-1094	347	157
H2C	419	-1175	1288	157
H3A	2179	-1536	1245	143
H3B	1840	-1482	298	143
H3C	3047	-961	872	143
H4A	1627	592	431	157
H4B	2711	336	375	157
H4C	1505	-186	-198	157
H6	1961	-962	2444	71
H10	3026	1158	1573	71
H14	3740	-456	6309	74

H16	2167	-1480	3977	73
H19	4968	554	7282	74
H20	6209	1943	7956	78
H30	5071	3260	5303	93
H31	5681	4610	4816	95
H34	8218	6039	7216	70
H38A	8068	7612	8181	170
H38B	8488	6819	8371	170
H38C	9158	7694	8916	170
H39A	10950	7410	7736	209
H39B	10907	7572	8644	209
H39C	10237	6698	8099	209
H40A	9174	8756	7658	184
H40B	10227	8809	8413	184
H40C	10330	8716	7516	184
H41	9089	8176	6321	68
H46	8822	8681	4798	69
H48	7506	7573	2459	78
H55	6958	6455	1517	104
H56	6097	4992	859	100
H60	4822	4193	3446	75
H61	3918	2891	3923	75
H51A	9955	9647	4308	294
H51B	9673	10271	3691	294
H51C	8841	9924	4201	294
H52A	7385	8856	2233	220
H52B	7298	9450	2955	220
H52C	8130	9797	2445	220
H53A	9112	8448	2353	253
H53B	9785	9406	2554	253
H53C	10148	8786	3153	253
H69A	1012	-2429	4417	140
H69B	2050	-2772	4410	140
H69C	1272	-3120	4958	140
H70A	2974	-2736	6151	137
H70B	3801	-2287	5676	137
H70C	3706	-1798	6464	137
H71A	979	-1632	5666	132
H71B	1281	-2344	6159	132
H71C	2013	-1406	6470	132
H69D	3655	-1761	6639	158
H69E	2614	-1465	6733	158
H69F	2519	-2427	6614	158
H70D	853	-2656	5443	130
H70E	946	-1694	5539	130

H70F	828	-2177	4681	130
H71D	3559	-2483	5211	154
H71E	2461	-3150	5254	154
H71F	2434	-2692	4478	154
H1	4321	1651	4553	64
H3	7730	4698	6977	77
H4	6758	5546	4262	69
H5	4590	2263	1903	67

Table S12-8 Atomic Occupancy for 2

Atom	Occupancy	Atom	Occupancy	Atom	Occupancy
C69	0.475 (16)	H69A	0.475 (16)	H69B	0.475 (16)
H69C	0.475 (16)	C70	0.475 (16)	H70A	0.475 (16)
H70B	0.475 (16)	H70C	0.475 (16)	C71	0.475 (16)
H71A	0.475 (16)	H71B	0.475 (16)	H71C	0.475 (16)
C69'	0.525 (16)	H69D	0.525 (16)	H69E	0.525 (16)
H69F	0.525 (16)	C70'	0.525 (16)	H70D	0.525 (16)
H70E	0.525 (16)	H70F	0.525 (16)	C71'	0.525 (16)
H71D	0.525 (16)	H71E	0.525 (16)	H71F	0.525 (16)

Table S12-9 Fractional Atomic Coordinates ($\times 10^4$) and Equivalent Isotropic Displacement Parameters ($\text{\AA}^2 \times 10^3$) for 2a. U_{eq} is defined as 1/3 of the trace of the orthogonalised U_{IJ} tensor.

Atom	x	y	z	U(eq)
C1	5869 (2)	1403 (2)	2698.6 (14)	68.3 (11)
C2	5902 (2)	1984 (2)	3187.7 (12)	54.8 (9)
C3	5579 (2)	1802 (2)	3665.1 (12)	54.3 (9)
C4	5652.9 (18)	2334.3 (19)	4105.5 (12)	48.0 (8)
C5	6065.9 (18)	3062.3 (18)	4072.6 (11)	45.1 (8)
C6	6365.9 (18)	3287.0 (19)	3587.1 (12)	48.8 (8)
C7	6274 (2)	2736 (2)	3159.3 (12)	55.1 (9)
C8	6700 (2)	4100 (2)	3510.6 (12)	51.9 (8)
C9	6342 (2)	4751 (2)	3229.1 (17)	73.8 (11)
C10	6832 (2)	5398 (2)	3261.8 (16)	69.7 (11)
C11	7502 (2)	5140 (2)	3556.0 (13)	53.4 (9)
C12	8198 (2)	5522 (2)	3673.5 (13)	53.3 (9)
C13	8815 (2)	5122 (2)	3937.9 (13)	52.7 (8)
C14	9575 (2)	5356 (2)	4043.6 (15)	66.5 (10)
C15	9952 (2)	4710 (2)	4286.3 (16)	71.9 (11)
C16	9429.0 (19)	4077 (2)	4337.7 (12)	50.1 (8)
C17	9599.2 (19)	3271 (2)	4590.0 (12)	49.8 (8)
C18	9371.7 (18)	3055.6 (19)	5102.8 (12)	47.2 (8)
C19	9627.5 (19)	2331.8 (19)	5357.2 (12)	48.4 (8)

C20	10077 (2)	1794 (2)	5094.8 (13)	59.0 (9)
C21	10299 (2)	1982 (2)	4579.0 (13)	63.2 (10)
C22	10062 (2)	2721 (2)	4349.0 (13)	60.6 (9)
C23	10818 (3)	1406 (3)	4284.3 (17)	91.5 (15)
C24	5441 (3)	1807 (4)	2208.1 (17)	114.7 (18)
C25	5474 (4)	601 (3)	2809.4 (19)	113.1 (18)
C26	6684 (3)	1195 (4)	2578 (2)	118.4 (19)
C30	8296 (2)	6388 (2)	3499.7 (14)	58.4 (9)
C31	8335 (3)	7018 (2)	3863.0 (17)	75.8 (11)
C32	8411 (3)	7820 (2)	3699 (2)	84.2 (13)
C33	8456 (3)	7991 (3)	3165 (2)	83.7 (13)
C34	8418 (3)	7383 (3)	2795.3 (18)	84.0 (13)
C35	8337 (2)	6590 (2)	2954.7 (17)	71.5 (11)
N1	8741.2 (15)	4320.4 (15)	4124.1 (10)	49.4 (7)
N2	7402.9 (16)	4329.5 (15)	3708.2 (10)	49.8 (7)
N3	6052.9 (15)	3502.3 (15)	4550.5 (10)	49.8 (7)
B1	8004 (3)	3812 (3)	4039 (2)	76.5 (15)
F1	8295 (2)	6854.2 (15)	4391.0 (10)	113.4 (10)
F2	8444 (2)	8417.0 (16)	4066.8 (13)	130.0 (11)
F3	8517.5 (19)	8767.7 (15)	3008.1 (14)	127.2 (11)
F4	8433.7 (19)	7562.9 (17)	2260.7 (11)	124.1 (11)
F5	8296.3 (18)	6006.8 (15)	2574.8 (10)	103.1 (9)
F6	7774 (2)	3489 (4)	4475.2 (18)	72.4 (18)
F7	8170 (2)	3106 (2)	3675 (3)	74.7 (15)
C27	10492 (10)	1356 (7)	3671 (3)	154 (6)
C28	10856 (11)	588 (8)	4501 (6)	179 (10)
C29	11566 (7)	1825 (10)	4270 (8)	209 (8)
F7'	7711 (5)	4088 (9)	4668 (4)	84 (4)
F6'	7993 (5)	3142 (6)	4092 (7)	93 (6)
C27'	11001 (12)	1642 (13)	3757 (9)	97 (6)
C28'	10519 (16)	490 (20)	4310 (12)	109 (9)
C29'	11646 (11)	1331 (14)	4662 (8)	96 (6)

Table 12-10 Anisotropic Displacement Parameters ($\text{\AA}^2 \times 10^3$) for 2a. The Anisotropic displacement factor exponent takes the form: $-2\pi^2[h^2a^{*2}U_{11} + 2hka^*b^*U_{12} + \dots]$.

Atom	U₁₁	U₂₂	U₃₃	U₂₃	U₁₃	U₁₂
C1	91 (3)	75 (3)	41 (2)	-10.5 (17)	15.4 (19)	-4 (2)
C2	69 (2)	62 (2)	34.2 (17)	-3.2 (15)	8.4 (15)	0.9 (18)
C3	70 (2)	52 (2)	41.9 (18)	-1.3 (15)	9.5 (16)	-6.6 (17)
C4	60 (2)	49.4 (19)	36.4 (16)	1.7 (14)	11.2 (15)	-5.2 (16)
C5	56 (2)	45.4 (18)	35.0 (16)	2.1 (13)	7.8 (14)	0.4 (15)
C6	55 (2)	51.0 (19)	41.2 (18)	8.5 (15)	9.1 (15)	-1.3 (16)
C7	70 (2)	62 (2)	34.7 (17)	7.4 (15)	14.2 (15)	0.6 (18)
C8	62 (2)	54 (2)	40.8 (17)	9.5 (15)	11.6 (16)	0.9 (17)

C9	67 (3)	72 (3)	81 (3)	30 (2)	-5 (2)	-2 (2)
C10	74 (3)	58 (2)	78 (3)	29 (2)	8 (2)	5 (2)
C11	69 (2)	46.2 (19)	47.1 (19)	11.5 (15)	16.2 (17)	0.9 (18)
C12	71 (2)	45.8 (19)	45.0 (18)	7.0 (15)	16.6 (17)	-3.3 (18)
C13	67 (2)	45.8 (19)	46.9 (19)	5.8 (15)	11.8 (17)	-4.9 (17)
C14	74 (3)	55 (2)	70 (2)	12.2 (18)	4 (2)	-14 (2)
C15	63 (2)	73 (3)	78 (3)	12 (2)	0 (2)	-14 (2)
C16	60 (2)	53 (2)	38.6 (17)	3.8 (15)	12.6 (15)	0.2 (17)
C17	57 (2)	52.1 (19)	41.7 (18)	4.6 (15)	10.1 (15)	3.2 (16)
C18	57 (2)	48.1 (19)	37.3 (17)	-2.1 (14)	10.2 (14)	4.0 (15)
C19	61 (2)	48.9 (18)	36.5 (16)	-0.1 (14)	10.2 (14)	6.3 (16)
C20	83 (3)	54 (2)	42.1 (19)	3.0 (15)	15.5 (17)	15.0 (18)
C21	86 (3)	64 (2)	41.9 (19)	1.3 (17)	18.6 (18)	19 (2)
C22	77 (3)	66 (2)	41.2 (18)	4.5 (17)	19.5 (17)	10 (2)
C23	129 (4)	87 (3)	65 (3)	4 (2)	45 (3)	39 (3)
C24	150 (5)	141 (5)	50 (3)	-16 (3)	-10 (3)	7 (4)
C25	174 (5)	95 (4)	74 (3)	-37 (3)	35 (3)	-32 (4)
C26	125 (5)	127 (5)	108 (4)	-47 (3)	41 (3)	6 (3)
C30	70 (2)	47 (2)	58 (2)	11.3 (17)	11.6 (18)	-5.4 (17)
C31	106 (3)	57 (2)	65 (3)	6 (2)	9 (2)	-4 (2)
C32	106 (4)	44 (2)	101 (3)	-8 (2)	1 (3)	-6 (2)
C33	97 (3)	48 (2)	106 (4)	27 (2)	12 (3)	-8 (2)
C34	112 (4)	62 (3)	82 (3)	27 (2)	32 (3)	-6 (2)
C35	91 (3)	56 (2)	70 (3)	16 (2)	25 (2)	-2 (2)
N1	57.1 (18)	46.2 (15)	46.1 (15)	10.5 (12)	11.8 (13)	-2.4 (13)
N2	62.2 (19)	44.6 (15)	44.1 (15)	11.8 (12)	12.5 (13)	-0.7 (13)
N3	66.0 (18)	42.3 (15)	42.7 (15)	-0.8 (12)	13.2 (13)	-5.5 (13)
B1	68 (3)	66 (3)	95 (4)	43 (3)	7 (3)	-7 (2)
F1	196 (3)	76.4 (17)	67.9 (16)	-4.7 (13)	12.3 (17)	1.3 (18)
F2	185 (3)	61.7 (16)	140 (3)	-20.4 (17)	-3 (2)	-4.6 (18)
F3	159 (3)	55.0 (15)	169 (3)	41.4 (17)	16 (2)	-14.5 (16)
F4	179 (3)	98 (2)	102 (2)	51.2 (17)	49.5 (19)	-2.5 (19)
F5	173 (3)	71.7 (16)	70.4 (15)	8.7 (13)	45.9 (16)	-4.6 (16)
F6	71 (2)	90 (5)	58 (3)	38 (3)	12.8 (19)	-9 (2)
F7	81 (2)	50 (2)	94 (4)	-10 (2)	10 (2)	2.8 (16)
C27	289 (18)	115 (8)	63 (5)	-24 (5)	39 (7)	90 (10)
C28	290 (20)	119 (10)	144 (12)	32 (9)	131 (14)	133 (15)
C29	111 (9)	241 (17)	290 (20)	-81 (16)	94 (12)	51 (10)
F7'	82 (5)	103 (9)	67 (5)	26 (6)	7 (4)	-6 (5)
F6'	77 (7)	52 (6)	144 (16)	31 (7)	-20 (8)	-9 (4)
C29'	88 (12)	106 (15)	95 (12)	-15 (10)	16 (10)	36 (11)

Table S12-11 Bond Lengths for 2a.

Atom	Atom	Length/Å	Atom	Atom	Length/Å
C1	C24	1.521 (6)	C18	N3 ¹	1.393 (4)
C1	C25	1.523 (6)	C18	C19	1.398 (4)
C1	C26	1.530 (6)	C19	C20	1.383 (4)
C1	C2	1.534 (5)	C20	C21	1.398 (5)
C2	C3	1.384 (4)	C21	C22	1.387 (5)
C2	C7	1.401 (5)	C21	C23	1.539 (5)
C3	C4	1.391 (4)	C23	C27'	1.42 (2)
C4	C5	1.403 (4)	C23	C28	1.443 (13)
C4	C19 ¹	1.455 (4)	C23	C29	1.490 (14)
C5	N3	1.384 (4)	C23	C27	1.572 (10)
C5	C6	1.401 (4)	C23	C28'	1.59 (3)
C6	C7	1.387 (4)	C23	C29'	1.667 (19)
C6	C8	1.475 (5)	C30	C31	1.364 (5)
C8	N2	1.344 (4)	C30	C35	1.393 (5)
C8	C9	1.394 (5)	C31	F1	1.338 (4)
C9	C10	1.364 (5)	C31	C32	1.386 (6)
C10	C11	1.396 (5)	C32	F2	1.332 (5)
C11	C12	1.387 (5)	C32	C33	1.356 (6)
C11	N2	1.394 (4)	C33	F3	1.338 (4)
C12	C13	1.383 (5)	C33	C34	1.348 (6)
C12	C30	1.497 (4)	C34	F4	1.355 (5)
C13	C14	1.395 (5)	C34	C35	1.368 (5)
C13	N1	1.402 (4)	C35	F5	1.336 (5)
C14	C15	1.360 (5)	N1	B1	1.542 (6)
C15	C16	1.401 (5)	N2	B1	1.536 (5)
C16	N1	1.340 (4)	B1	F6'	1.105 (9)
C16	C17	1.478 (4)	B1	F6	1.295 (6)
C17	C22	1.384 (4)	B1	F7	1.508 (7)
C17	C18	1.406 (4)	B1	F7'	1.736 (13)

¹3/2-X,+Y,1-Z

Table S12-12 Bond Angles for 2a.

Atom	Atom	Atom	Angle/°	Atom	Atom	Atom	Angle/°
C24	C1	C25	108.4 (4)	C20	C21	C23	121.4 (3)
C24	C1	C26	110.5 (4)	C17	C22	C21	124.1 (3)
C25	C1	C26	107.2 (4)	C28	C23	C29	115.1 (10)
C24	C1	C2	109.7 (3)	C27'	C23	C21	117.2 (9)
C25	C1	C2	112.3 (3)	C28	C23	C21	113.8 (5)
C26	C1	C2	108.7 (3)	C29	C23	C21	107.0 (6)
C3	C2	C7	117.5 (3)	C28	C23	C27	108.0 (9)
C3	C2	C1	123.1 (3)	C29	C23	C27	104.5 (9)
C7	C2	C1	119.4 (3)	C21	C23	C27	107.8 (5)
C2	C3	C4	120.8 (3)	C27'	C23	C28'	113.3 (14)

C3	C4	C5	120.1(3)	C21	C23	C28'	110.2(12)
C3	C4	C19 ¹	134.0(3)	C27'	C23	C29'	105.9(11)
C5	C4	C19 ¹	105.9(3)	C21	C23	C29'	107.9(7)
N3	C5	C6	128.9(3)	C28'	C23	C29'	100.6(12)
N3	C5	C4	110.2(2)	C31	C30	C35	116.8(3)
C6	C5	C4	120.6(3)	C31	C30	C12	121.9(3)
C7	C6	C5	116.9(3)	C35	C30	C12	121.3(3)
C7	C6	C8	120.7(3)	F1	C31	C30	119.0(3)
C5	C6	C8	122.1(3)	F1	C31	C32	119.3(4)
C6	C7	C2	123.9(3)	C30	C31	C32	121.7(4)
N2	C8	C9	109.2(3)	F2	C32	C33	120.6(4)
N2	C8	C6	124.9(3)	F2	C32	C31	119.8(4)
C9	C8	C6	125.9(3)	C33	C32	C31	119.6(4)
C10	C9	C8	107.9(3)	F3	C33	C34	120.5(4)
C9	C10	C11	107.3(3)	F3	C33	C32	119.4(5)
C12	C11	N2	120.2(3)	C34	C33	C32	120.1(4)
C12	C11	C10	131.7(3)	C33	C34	F4	119.6(4)
N2	C11	C10	108.0(3)	C33	C34	C35	120.4(4)
C13	C12	C11	122.1(3)	F4	C34	C35	119.9(4)
C13	C12	C30	118.6(3)	F5	C35	C34	118.5(4)
C11	C12	C30	119.3(3)	F5	C35	C30	120.2(3)
C12	C13	C14	131.4(3)	C34	C35	C30	121.3(4)
C12	C13	N1	120.4(3)	C16	N1	C13	107.5(3)
C14	C13	N1	108.1(3)	C16	N1	B1	127.9(3)
C15	C14	C13	107.0(3)	C13	N1	B1	124.3(3)
C14	C15	C16	108.4(3)	C8	N2	C11	107.5(3)
N1	C16	C15	108.9(3)	C8	N2	B1	127.6(3)
N1	C16	C17	125.1(3)	C11	N2	B1	124.9(3)
C15	C16	C17	126.0(3)	C5	N3	C18 ¹	107.4(3)
C22	C17	C18	116.6(3)	F6	B1	F7	105.8(5)
C22	C17	C16	120.4(3)	F6'	B1	N2	126.3(6)
C18	C17	C16	122.7(3)	F6	B1	N2	114.6(4)
N3 ¹	C18	C19	109.8(3)	F7	B1	N2	105.5(4)
N3 ¹	C18	C17	129.2(3)	F6'	B1	N1	123.0(6)
C19	C18	C17	120.8(3)	F6	B1	N1	115.4(4)
C20	C19	C18	120.3(3)	F7	B1	N1	106.8(4)
C20	C19	C4 ¹	133.1(3)	N2	B1	N1	107.9(3)
C18	C19	C4 ¹	106.6(3)	F6'	B1	F7'	98.2(9)
C19	C20	C21	120.3(3)	N2	B1	F7'	94.9(4)
C22	C21	C20	117.7(3)	N1	B1	F7'	93.0(5)
C22	C21	C23	120.8(3)				

¹3/2-X,+Y,1-Z

Table S12-13 Hydrogen Atom Coordinates ($\text{\AA} \times 10^4$) and Isotropic Displacement Parameters ($\text{\AA}^2 \times 10^3$) for 2a.

Atom	x	y	z	U(eq)
H3	5310.4	1317.08	3691.65	65
H7	6472.31	2874.29	2834.38	66
H9	5854.85	4746.16	3050.55	89
H10	6737.27	5914.71	3115.38	84
H14	9784.38	5858.22	3963.29	80
H15	10469.45	4691.98	4399.06	86
H20	10232.09	1306.15	5262.01	71
H22	10223.48	2856	4011.62	73
H24A	5683.31	2314.33	2132.44	172
H24B	5445.08	1453.16	1898.26	172
H24C	4924.52	1908.71	2283.98	172
H25A	5737.03	337.22	3118.34	170
H25B	4956.89	707.78	2882.65	170
H25C	5477.44	252.23	2496.93	170
H26A	6945.97	940.56	2891.13	178
H26B	6671.3	827.3	2274.21	178
H26C	6945.92	1685.98	2492.69	178
H3A	6267.55	3966.46	4620.53	60
H27A	10461.79	1895.35	3518.54	231
H27B	10822.98	1026.1	3473.16	231
H27C	9993.5	1116.6	3648.5	231
H28A	10351.22	365.83	4495.15	269
H28B	11157.73	253.35	4283.5	269
H28C	11084.19	600.04	4868.69	269
H29A	11487.95	2362.8	4120.81	314
H29B	11809.82	1864.26	4632.46	314
H29C	11883.35	1517.57	4047.27	314
H27D	11324.71	1237.42	3616.43	145
H27E	10541.19	1690.71	3520.12	145
H27F	11259.8	2158.37	3778.97	145
H28D	10405.58	370.43	4674.94	164
H28E	10067.27	432.06	4067.33	164
H28F	10904.99	127.01	4204.98	164
H29D	11555.07	1172.13	5025.35	144
H29E	11958.45	928.6	4507.38	144
H29F	11900.66	1849.59	4671.6	144

Table S12-14 Atomic Occupancy for 2a.

Atom	Occupancy	Atom	Occupancy	Atom	Occupancy
F6	0.683(11)	F7	0.683(11)	C27	0.683(11)
H27A	0.683(11)	H27B	0.683(11)	H27C	0.683(11)
C28	0.683(11)	H28A	0.683(11)	H28B	0.683(11)

H28C	0.683(11)	C29	0.683(11)	H29A	0.683(11)
H29B	0.683(11)	H29C	0.683(11)	F7'	0.317(11)
F6'	0.317(11)	C27'	0.317(11)	H27D	0.317(11)
H27E	0.317(11)	H27F	0.317(11)	C28'	0.317(11)
H28D	0.317(11)	H28E	0.317(11)	H28F	0.317(11)
C29'	0.317(11)	H29D	0.317(11)	H29E	0.317(11)
H29F	0.317(11)				